CHALMERS

Vibration response of lightweight pedestrian bridges

Master of Science Thesis in the Master's Programme Structural Engineering and Building Technology

PER ERIKSSON
HALLVARD PAGANDER TYSNES

Department of Civil and Environmental Engineering
Division of Structural Engineering
Steel and Timber Structures
CHALMERS UNIVERSITY OF TECHNOLOGY
Göteborg, Sweden 2013

Master's Thesis 2013:51

MASTER'S THESIS 2013:51

Vibration response of lightweight pedestrian bridges

Master of Science Thesis in the Master's Programme Structural Engineering and Building Technology

PER ERIKSSON

HALLVARD PAGANDER TYSNES

Department of Civil and Environmental Engineering
Division of Structural Engineering
Steel and Timber Structures
CHALMERS UNIVERSITY OF TECHNOLOGY
Göteborg, Sweden 2013

Vibration response of lightweight pedestrian bridges

Master of Science Thesis in the Master's Programme Structural Engineering and Building Technology

PER ERIKSSON
HALLVARD PAGANDER TYSNES

Examensarbete / Institutionen för bygg- och miljöteknik,
Chalmers tekniska högskola2013:51

Department of Civil and Environmental Engineering
Division of Structural Engineering
Steel and Timber Structures
Chalmers University of Technology
SE-412 96 Göteborg
Sweden
Telephone: + 46 (0)31-772 1000

Cover:
The three studied bridges, the steel truss bridge in Anneber (upper left), the box-beam bridge in Kristinehamn (upper right) and the multi-span bridge (bottom) Description of the bridges can be found in Chapter 5.

Department of Civil and Environmental Engineering Göteborg, Sweden 2013

Vibration response of lightweight pedestrian bridges

Master of Science Thesis in the Master's Programme Structural Engineering and Building Technology

PER ERIKSSON
HALLVARD PAGANDER TYSNES
Department of Civil and Environmental Engineering
Division ofStructural Engineering
Steel and Timber Structures
Chalmers University of Technology

ABSTRACT

Pedestrian bridges are built lighter and with longer spans as the years go by. These lightweight bridges are often susceptible for human induced vibrations, but it is still important to ensure pedestrian comfort. Hence, the Swedish Transport Administration, Trafikverket, realises the need to design for pedestrian loading at an early stage. In design, it is difficult to predict the actual dynamic behaviour of the bridge, and hence it is important to study bridges in use and compare them to the design guidelines.

The aim of this thesis was to compare the peak vertical accelerations from four different design guidelines, and compare to accelerations measurements performed in situ at three different bridges. From this comparison, a proposal for a suitable design guideline to use in future design of bridges was proposed. In addition, some of the issues affecting the damping of bridges were highlighted.

The three studied bridges were a 27 m long steel truss bridge, a 33 m long timber box-beam bridge, with a vertical radius, and a five span timber beam bridge of 103.4 m. Heel impact tests, jumping tests and controlled walking tests were performed on these bridges to determine the peak accelerations, natural frequencies and damping under vandal loading and normal use. These measurements were compared to the calculated peak accelerations according to Annex B of Eurocode 5 – Part 2, UK National Annex to Eurocode 1, the design guideline from the French Sétra and ISO 10137.

The field measurements showed natural frequencies that differed from the design models, and the models had to be modified by adding the effect of elements not expected to contribute to the stiffness, like railings. The measured total damping ratios were four to ten times larger than what is given in design guidelines. This was assumed to be related to the influence of non-structural elements and people on the bridge. The two design guidelines, UK NA and Sétra, were deemed to give a good correlation to the measurements of the vertical accelerations and the perception of the bridges. For the future design of pedestrian bridges, this study concludes that, EC 5-2 and ISO 10137 standards are outdated due to oversimplification. Sétra and UK NA guidelines provided good correlation, however Sétrais easier to use and are hence recommended in future designs.

Key words: Vertical accelerations, Pedestrian bridge, footbridge, lightweight bridge, steel bridge, timber bridge, pedestrian loading, field measurements, Sétra, UK NA, ISO 10137, EC 5-2, comfort criteria, pedestrian force models

Vibrations respons ilätta gångbroar

Examensarbete inom Structural Engineering and Building Technology

PER ERIKSSON
HALLVARD PAGANDER TYSNES
Institutionen för bygg- och miljöteknik
Avdelningen för konstruktionsteknik
Stål- och träbyggnad
Chalmers tekniska högskola

SAMMANFATTNING

Gång- och cykelbroar byggs idag lättare och med längre spännvidder. Dessa lätta broar är ofta känsliga för vibrationer orsakade av gångtrafikanter och det är viktigt att komforten upprätthålls. Därförser Trafikverket behovet av att ta hänsyn till dynamiska laster från fotgängare i ett tidigt stadium. I dimensioneringen är det svårt att förutse brons dynamiska beteende, och därför är det viktigt att studera befintliga broar och jämföra dem med standarder.

Syftet med denna avhandling var att jämföra beräknade och uppmätte maximala vertikala accelerationer från fyra olika standarder på tre broar. Från denna jämförelse skulle ett förslag på en lämplig standard att använda i framtiden tas fram. Även några av de faktorer som påverkar dämpningen av broar skulle belysas.

De tre studerade broarna var en 27 m fackversbro i stål, en 33 m lådbalksbro i trä, med en vertikal radie och en fem spanns plattbro i trä på 103,4 meter. På dessa tre broar utfördes hälstöt-, hopp- och kontrollerade gångtester för att bestämma maximala accelerationer, egenfrekvenser och dämpning. Dessa mätningar jämfördes med maximala beräknade accelerationer enligt bilaga B i Eurokod 5 - Del 2, UK National Annex till Eurocode 1, franska Sétra och ISO 10137.

Fältmätningarna indikerade egenfrekvenser som skilde sig från beräkningsmodellerna. För att återskapa verkligheten ändrades modellerna genom att lägga till effekten från faktorer som inte förväntades bidra till styvheten, till exempel räcken. Den uppmätta dämpningen var fyra till tio gånger större än vad som anges i standarder. Den höga dämpningen antogs vara relaterad till inverkan av icke bärande element och människor.Modellerna UK NA och Sétra ansågs ge en bra korrelation med mätningarna. Denna avhandling slutar med att konstantera att EC 5-2 och ISO 10137 är inte bör användas på grund av grova förenklingar,medan både Setra och UK NA gav god korrelation. Setra är lättare att applicera och rekommenderas därför för framtidaanvändning.

Nyckelord: Vertikala accelerationer, gång- och cykelbro, lätt bro, stålbro, träbro, laster från fotgängare, fältmätningar, Setra, UK NA, 10137 ISO, EC 5-2, komfortkriterier

Contents

Preface

This project is the culmination of five years of civil engineering studies at Chalmers University of Technology in Göteborg, Sweden, finishing our Master's degree with specialisation in structural engineering. The project has been performed in collaboration with COWI AB in Göteborg as a continuation of a previous thesis. The project investigated the vibration response of pedestrian bridges subjected to pedestrian loading. Acceleration measurements were performed on three bridges at three different occasions, to investigate the behaviour or the bridges. We would like to thank everyone who participated in these field measurements, our friends from Chalmers, employees at COWI, the students and teachers at Ölmeskolan, and KristinehamnsKommun, which helped us with a vehicle for the static test.

At COWI, they have given us tremendous help during the work. Especially we would like to thank our main supervisor, Tomas Svensson, for all the help given with practical guidance. With regards to the modelling in BRIGADE/Plus we would like to thank Isak Svensson, who always answered and came with advice when we disturbed him in his work. And last, Hanna Jansson, which have been sitting further away and hence not been disturbed as much – you have also been a tremendous help, especially with regards to the writing.

At Chalmers, we would like to thank our supervisor and examiner Professor Robert Kliger, who has a huge knowledge when it comes to timber structures. We also have to thank him for allowing Hallvard to start this Master's project even without all prerequisites and let him participatein the Timber Engineering course during the first half of the project.

In the end, we would like to thank our opposition, Anders Pagoldh Johansson and Carl Westerlund, which has given us feedback and support throughout the work. They even participated in the field experiments at two of the bridges.

Göteborg, June 2013

Per Eriksson

Hallvard Pagander Tysnes

Notations

Roman upper case letters

A	Area of bridge deck	[m²]
$\mathbf{C}$	Viscous damping matrix	[Ns/m]
$C(N)$	Coordination factor, for randomness in walking	[-]
D	Pedestrian mass damping parameter	[-]
$F(t)$	Applied force	[N]
$F(t)$	Pedestrian force from all pedestrians	[N]
$\mathbf{F}(t)$	Applied force vector	[N]
F_0	Force amplitude	[N]
G	Weight of one pedestrian	[N]
ΔG_n	Load component (amplitude) of n-th harmonic	[N]
$\mathbf{K}$	Stiffness matrix	[N/m]
M	Generalised mass	[kg]
M	Total mass of bridge	[kg]
$\mathbf{M}$	Mass matrix	[kg]
N	Number of pedestrians	[-]
N	Number of measurements	[-]
N_{eq}	Equivalent number of pedestrians	[-]
N_L	Limiting number of pedestrians	[-]
N_{tot}	Total number of pedestrians	[-]
Q	Static load from pedestrians	[N]
S	Span length	[m]
S_{eff}	Effective span length	[m]

Roman lower case letters

$a_{hor,1}$	Horizontal peak acceleration from one person	[m/s^2]
$a_{hor,n}$	Horizontal peak acceleration for n pedestrians	[m/s^2]
a_i	Acceleration at the peak in cycle i	[m/s^2]
a_{i+1}	Acceleration at the peak in cycle i+1	[m/s^2]
a_{limit}	Maximum peak acceleration	[m/s^2]
$a_{vert,1}$	Vertical peak acceleration from one person	[m/s^2]
$a_{vert,n}$	Vertical peak acceleration for n pedestrians	[m/s^2]
b	Width of walkway	[m]
c	Viscous damping coefficient	[Ns/m]
c_{cr}	Critical damping	[Ns/m]
d	Crowd density	[m^{-2}]
f	Natural frequency	[Hz]

f	Forcing frequency	[Hz]
f_{hor}	Horizontal natural frequency	[Hz]
f_v	Vertical natural frequency	[Hz]
f_n	Natural frequency	[Hz]
f_w	Walking frequency	[Hz]
f_{vert}	Vertical natural frequency	[Hz]
k	Spring stiffness	[N/m]
k	Proportionality factor	[N/m]
k_1	Response modifier to account for site usage	[-]
k_2	Response modifier to account for route redundancy	[-]
k_3	Response modifier to account for height of structure	[-]
k_4	Response modifier to account for exposure	[-]
$k(f_v)$	Factor for description of real behaviour	[-]
k_{vert}	Coefficient depending on the natural frequency	[-]
k_{hor}	Coefficient depending on the natural frequency	[-]
m	Mass	[kg]
m_{bridge}	Mass of the bridge per unit length	[kg/m]
$m_{pedestrian}$	Mass of pedestrians per unit length of the bridge	[kg/m]
n	Number of pedestrians	[-]
n	Harmonic number	[-]
t	Time	[s]
u	Displacement	[m]
u	Displacement vector	[m]
$\dot{u}$	Velocity	[m/s]
$\dot{\mathbf{u}}$	Velocity vector	[m/s]
$\ddot{u}$	Acceleration	[m/s^2]
$\ddot{\mathbf{u}}$	Acceleration vector	[m/s^2]
v_t	Pedestrian crossing speed	[m/s]
$w(t)$	Pedestrian force	[N/m^2]

Greek letters

α_n	Numerical coefficient for n -th harmonic	[-]
γ	Reduction factor for unsynchronised crowds	[-]
γ	Reduction factor for synchronised walking	[-]
ρ	Crowd density	[m^{-2}]
δ	Logarithmic decrement of decay of vibrations	[-]
λ	Reduction factor for effective number of pedestrians	[-]
ζ	Critical damping ratio	[-]
ψ	Minus factor correlated to risk of resonance	[-]

φ_n	Phase angle for the n -th harmonic	[-]

Abbreviations

BRIGADE/Plus	FE modelling software
Box-beam bridge	Refers in general to the box-beam bridge crossing the highway E18 in Kristinehamn.
BSI	British Standard Institution
Cable stayed bridge	Refers in general to the cable stayed bridge in Skellefteå, called Älvsbackabron
CEB	Euro-International Concrete Committee – now the International Federation for Structural Concrete (fib)
CEN	European comittee for standardization
EC5-2	Referring to the load model for pedestrian loading described in Annex B of Eurocode 5 – Part 2
FFT	Fast Fourier Transform
FE	Finite Element
Harmonic	Pulsating load in double and triple the walking frequency
Heel impact test	A group of people standing on their tiptoes and fall down simultaneously down on their heels to create a impact force.
ISO 10137	Referring to the load model for pedestrian loading described in this document.
JRC	European Commission, Joint Research Centre
Jumping test	A group of people jumping in a certain frequency.
MDOF	Multiple degrees of freedom
Multi-span	Refers in general to the five-span timber bridge in Mariestad
Multi-span bridge	Refers to the same bridge as above
SDOF	Single degree of freedom
Sétra	*Service d'études techniques des routes et autoroutes*, in English: Technical Department for Transport, Roads and Bridges Engineering and Road Safety, and in general referring to the guidelines presented by this authority.
SIS	Swedish Standard Institute
Steel truss bridge	Refers in general to the steel truss bridge crossing the railway in Anneberg south of Gothenburg.
Spring-to-ground	A command in BRIGADE/Plus that assignsa spring with a given stiffness, between the model and solid ground.
TIE-command	A command in BRIGADE/Plus that connect elements together with a selected interaction.

UK NA	Referring to the load model, including design criteria, for the United Kingdom National Annex to Eurocode 1 – Part 2.
x-direction	Always defined as the longitudinal direction of the bridge.
y-direction	Always defined as the transversal direction of the bridge.
z-direction	Always defined as the vertical direction of the bridge.

1 Introduction

In recent years, the architecture and design of pedestrian bridges have become more daring, trending towards longer spans and slender looks, which are possible by higher allowable stress levels achieved by development of building materials. When higher stress levels are allowed, a decrease in stiffness often occurs. The decrease in stiffness and increased span length also decreases the natural frequencies of the bridges. If the natural frequency of the bridge is in the same range as the human walking frequency, resonance may be possible.

These lightweight bridges may feel uncomfortable to cross due to excessive vibrations, even though they are structurally safe. When vibrations are considered in this thesis, it is always caused by pedestrians. Within the last two decades several bridges have had problems with this. Famous examples are the Millenium Bridge in London and Pont de Solférino in Paris. New guidelines have been developed to better reflect the actual loading exerted by pedestrians and still have a load that is easy to apply for design purposes.

Bridges only designed for static loading are particularly prone to uncomfortable vibrations, which are often the main problem in lightweight bridges. Hence, The Swedish Transport Administration (Trafikverket) urges the need for preliminary designs to include the dynamic pedestrian loading, not only the static loading[1]. In recent years some new design guidelines including load models have been developed. This thesis will investigate the three following design guidelines: United Kingdom National Annex to Eurocode 1-Part 2 (UK NA),from the French road authorities, Service d'études techniques des routes et autoroutes (Sétra), in addition to Eurocode including the acceleration response given by Annex B of Eurocode 5-Part 2 (EC 5-2).

Force models cannot capture the real dynamic behaviour and response of a bridge before it is built. Several parameters in the dynamic design are uncertain. It is difficult to determine the influence of paving and non-structural elements, the damping ratio and the interaction with people on the bridge.Because of these uncertainties, Jansson and Svensson (2012) investigated the cable stayed timber bridge Älvsbackabron in Skellefteå, Sweden, in their Master's Thesis. Their aim was to compare the resulting accelerations from the force models in BRO 2004 and Eurocode, determine the acceleration response of the bridge through measurements and estimate a damping ratio from these. The pedestrian force model for Eurocode was modelled with ISO 10137 since the model presented in EC 5-2 only is valid for simply-supported bridges. Their conclusions were that the measured accelerations never exceeded the allowable levels in tests simulating normal usage, even though both design guidelines gave unacceptable accelerations. The measurements gave a calculated damping ratio of 1.2%, which is double the damping ratio specified in BRO 2004, but consistent with Eurocode.

Älvsbackabron is not a bridge commonly designed in Sweden, so the partner in the mentioned thesis, which also was the designer of the bridge - COWI AB, wanted to investigate more common bridges, where EC 5-2 is applicable. Hence, the following bridges were investigated in this project; a 27 meter long steel truss bridge, a 33 meterlong timber box-beam bridge with a vertical radius and a five span timber beam bridge of 103.4 meters. The three bridges were subjected to field experiments and

[1]Johan Jonsson, Trafikverket, meeting November 21, 2012

they were modelled with the three design guideline mentioned in the previous paragraphs, and in addition ISO 10137.

1.1 Aim and objective

The main aim of this thesis was to propose a suitable design guideline for the dynamic design of lightweight bridges with regards to pedestrian loading. To achieve this, the following objectives were identified.

- Determine the peak acceleration, vertical natural frequencies and total damping on three existing bridges through field measurement. The three bridges were a simply-supported steel truss bridge, a simply-supported timber box-beam bridge and a five span timber bridge with a stress laminated deck.
- Determine how peak accelerations from the modelled design guidelines relate to the relevant comfort criteria and performed measurements at the bridges.
- Calibrate the FE models of the three bridges to reflect the behaviour that can be seen in the measurements by adjusting material properties and boundary conditions, and adding non-structural elements originally not expected to contribute to the dynamic behaviour
- Highlight some of the issues affecting the damping of lightweight pedestrian bridges.

1.2 Limitations

Only vibrations in the vertical direction which are caused by pedestrians were studied in this thesis. This was because the largest vibrations caused by pedestrians are in the vertical direction, and calculation at the three studied bridges gave lateral natural frequencies sufficiently far away from the lateral walking frequency to be considered negligible.

Pedestrian induced vibration in bridges is mainly a serviceability problem, hence only the service state was considered in this thesis. To simulate the actual behaviour of the bridges no partial factors were used on loads or materials. In a real design situation, the ultimate state would be checked against dynamic wind actions, and possibly vandal loading by humans. But these problems were considered to be outside the scope of this thesis.

Only the following design guidelines were studied and modelled; EC 5-2, UK NA and Sétra, in addition ISO 10137 was modelled and applied in the design of the studied bridges. EC 5-2 and ISO 10137 were studied since they are codes commonly used in the design pedestrian bridges. Sétra and UK NA on the other hand were design guidelines not yet common in Sweden, and are hence interesting for the future design of pedestrian bridges. Which parameters, experiments and theory the studied design guidelines have used to define their loads and comfort criteria were not studied in this thesis.

Only the total damping of the bridges was evaluated from the field measurements. In the evaluation, logarithmic decrement was the only method used.

1.3 Method

The work with this thesis was divided in two parts. The first part consisted of a literature review to increase the knowledge before the case studies. The second part included case studies, first field experiments and second dynamic design of the studied bridges with regards to pedestrian loading.

Three different aspects, all relevant to the dynamic behaviour and design of bridges subjected to pedestrian loading, were studied in the literature review. The first, treated the dynamic forces induced by walking humans, including magnitude direction and variation with time. The second topic studied was related to the design of footbridges, namely design guidelines, with associated force models and comfort criteria. The studied codes were EC 5-2, UK NA and Sétra. The last studied topic was the damping of bridges. Within this topic, the effect of asphalt pavement and human structure interaction was studied, as well as how it is treated by different design guidelines.

The case studies investigated three bridges, a 27 meter steel truss bridge, a 33 meter timber box-beam bridge with a vertical radius and a five span timber beam bridge of 103.4 meters with a stress laminated deck. The bridges were first modelled in the Finite Element software BRIGADE/Plus according to the drawings to determine their natural frequencies and associated mode shapes. Field experiments measuring the accelerations caused by several tests were then performed on the bridges. On each of the bridges, jumping tests, heel impact tests and controlled walking tests were performed. The natural frequencies were also evaluated through frequency analysis during the tests, to account for errors in the modelling. The heel impact- and jumping tests were performed to evaluate the structural damping and the natural frequencies of the bridges. The controlled walking tests were performed to simulate a normal loading situation in addition to evaluate the natural frequencies. For the heel impact- and controlled walking tests, the natural frequencies were evaluated by the use of frequency analysis through Fast Fourier Transform (FFT), while for the jumping test they were evaluated by the jumping frequency giving the largest accelerations. The damping for both the heel impact- and jumping tests were evaluated by logarithmic decrement.

With the results from the field experiments, the FE models were calibrated. Changing stiffness and mass, using the measured damping ratios and adding some non-structural elements clearly influencing the stiffness and natural frequency. For each of the studied bridges one heel impact and one jumping test were simulated in BRIGADE/Plus, to be used as a comparison between measurements and models.

In the last part of the project, the models were subjected to the loads from each of the studied design guidelines and in addition ISO 10137. This was meant to simulate the actual design situation of the bridges, if they were to be designed again. The results of the field experiments were compared to the results of the design guidelines to see which of them were most applicable in the future design of footbridges.

1.4 Thesis outline

The outline of the coming chapters in this thesis is:

Chapter 2 to 4 consists of the literature review.Chapter 2 is an introduction to structural dynamics in general and more specific to vibrations caused by pedestrians.

In Chapter 3, design guidelines considering the dynamic load from pedestrians are treated. The literature review ends with an introduction to damping and how it is influenced by asphalt pavement and humans Chapter 4.

Chapter 5 and 6 describe the case studies performed on the three studied bridges. The bridges and the modelling of them are described in Chapter 5, while the performed experiments are described in Chapter 6.

Chapter 7 presents the results from case study. This includes measured damping ratios, maximum accelerations and natural frequencies determined during the field measurements, simulation of the same tests in BRIGADE/Plus and the peak accelerations achieved by each of the tested design models.

In **Chapter 8**, the results presented in Chapter 7 are analysed, and in **Chapter 9** the authors discusses important results presented in the thesis.

Chapter 10 presents the conclusions made by the authors after working with this project.

In the **Appendices** the following addition information can be found:

- **Appendix A** – Calibration certificates for the accelerometers.
- **Appendix B** – Description of FE models.
- **Appendix C** – MATLAB scripts for calculation of damping and FFT.
- **Appendix D** – Hand Calculations for EC 5-2.

2 Vibration of lightweight bridges

Vibration is a phenomenon that occurs in all structures and is caused by an energy pulse acting on a structural member. In walkways and lightweight bridges the energy source arises from humans crossing the bridge or the wind blowing from the side. While the wind action must be considered when designing for failure, the forces from pedestrians are so small that they are considered as serviceability problem. Dynamic actions are a function of time and space and for exact calculations the characteristics of the source, the transmission path and the receiver is needed.

In this chapter the basic theory of structural dynamics and human-induced vibrations are introduced, which both relates to the vibration source.

2.1 Introduction to structural dynamics

The simplest dynamic system is an oscillating system with one single degree of freedom (SDOF). The system consists of a mass m, connected to a linear spring with stiffness k and a linear damper with viscosity c, and an external force $F(t)$ as shown in Figure 2.1.

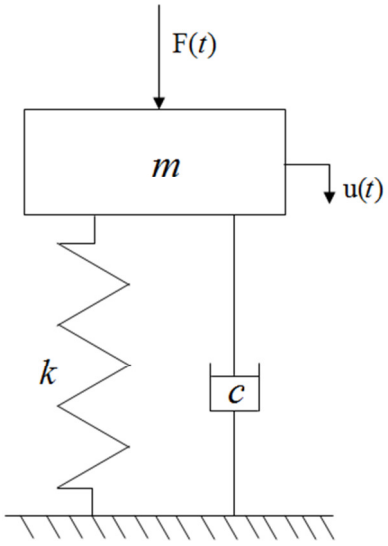

Figure 2.1 Schematic drawing of the simplest single degree of freedom system, containing a mass, linear spring and a viscous damper.

The differential equation in Equation (2.1) is called the *equation of motion,* and describes the behaviour of a moving SDOF system. The equation can be derived by using Newton's second law or the principle of virtual displacement (Craig Jr & Kurdila, 2006).

$$m\,\ddot{u} + c\,\dot{u} + k\,u = F(t) \tag{2.1}$$

Where

m	Mass
c	Damping
k	Spring stiffness
$F(t)$	Force
u	Displacement
$\dot{u}$	Velocity
$\ddot{u}$	Acceleration

When a system has more than one degree of freedom it is called a multi degree of freedom system (MDOF) and the equation of motion is rewritten to Equation (2.2) with mass, damping and stiffness as matrices, and displacement and the applied force as vectors.

$$\mathbf{M}\ddot{u} + \mathbf{C}\dot{u} + \mathbf{K}u = \mathbf{F}(t) \tag{2.2}$$

The dynamic behaviour of a system can be evaluated by modal analysis. This method allows decoupling of the system of differential equations into a set of linearly independent differential equations of SDOF oscillators by the use of modal decomposition (Craig Jr & Kurdila, 2006). By determining the mass, stiffness, geometry and boundary conditions of a beam or a structure, it becomes possible to calculate the natural frequency and mode shape for all relevant modes (Craig Jr & Kurdila, 2006). The first two mode shapes of an arbitrary simply-supported beam are shown in Figure 2.2.

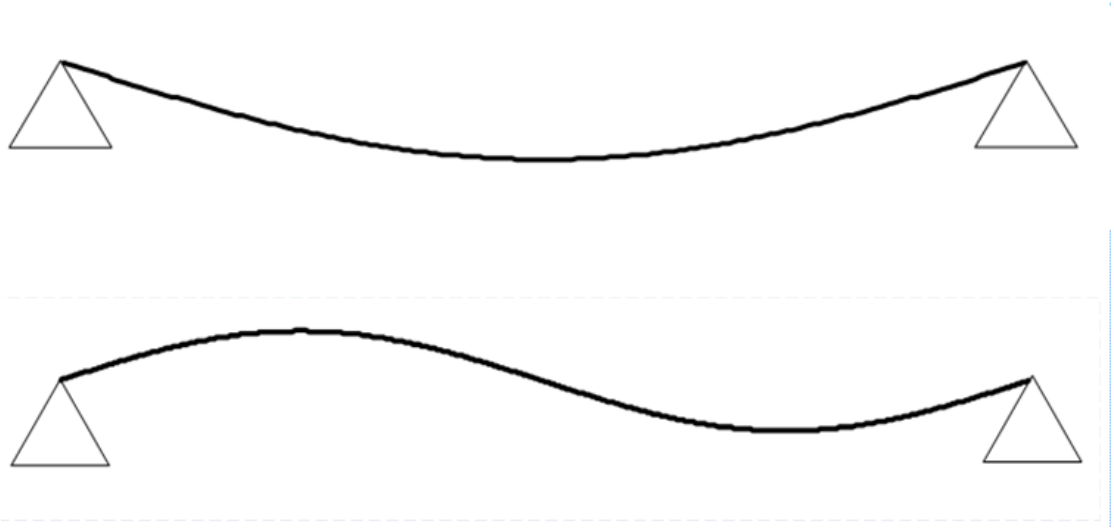

Figure 2.2 First and second vibration modes of a simply-supported beam, assumed to be sinusoidal.

These mode shapes represent how a structure will behave during free vibration. This is used to determine the total response of the structure when an external force is

applied. The total response of a linear system consists of two important parameters, the superposition of the force motion and the natural motion. If these two motions have the same amplitude and in are in the same phase a phenomenon called resonance may occur (Craig Jr & Kurdila, 2006), which can be seen as the peaks in Figure 2.3.It can also be seen that with an increased damping ratio, ζ, the resonance amplitude decreases. The definition of ζ is found in Equation (2.3).

$$\zeta = \frac{c}{c_{cr}} \tag{2.3}$$

Where

ζ	Damping ratio
c	Damping
c_{cr}	Critical damping, where $c_{cr} = 2\sqrt{km}$
k	Spring stiffness
m	Mass

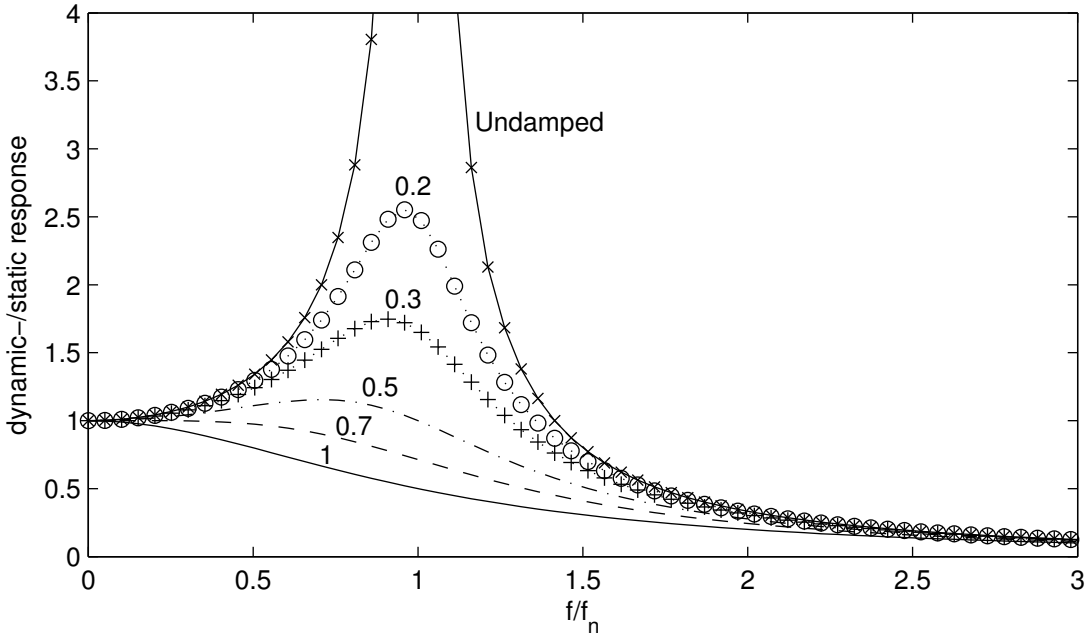

Figure 2.3 Resonance phenomena plotted as a function between the ratio of the forcing frequency, f, and the natural frequency f_n, versus the ratio of the dynamic- and static response.

2.2 Dynamic forces induced by humans

When humans walk, the weight of the person will be transferred to the ground at approximately even intervals, which will lead to a periodic force. This force is dependent on the walking speed and stride length, in other words the pacing rate or the step frequency. Figure 2.4, shows that when the pacing rate increases, the time in which one foot has contact with the ground decreases and at the same time the

dynamic amplification increases. Normal walking usually has a pacing frequency varying between 1.6 and 2.4 Hz with 2.0 Hz often used as a mean value, while running varies between 2.0 and 3.5 Hz (Živanović, Pavić, & Reynolds, 2005). From Figure 2.4 it can be seen that a walking frequency of 2.0 Hz gives a dynamic effect where around 40% of the self-weight is added to the static force. When running, the dynamic force can be over 150% of the self-weight, and hence running will often be governing. However, Sétra guidelines (2006) states that it sometimes should be allowed to exceed design limits for running due to the short duration of the crossing. The short duration is not long enough to cause resonance and will onlydisturb other pedestrians for a short period of time.

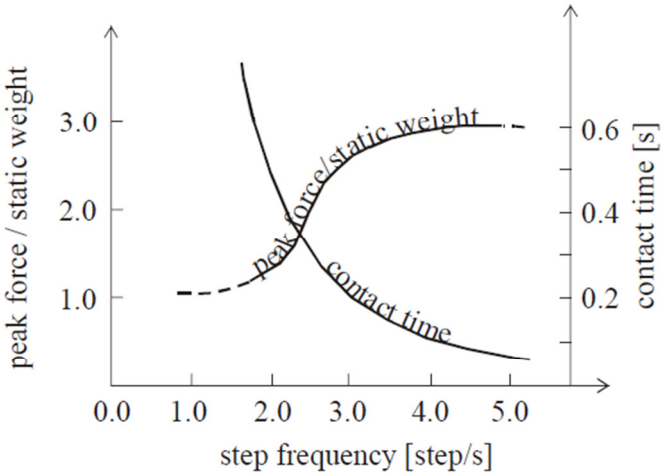

Figure 2.4 Variation of vertical peak force and contact time with respect to walking frequency (Živanović, Pavić, & Reynolds, 2005).

When walking, dynamic forces arise in three directions: vertical, lateral and longitudinal. The vertical and longitudinal components have the same frequency, while the lateral component has half this frequency because only every other step is with the same foot and hence in the same direction. The vertical direction is the most investigated due to the largestmagnitude (Živanović, Pavić, & Reynolds, 2005). However, in the last decade the lateral force was more thoroughly studied and is discussed in Section2.2.1. The difference in periods and frequencies can be seen in Figure 2.5. In addition, it is possible to see how each step overlaps the previous one and that more than one harmonic is needed to describe these periodic forces. The harmonic is the pulsating loads also exerted in double and triple the walking frequency. The total effect of a walking pedestrian can then, according to Bachmann and Amman (1987), be described as the Fourier series in Equation (2.4).

$$F(t) = G + \sum_{n=1}^{3} \Delta G_n \sin(n \cdot 2\pi f_w t - \varphi_n) \tag{2.4}$$

Where:

$F(t)$	Time varying force from one pedestrian
G	Weight of the pedestrian
ΔG_n	Load component (amplitude) of n-th harmonic
n	Harmonic number

f_w	Walking frequency
φ_n	Phase angle for the n -th harmonic, where $\varphi_0 = 0$
t	Time

Since pedestrians are entering the bridge at different time intervals, which creates several phase shifts, and with slightly different walking frequencies the behaviour of a pedestrian crowd can be seen as random.

Together with the complexity of the exerted force from pedestrians this makes it hard to execute a simulation of a full crowd's actual impact on a footbridge (Sétra, 2006). As long as the pedestrians are walking completely unaffected by each other, Živanović, Pavić and Reynolds (2005) state that the response of N pedestrians will be $\sqrt{N}$ times higher than the response from one pedestrian. Equation (2.5) can then be used in calculations as an equivalent number of pedestrians on the bridge walking in the same frequency and phase.

$$N_{eq} = \sqrt{N_{tot}} \tag{2.5}$$

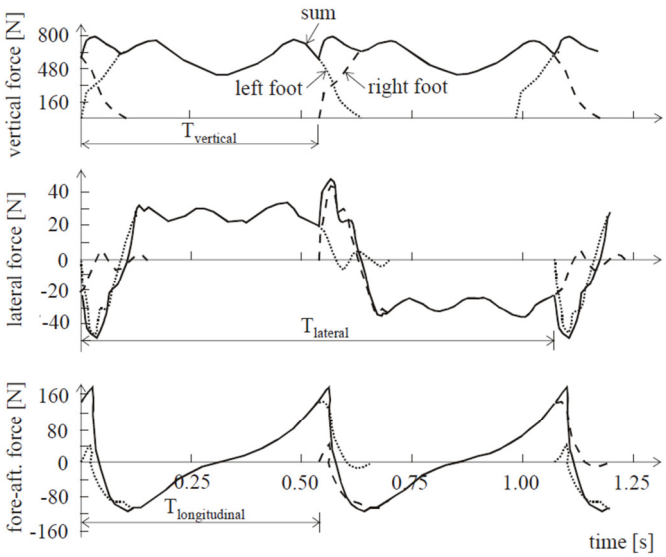

Figure 2.5 Periodic walking time histories in vertical, lateral and longitudinal direction (Živanović, Pavić, & Reynolds, 2005).

2.2.1 Pedestrian-induced lateral forces

When walking, a person will shift the centre of gravity from left to right with around 2 cm, see Figure 2.6. This will induce a dynamic lateral force of a magnitude 10 times smaller than the vertical force. This lateral force is mainly of interest due to a behaviour that occurs in some bridges when subjected to a large crowd of pedestrians. If the bridge has a lateral natural frequency of approximately half the usual walking frequency, it becomes easier to walk in this frequency than any else when the vibration amplitude increases. Hence, this may cause even larger lateral vibrations, and some people then might feel uncomfortable, even though the bridge is structurally sound and safe to cross (Nakamura & Kawasaki, 2006).

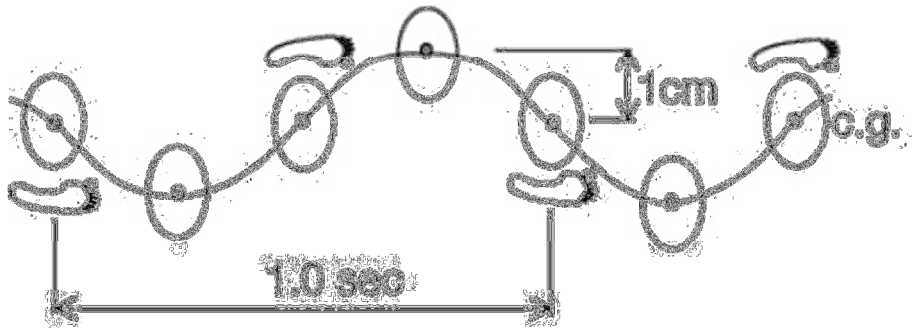

Figure 2.6 The origin of lateral forces by shifting the gravity centre (Nakamura & Kawasaki, 2006).

Two recent and famous cases of this phenomenon, called *Lock-in* or *Synchronous Lateral Excitation (SLE)*, are the Millennium Bridge in London and Pont de Solférino in Paris Both were closed shortly after opening and subjected to testing to determine the cause of the excessive and improve the bridges (Sétra, 2006). These two bridges have a very slim construction and special structural systems, but this problem is not restricted to slender bridges. According to Ingólfsson, Georgakis and Jönsson (2012), even more robust bridges exposed to unnatural huge crowds have experienced excessive lateral vibrations, among others the Brooklyn Bridge in New York City during a power blackout. The studies of the London Millennium Bridge by Dallard et al. (2001) shows that the load effect arises from synchronization of the lateral footfall of the crowd to the natural swaying of the bridge since it is more comfortable for the pedestrian. However, according to Nakamura (2004) when the velocity becomes large the pedestrians feel unsafe and this gives a maximum level of the vibrations. According to Ingólfsson, Georgakis, and Jönsson (2012) there is a discussion about the basic mechanism behin lateral forces and several hypothesis and load model exist, even thoug it may seem that the lock-in effect is the cause of excessive lateral vibrations.

According to Ingólfsson, Georgakis and Jönsson (2012), the most used method to assess suspectability of a bridge to excessive pedestrian-induced lateral vibrations is the theory formulated for the Millennium Bridge. The model is thoroughly explained by Dallard, et al.(2001) and gives a limiting number of pedestrians before excessive vibrations occur. Equation (2.6) gives an example of how this is expressed for a given level of damping and a sinusoidal mode shape normalised to unity.

$$N_L = \frac{8\pi cfM}{k} \tag{2.6}$$

Where:

N_L	Limiting number of pedestrians
c	Damping
f	Frequency corresponding to relevant modeshape
M	Generalised mass in the relevant modeshape
k	Proportionality factor, approximately value of 300 Ns/m

The investigations on Pont de Solférino agree with the investigations on the Millennium Bridge that there is a threshold for when lock-in occurs. However, the threshold is instead expressed in terms of accelerations stating that the crowd behaviour is no longer random when the acceleration exceeds 0.10-0.15 m/s^2 (Sétra, 2006), and hence theories based on the randomness of pedestrians are no longer valid. This threshold of a maximum acceleration of 0.10 m/s^2 is also adopted as a design requirement limit in the design guideline by Sétra(2006). The design guideline will be discussed in Section 3.3.

3 Design guidelines

Eurocode 1 (SIS, 2003) does not give any design models for the human-induced loading exerted on a pedestrian bridge and leaves it to the designer to select which model to use. For this reason, it becomes very important for the designer to know which models are available, how to use them and how closely they predict the response of the bridge.

This chapter describes how to use three different design guidelines. The first one is from Annex B of Eurocode 5 part - 2 (EC 5-2). The second and third ones are UK National Annex to Eurocode 1 (UK NA) and the design guideline from the French Technical Department for Transport, Roads and Bridges Engineering and Road Safety (Service d'études techniques des routes et autoroutes – Sétra). It will continue by summarising two studies about how the design guidelines capture the actually measured response on two existing bridges. The last sections are analyses of the comfort criteria and force models described by the design guidelines treated in this chapter.

3.1 EC 5-2 (SIS, 2004)

For pedestrian-induced vibrations in footbridges Eurocode states that a control of the maximum peak acceleration in all directions must be performed if the first natural frequency of the bridge deck is less than 5 Hz for vertical vibrations or less than 2.5 Hz for lateral and torsional vibrations (SIS, 2005). The maximum allowable accelerations according to Eurocode are found in Table 3.1 and should according to (SIS, 2005) be fulfilled by a considerable margin due to high uncertainties in the calculation of the response. The approach described here is only valid for timber bridges with simply-supported beams or truss systems excited by pedestrians (SIS, 2004). However, according to Zivanovic, Pavic and Ingólfsson (2010) the model could be used to check bridges of any material, since it is not timber specific. In EC 5-2, it is stated that the model will be found in future versions of EN 1991-2.

Table 3.1 Maximum allowable accelerations according to Eurocode(SIS, 2005).

Direction of vibrations	Maximum accelerations [m/s^2]
Vertical	0.7
Horizontal – normal use	0.2
Horizontal – exceptional crowd loads	0.4

The resulting vertical and horizontal accelerations for one person crossing the bridge, are dependent on the natural frequency, mass of the bridge and damping ratio and are given in Equations (3.1) and (3.2).

$$a_{vert,1} = \begin{cases} \dfrac{200N}{M\zeta} & \text{for } f_{vert} < 2.5Hz \\ \dfrac{100N}{M\zeta} & \text{for } 2.5Hz < f_{vert} < 5Hz \end{cases} \quad (3.1)$$

$$a_{hor,1} = \frac{50N}{M\zeta} \qquad \text{for } 0.5Hz < f_{hor} < 2.5Hz \quad (3.2)$$

Where

$a_{vert,1}$	Vertical accelerations from one pedestrians
$a_{hor,1}$	Horizontal accelerations form one pedestrian
M	Mass of the bridge
ζ	Damping ratio of the bridge

For groups of people crossing the bridge the vertical and horizontal accelerations are given by:

$$a_{vert,n} = 0.23 a_{vert,1} n k_{vert} \quad (3.3)$$

$$a_{hor,n} = 0.18 a_{hor,1} n k_{hor} \quad (3.4)$$

Where

$a_{vert,n}$	Vertical accelerations from n pedestrians
$a_{hor,n}$	Horizontal accelerations from n pedestrians
n	Number of pedestrians on the bridge
k_{vert} / k_{hor}	Coefficient dependent on the natural frequency of the bridge, and can be found in Figure 3.1

The number of pedestrians should be taken as:

$$n = \begin{cases} 13 & \text{for a distinct group} \\ 0.6A & \text{for a continuous stream} \end{cases}$$

A Area of the bridge deck [m²]

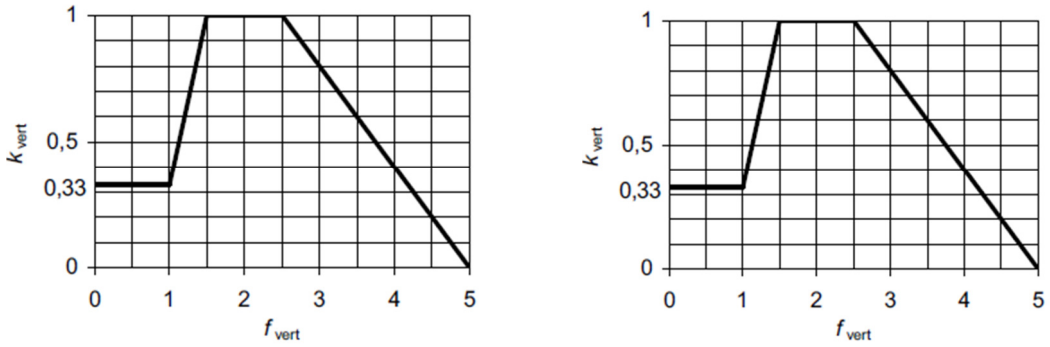

Figure 3.1 Relationship between the first natural frequency and the coefficients k_{vert} and k_{hor} according to EC 5-2

3.2 UK NA (BSI, 2008)

The load model described in this chapter can be found in section NA.2.44 in the United Kingdom National Annex to Eurocode 1 (BSI, 2008). To verify a design two different controls have to be made:

- The peak acceleration should be smaller than the maximum allowable given by Equation (3.5).
- The likelihood of synchronised lateral response needs to be determined by Equation (3.6).

Both criteria are described in Section 3.2.1, and the force models are used for the calculation of maximum vertical acceleration are described in Section 3.2.2.

3.2.1 Comfort Criteria

The maximum allowable vertical acceleration are:

$$a_{\lim it} = 1.0 \cdot k_1 \cdot k_2 \cdot k_3 \cdot k_4 \quad [\mathrm{m/s^2}] \qquad (3.5)$$

$$\text{and } 0.5 \le a_{\lim it} \le 2.0\,[\mathrm{m/s^2}]$$

Where

k_1 Site usage factor according to Figure 3.2

k_2 Route redundancy factor according to Figure 3.2

k_3 Structure height factor according to Figure 3.2

k_4 Exposure factor, generally set to 1.0, but may vary between 0.8 and 1.2 depending on the walking surface.

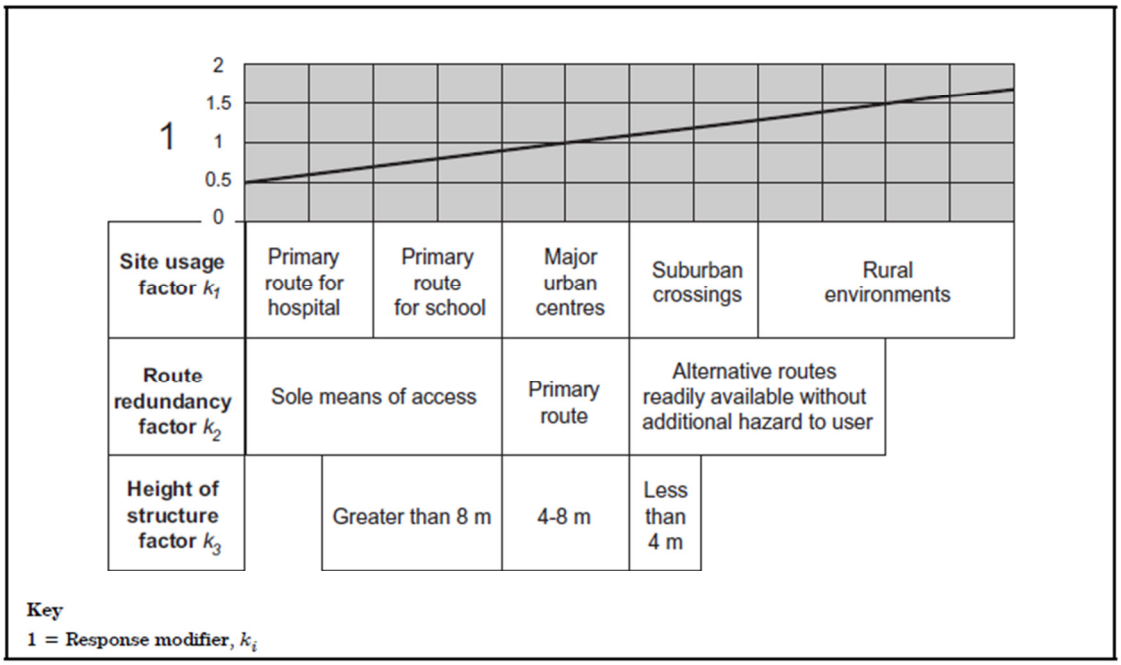

Figure 3.2 Values for the response modifiers k_i. The values can also be taken from Table NA.9 to NA.11 in the reference (BSI, 2008).

There is no reason to do more thorough checks for lateral vibrations if the first lateral mode is higher than 1.5 Hz. However, if this is not the case, all the modes with lateral natural frequencies below 1.5 Hz have to compare their pedestrian mass damping parameter, D, from Equation (3.6) with the stability boundary as defined in Figure 3.3.

$$D = \frac{m_{bridge} \cdot \zeta}{m_{pedestrian}} \tag{3.6}$$

Where:

D	Mass damping parameter
m_{bridge}	Mass per unit length of the bridge
$m_{pedestrian}$	Mass per unit length of pedestrians for the relevant crowd density according to relevant bridge class, assuming that each pedestrian weighs 70 kg
ζ	Structural damping when expressed as a damping ratio $\zeta = \delta/(2\pi)$
δ	Logarithmic decrement of decay of vibration between successive peaks

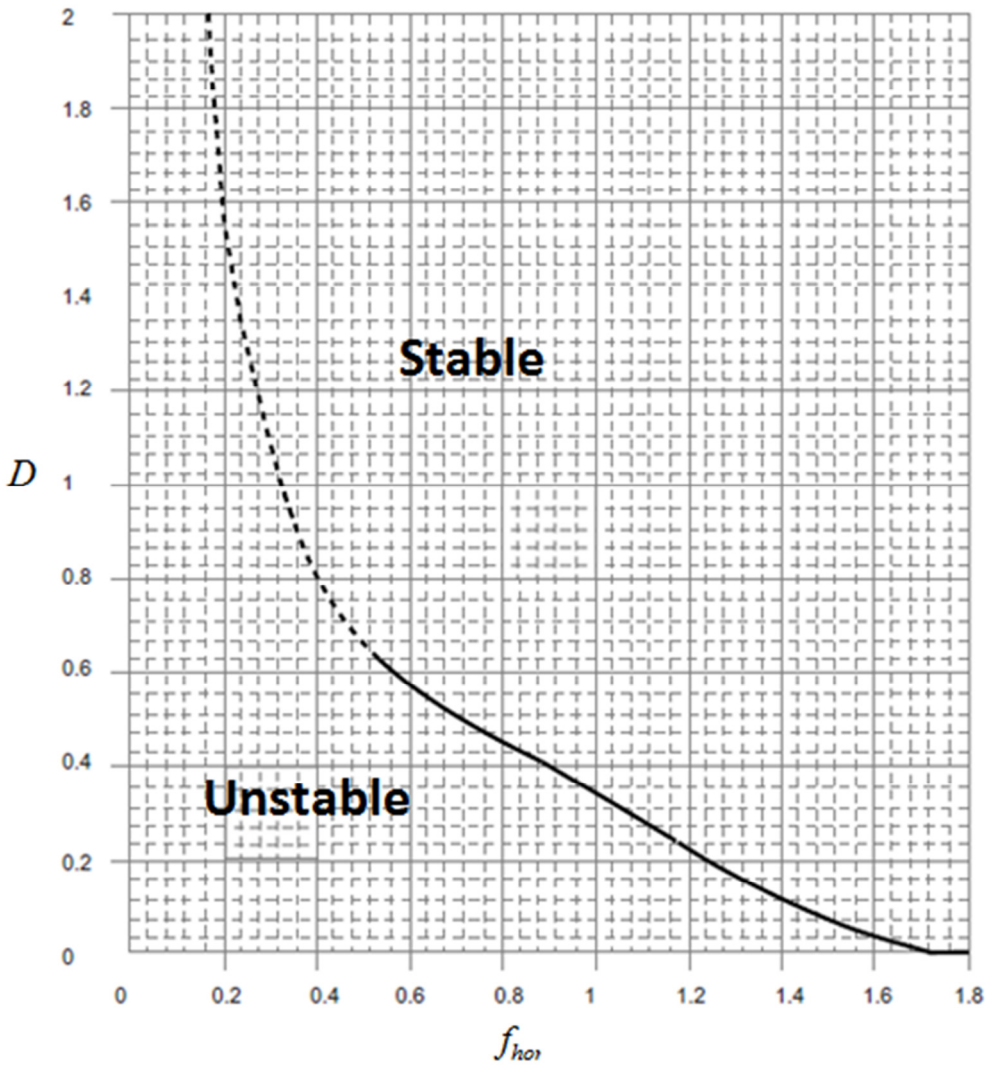

Figure 3.3 *Lateral lock-in stability boundaries, plotted for lateral natural frequency against the pedestrian mass damping parameter in Equation (3.6).Reliable test measurements are only available in the lateral frequency range of 0.5 Hz to 1.1 Hz, natural frequencies outside this range should be used with caution (Modified after BSI, (2008)).*

3.2.2 Application of load

Two different load cases are to be considered in the dynamic design. The first, Equation (3.7), simulates a single pedestrian, or a group of pedestrians as a point load crossing the bridge at a constant speed v_t. The crossing speed is 1.7 m/s for walking and 3 m/s for running.

The other case is steady state modelling of crowded conditions. The load, found in Equation (3.8), is to be applied as a uniformly-distributed load on the entire area of the bridge. To obtain the most unfavourable effect, the load should be applied with directions that coincide with the mode in which the response is calculated for, as shown in Figure 3.4. The size of relevant groups, to be used in both load cases, is dependent on the usage of the bridge and can be found in Table 3.2. Bridges are

classified in bridge classes according usage, from rural locations (Bridge class A) to primary access routes (Bridge class D).

Table 3.2 Bridge class and recommended crowd densities for design

Bridge class	Group size (walking)	Group size (jogging)	Crows density, ρ [pedestrian/m²] (walking)
A	N=2	N=1	0
B	N=4	N=2	0.4
C	N=8	N=3	0.8
D	N=16	N=4	1.5

Only one mode is checked in each analysis, and if the modes are closely spaced interaction between the modes is not captured. If this is the case, a more sophisticated method or the vector response of the modes should be used, which gives a conservative design.

$$F(t) = F_0 \cdot k(f_v) \cdot \sqrt{1+\gamma \cdot (N-1)} \cdot \sin(2\pi \cdot f_v \cdot t) \tag{3.7}$$

Where:

$F(t)$ Applied point load, representing a group moving at the speed v_t

N Number of pedestrians in the group depending of the bridge class

F_0 Reference amplitude of the applied force in Newton, and is 280 N for walking pedestrians, and 910 N for running

f_v Natural frequency of the vertical mode under consideration

$k(f_v)$ Factor to deal with (a) the effect of a more realistic pedestrian population, (b) harmonic responses and (c) relative weighting of pedestrian sensitivity to response, and is displayed in Figure 3.5

t Elapsed time

γ Reduction factor to allow for the unsynchronised combination of actions in a pedestrian group and is a function of damping and effective span length

$$w(t) = 1{,}8(\frac{F_0}{A})k(f_v)\cdot\sqrt{\gamma\cdot N/\lambda}\cdot\sin(2\pi\cdot f_v\cdot t) \tag{3.8}$$

Where:

$w(t)$	Time varying load applied on one square metrewith the directions according toFigure 3.4
A	Area of the bridge
γ	Gactor to allow for the unsynchronised combination of actions in a crowd
N	Total number of pedestrians distributed of the span length $N = \rho\cdot A = \rho\cdot S\cdot b$
ρ	Crowd density depending on the usage and with a maximum of 1.5 pedestrians/m²
S	Span of the bridge
b	Width of the bridge subjected to pedestrian loading
λ	Factor that reduces the effective number of pedestrians when loading from only part of the span contributes to the mode of interest, $\lambda = 0.634(S_{eff}/S)$

The rest of the variable are the same as in Equation (3.7).

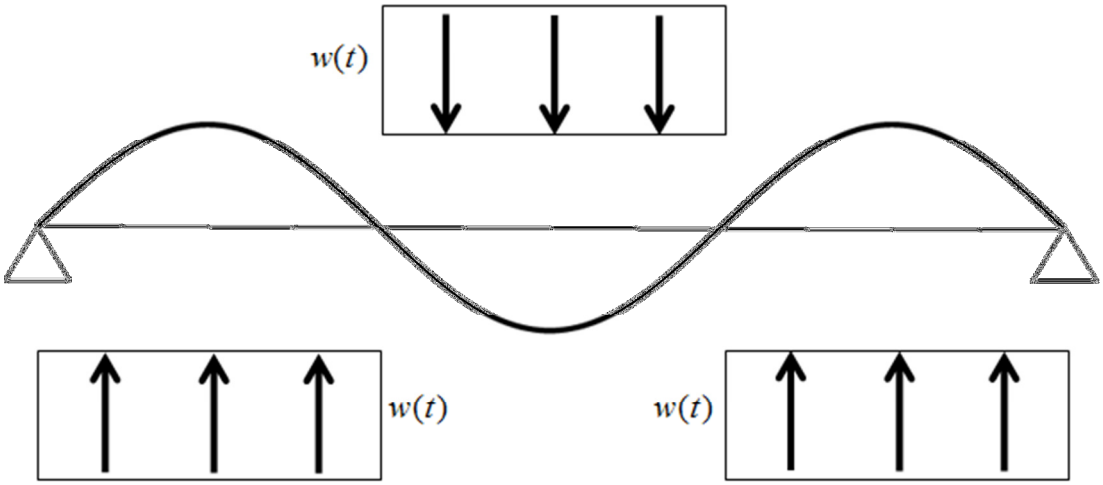

Figure 3.4 Sign of the amplitude of the load $w(t)$, in case of a mode with multiple sags.

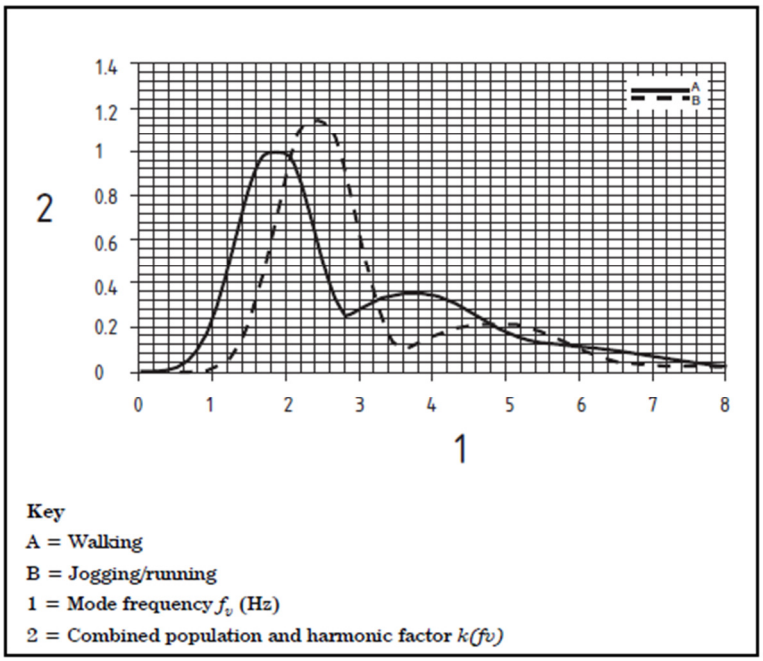

Figure 3.5 Relationship between the natural frequency of the mode of interest and the reduction factor $k(f_v)$ (BSI, 2008).

3.3 Sétra (Sétra, 2006)

This design guideline was prepared by a working group on the "Dynamic behaviour of footbridges" from the French Technical Department for Transport, Roads and Bridges Engineering and Road Safety (Sétra). The code gives a methodology to evaluate the response of bridge structures subjected to pedestrian loading. This methodology is shown in Figure 3.6.

The code gives two choices to the client, which are decisive for the design of the bridge. The client must decide what traffic class the bridge belongs to and what the comfort criteria for the bridge shall be. The traffic class describes the density of the pedestrian loading on the bridge and is divided in four classes ranging from urban bridges subjected to large crowds (Class I) to bridges in remote areas that are seldom used (Class IV). It means that if the owner selectsa lower class a more slim construction can be used to reduce the cost or ensure greater freedom of architectural design. However, a lower class increases the risk of people feeling uncomfortable due to strong acceleration, if the structure is densely loaded and exceeds the proposed limits

The comfort level is divided in four categories, three four acceptable and the last for unacceptable vibrations. For the maximum comfort criterion the vibrations should be practically imperceptible to the user, while for the minimum comfort criterion the vibrations may be perceived, but not become intolerant under seldom-occurring load configurations. The choice of the comfort level often depends on the location and population using the bridge. It is possible to be more demanding for sensitive users, such as schoolchildren, elderly or disabled people, and more tolerant in case of short footbridges.

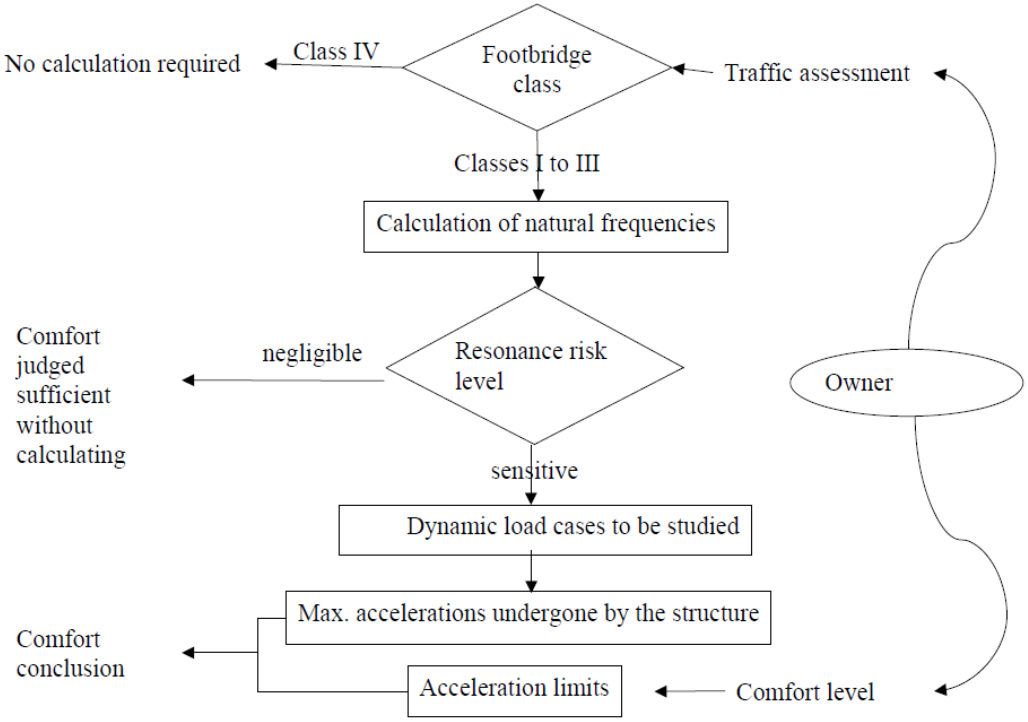

Figure 3.6 The design procedure as defined by Sétra (2006).

The comfort requirement level is linked to the accelerations of the bridge deck, which are determined though the different load cases as described in the following sections. Sétraassociates the allowable accelerations in terms of acceleration ranges instead of fixed values. These ranges are presented in Figure 3.7 for vertical vibration and Figure 3.8 for horizontal vibrations. The first three ranges correspond to the maximum, average and minimum comfort levels as described before and the last range is unacceptable and corresponds to uncomfortable acceleration levels.

	0	0.5	1.0	2.5 [m/s²]
Range 1	Max			
Range 2		Mean		
Range 3			Min.	
Range 4				Unaccept.

Figure 3.7 Comfort criteria for vertical vibrations. Described in acceleration ranges where Max, Mean and Min describes the comfort level.

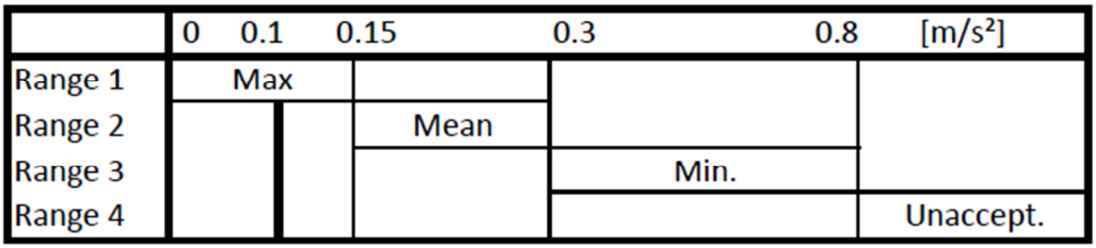

Figure 3.8 *Comfort criteria for horizontal vibrations. Described in acceleration ranges where Max, Mean and Min describes the comfort level. The limit at 0.1 m/s^2 corresponds to the limit if lateral lock-in can be expected.*

The natural frequencies of the structure in vertical-, lateral- and longitudinal direction are necessary to evaluate if the pedestrian bridge is subjected to intense traffic loads. The frequencies are determined for two mass assumptions, one is an empty bridge and the other one is a footbridge loaded throughout its bearing area with one pedestrian per square metre, each weighing 700 N. The risk of resonance is evaluated according to Figure 3.9 and Figure 3.10.

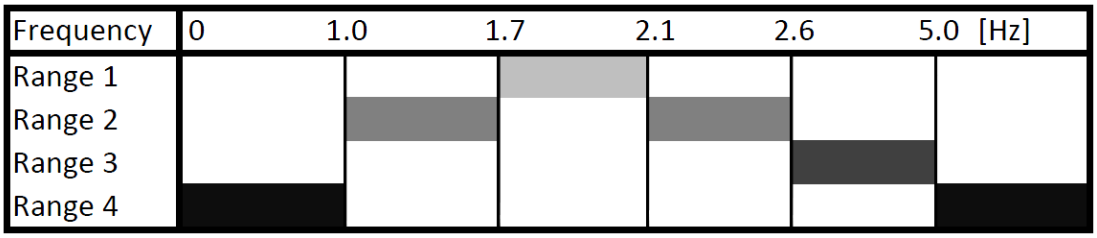

Figure 3.9 *Frequency range in Hz for vertical and longitudinal vibrations. Range 1 corresponds to maximum risk of resonance and Range 4 corresponds to negligible risk of resonance.*

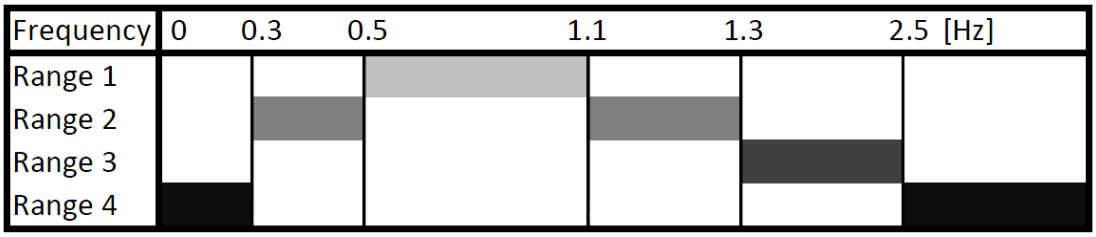

Figure 3.10 *Frequency range in Hz for lateral vibrations. Range 1 corresponds to maximum risk of resonance and Range 4 corresponds to negligible risk of resonance.*

3.3.1 Load application

The Setra group has done several crowd load calculations using probability calculation and statistical processing trying to understand how to represent a crowd in the best way. The simulations assumed that pedestrians move with random phases and frequencies. Each time assessing, the number of evenly distributed equivalent pedestrians, in phase and at the natural frequency of the bridge, which created the same response as the randomly distributed pedestrians.

The load need to be applied on the whole footbridge, and the sign of the force must always, at any point, be selected to produce the maximum effect to create the worst case for each vibration mode, as shown in Figure 3.4.

A number of 500 digital tests were repeated with a fixed number of pedestrians in different phases, fixed damping and a fixed number of mode antinodes. Then by repeating the tests with varying number of pedestrians, damping and mode antinodes. From this, the law of equivalent number of pedestrians in Equation (3.9) were retained.

$$N_{eq} = \begin{cases} 10.8\sqrt{N \times \zeta} & \text{for a sparse or dense crowd} \\ 1.85\sqrt{N} & \text{for a very dense crowd} \end{cases} \quad (3.9)$$

Where:

N Number of pedestrians

ζ Critical damping ratio

The combination between natural frequency and the traffic class of the footbridge will indicate if it is necessary to perform dynamic calculation to ensure the comfort and safety on the bridge. In Figure 3.11 the different load combinations for analysis depending on the traffic class are displayed. The three different load cases correspond to these crowd loadings:

- Case 1 – Sparse or densecrowd
- Case 2 – Verydensecrowd
- Case 3 – Complement for the 2nd harmonic effect

		Load cases to select for acceleration checks		
		Natural frequency range		
Traffic	Class	1	2	3
Sparse	III	Case1	Nil	Nil
Dense	II		Case 1	Case 3
Very dense	I	Case 2	Case 2	Case 3

Figure 3.11 Verification of traffic, load class and natural frequency (Sétra, 2006).

3.3.2 Load cases

Load case 1, which is applicable to category II and III and depicts groups of sparse and dense crowds, is given by Equation (3.10). The three different directions are not to be applied simultaneously and also the static weight of the pedestrians is not included in the equations since it does not give rise to accelerations. The static weight of the pedestrians, has to be included in the mass of the footbridge. Calculation including the pedestrians and calculations excluding them is necessary to get an upper and lower boundary of the frequency range. This also applies for load case 2 and 3.

$$w(t)=\begin{cases} d\times(280N)\times\cos(2\pi f_v t)\times 10.8\times(\zeta/n)^{1/2}\times\psi & \text{Vertical} \\ d\times(140N)\times\cos(2\pi f_v t)\times 10.8\times(\zeta/n)^{1/2}\times\psi & \text{Longitudinal} \\ d\times(35N)\times\cos(2\pi f_v t)\times 10.8\times(\zeta/n)^{1/2}\times\psi & \text{Horizontal} \end{cases} \quad (3.10)$$

Where

$w(t)$	Applied time-varying area-load applied as in Figure 3.4 [N/m²]
d	Density of the pedestrians, set to 0.8 pedestrians/m^2 for traffic class II and 0.5 pedestrians/m^2 for traffic class III
f_v	Natural frequency (Hz) of the vertical mode under consideration. Both mass assumptions are used
t	Elapsed time, in second
ζ	Critical damping ratio
n	Number of pedestrians on the footbridge ($n = S\times d$)
ψ	Minus factor, which makes allowance for the actual walking frequencies of a person and is displayed in Figure 3.12 and Figure 3.13
S	Surface area of the bridge deck

Load case 2 is only to be considered for bridges in traffic class I and is very similar to load case 1 and is supposed to describe a very dense crowd. The difference depends on how the equivalent number of pedestrians is calculated and on that the density of pedestrians is now set to 1.0 pedestrians/m^2. The applied load is given by:

$$w(t)=\begin{cases} 1.0\times(280N)\times\cos(2\pi f_v t)\times 1.85\times(1/n)^{1/2}\times\psi & \text{Vertical} \\ 1.0\times(140N)\times\cos(2\pi f_v t)\times 1.85\times(1/n)^{1/2}\times\psi & \text{Longitudinal} \\ 1.0\times(35N)\times\cos(2\pi f_v t)\times 1.85\times(1/n)^{1/2}\times\psi & \text{Horizontal} \end{cases} \quad (3.11)$$

Where all the notations are the same as in Equation (3.10).

Load case 3 considers the effect of the second harmonic caused by the crowd for either load case 1 or load case 2. The density of the pedestrian crowd is 1.0 pedestrians/m^2 for traffic class I and 0.8 pedestrians/m^2 for traffic class II. The magnitude of the force in Equations (3.10) and(3.11), are reduced down to 70 N in vertical-, 7 N in transversal- and 35 N in longitudinal direction. The minus factor, ψ, is also changed to reflect the contribution from the second harmonic. The new values for the forcing frequency, density and minus factor are then used in Equations(3.10) or (3.11), depending on the traffic class.

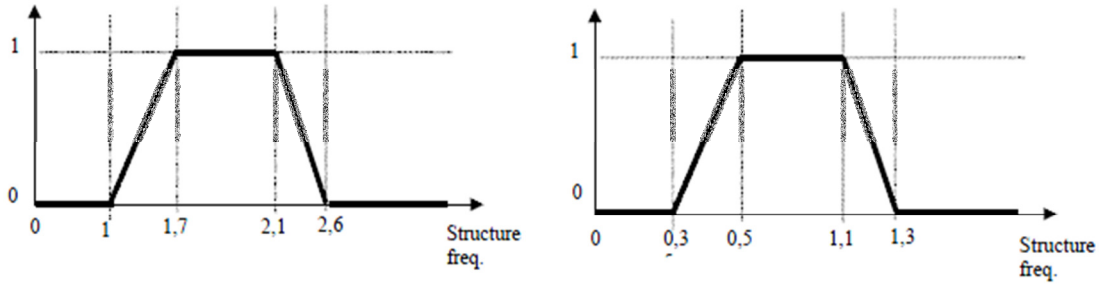

Figure 3.12 Relationship between the natural frequency of the investigated mode and the minus factor ψ for load case 1 and 2, corresponding to the first harmonic (Sétra, 2006).

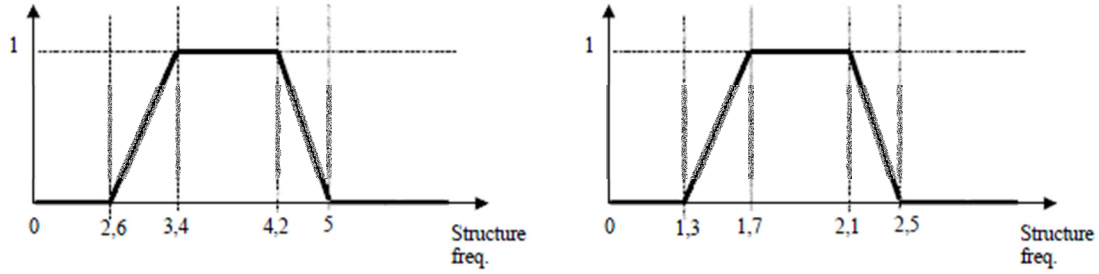

Figure 3.13 Relationship between the natural frequency of the investigated mode and the minus factor ψ for load case 3, corresponding to the second harmonic (Sétra, 2006).

3.4 Reliability of force models

Zivanovic, Pavic and Ingólfsson (2010) studied a pedestrian bridge in Reykjavik, Iceland and another in Podgorica, Montenegro. The bridge in Rekjavik was a 160 m continuous posttensioned concrete beam without any expansion joints in eight spans with a spiral shape in plan. The main span was 27.1 m, and the whole bridge had a 3.2 m wide deck with a varying thickness of 170 mm at the edges to 700 mm at the centreline. The bridge in Podgorica was 104 m, with a main span of 78 m between inclined columns. It was a steel box girder with longitudinal and transversal stiffeners and a composite concrete-steel slab on top.

On both bridges controlled tests were performed so it would be possible to model the same number of pedestrians in the force models. On the steel box bridge the damping were adjusted from 0.26% to 0.67% to better fit the measured response. This was done to take into account people standing on the bridge. The ISO 10137 is modelled as a point load crossing the bridge at a constant speed and both Sétra and UK NA are modelled as uniformly distributed loads. The relative error between the predicted and measured response is displayed in Table 3.3. The models tend to overestimate the response and Zivanovic, Pavic and Ingólfsson (2010) suggests some reasons for what this overestimation may come from. In EC 5 the avoidance from the assumed sinusoidal mode shape, the mulitplication factor, k, and the multiplication factor for multi person traffic are possible sources of error. The conservative multiplication factor for multi person traffic, $\sqrt{N}$, is proposed as the main possible source of error in ISO 10137. The report concludes that the simple procedures, such as ISO 10137 and EC5-2 are outdated due to oversimplification.

Table 3.3 *Relative error between measured and predicted accelerations on the posttensioned concrete- and steel box bridge (calculated as (predicted – measured)/measured). After Zivanovic, Pavic, and Ingólfsson (2010). A positive value means the response is overestimated in design.*

Model	Post-tensioned concrete	Steel box - empty	Steel box - Occupied
EC5	77%	69%	- 34%
ISO	261%	178%	69%
Sétra	26%	25%	-21%
UK NA – Stream	146%	59%	9%

Shahabpoor and Pavic (2012) studied the effect of people standing still on the bridge and how it affects the relationship between predicted and measured response. The study used the same measured response as Zivanovic, Pavic and Ingólfsson (2010) for the steel box bridge in Podgorica. A 10.8 m posttensioned concrete slab was cast and investigated in the laboratory. The slab had a width of 2.0 m and a depth of 275 mm. In addition to the uniformly distributed loads from Setra and UK NA (Stream) a group crossing the bridge is modelled with UK NA. All three models are calculated with a damping ratio corresponding to an empty and an occupied bridge. The results are presented in Table 3.4 as relative error. These tests also showed an overestimation of the result for random walking, but found that for the synchronous walking at the slab and on the steel box bridge were a better match. The study suggests this is due to a better match between assumption and the real life situation. It also concludes that the added damping from humans gave better results. Both studies urge the need to increase the knowledge on how walking and passive humans affect the response of bridges.

Table 3.4 Relative error between measured and predicted peak accelerations from two tests on an experimental slab and the Podgorica footbridge (calculated as (predicted – measured)/measured). After Shahabpoor and Pavic (2012). A positive value means the response is overestimated in design.

	Concrete slab – random frequencies		Concrete slab – synchronous walking		Steel box	
Model	Empty	Occupied	Empty	Occupied	Empty	Occupied
Sétra	877%	115%	263%	- 31%	45%	- 5%
UK NA – Group	773%	213%	276%	32%	194%	65%
UK NA – Stream	500%	7%	1 070%	46%	91%	24%

3.5 Analysis of comfort criteria

The three studied design guidelines in this chapter all give a limit for the maximum allowed vertical vibrations of the bridge deck. However, they have three different approaches to describe these. Eurocode 0 gives a strict limit of 0.7 m/s^2 no matter what the usage or location of the bridge. UK NA have factors, k_i, to account for different usage and location, which may give an acceleration limit varying between of 0.5 m/s^2 and 2.0 m/s^2. These limits can be selected by the designer to reflect the actual conditions of the bridge. Sétra gives the client a choice of comfort ranges, with associated acceleration limits. For maximum comfort the limit is 0.5 m/s^2, for medium comfort it is 1.0 m/s^2 and for minimum comfort 2.5 m/s^2. The comfort criteria for vertical vibrations from the different cods are visualised in Figure 3.14.

When it comes to lateral vibrations the codes also have different ways to portray the governing criterion. Eurocode 0 uses, as for the vertical vibrations a strict peak acceleration level, however two limits exists for the lateral vibrations, 0.2 m/s^2 for normal use and 0.4 m/s^2 for exceptional crowd loads. UK NA does not have any acceleration limit and is only concerned about lateral lock-in of a moving crowd. Whether this may be expected depends on the mass of the bridge, the damping ratio, the natural frequency in lateral direction and the mass of pedestrians on the bridge. A low frequency, damping ratio and mass of the bridge with a large mass of the crowd give a high risk of lock-in and the opposite gives a low risk. As for vertical vibrations Sétra uses acceleration ranges describing the comfort level together with peak horizontal acceleration. The limits for each range are: 0.15 m/s^2 for maximum comfort, 0.3 m/s^2 for mean comfort and 0.8 m/s^2 for minimum comfort. However, an absolute limit of 0.1 m/s^2 is set to avoid lateral lock-in for large crowds. The limits from Sétra and Eurocode are shown in Figure 3.15.

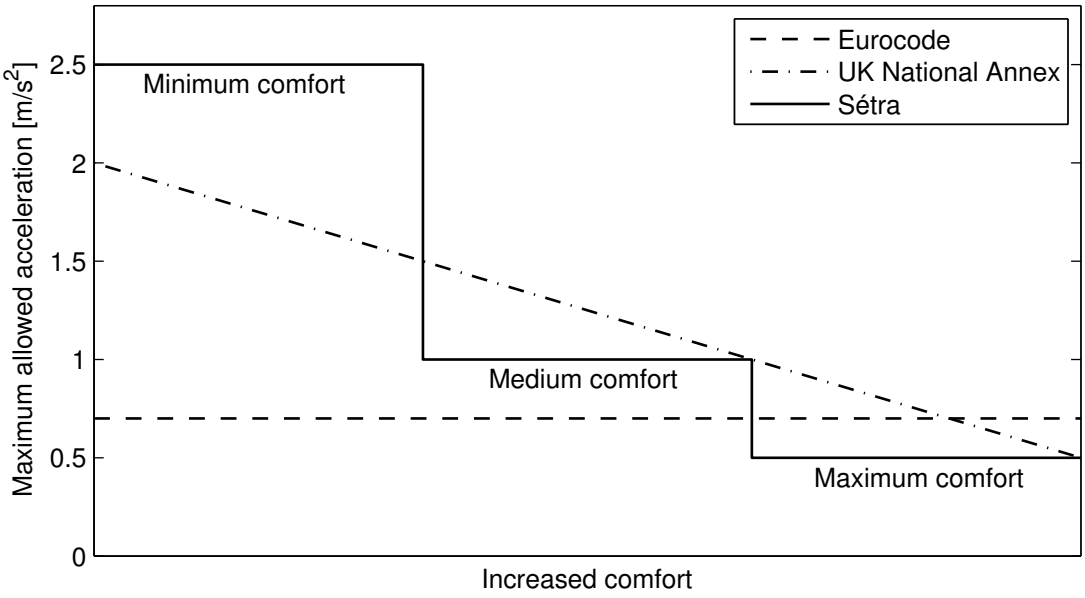

Figure 3.14 Vertical peak acceleration limits plotted against an increased comfort for the three different codes. The levels for UK NA are based on the maximum and minimum levels allowed for the vertical comfort criterion.

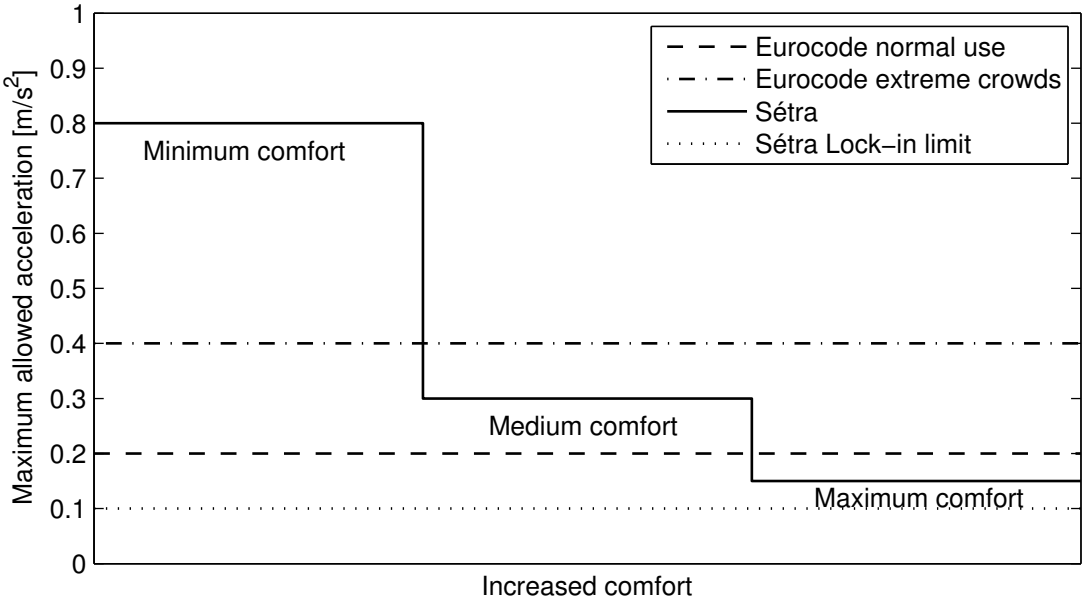

Figure 3.15 Lateral peak acceleration limits plotted against an increased comfort for Eurocode and Sétra.

3.6 Analysis of force models

EC 5-2 does not give a load to be applied, but the magnitude of the horizontal- and vertical peak accelerations depending on the natural frequency, mass of the bridge and damping ratio. UK NA and Sétra both apply the load as a uniformly distributed load with signs corresponding to the investigated mode and the natural frequency of

this mode is used as the frequency of the exciting force. The results of the model in UK NA are 44% less conservative than if using Sétra(Shahabpoor & Pavic, 2012).

In addition to this uniformly-distributed load, UK NA describes groups of pedestrians walking or running across the bridge. This is to be modelled with different group size, depending on the usage of the bridge, as a point load crossing the bridge. EC 5- 2 also has a case for running pedestrians.Sétra on the other side, considers it unnecessary due to the short time the runner disturbs the other pedestrians.

For all the models, the magnitude of the load to be applied depends on the natural frequency of the bridge. For EC 5-2, the highest vertical accelerations are reached for a natural frequency between 0 Hz and 2.5 Hz, and no calculations are necessary if the natural frequency is above 5 Hz. Sétra also gives an upper limit of 5 Hz, but also gives a lower limit 1 Hz for calculations for all bridges. If the bridge is in class III however, the upper limit for performing calculations is only 2.1 Hz. UK NA does not give any explicit limit of where calculations are needed, but by studying Figure 3.5 an upper limit of 8 Hz can be distinguished.

The effect of the first and second harmonic of the walking frequency is treated differently in Sétra and UK NA. Sétra gives a third load case, in addition to the ones stated in Equations (3.10) and (3.11), where the load is reduced to 25% of the original and with a minus factor favouring the frequency range of the second-, instead of the first, harmonic. The third load case however, could be omitted by introducing a modified minus factor, ψ_{mod}, for the whole frequency range as shown in Figure 3.16. An effect of the minus factors is that a natural frequency of 2.6 Hz gives a magnitude of 0 N for the load. However, the load will never be 0 N since calculations must be performed on both an empty and an occupied bridge which will give two different natural frequencies, and hence two different applied forces, for the same mode. UK NA uses the same reference load over the whole frequency spectrum, but with the reduction factor in Figure 3.5, which has two peaks matching the harmonics of normal walking.

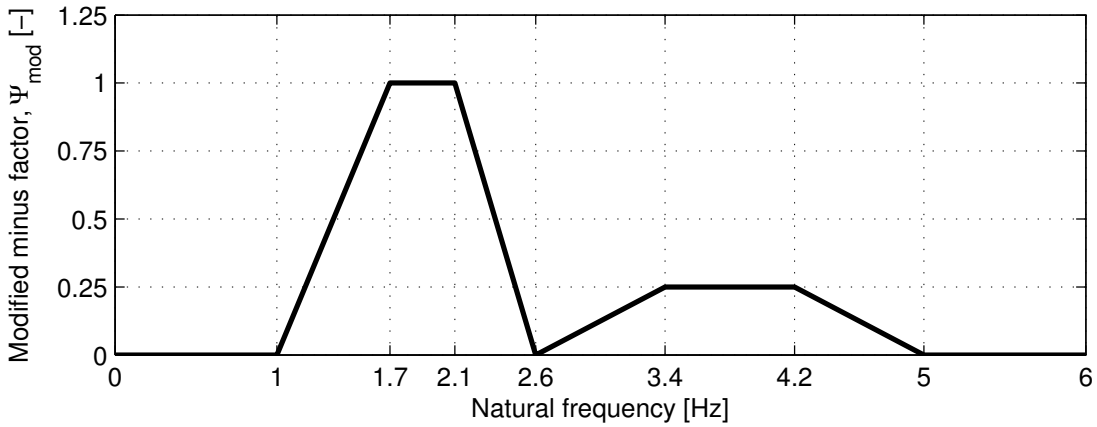

Figure 3.16 Modified minus factor, ψ_{mod}, for the applied load in Sétra, applicable for the whole frequency range of the bridge.

4 Damping

Damping describes how good the energy dissipation in a vibrating structure is. All structures possess some kind of capability to absorb and dissipate energy pulses (Živanović, Pavić, & Reynolds, 2005), and the beneficial importance of damping is that it lowers the structures response to a dynamic excitation near the resonance frequency of the structure (SIS, 2008).

When talking about damping there are several mechanisms acting on and in a structure that can dissipate energy. These mechanisms can be divided into two groups. The first mechanism is called dissipation, and it includes all the dissipated energy within the structure such as through bolts, welds, paving and joints. The second mechanism is called dispersion, and propagates energy away from the structure. These two mechanisms determine the overall damping of the structure and is in practice measured as the structural damping (Živanović, Pavić, & Reynolds, 2005).

The amount of damping depends in general on the level of vibration. Large vibration amplitude causes more friction between non-structural and structural elements. The co-existence of the mentioned mechanisms within the structure makes damping a complex phenomenon (Heinemeyer et al., 2009). The damping of a structure cannot be fully predicted or calculated exactly before the real structure is built. Experience from similar structures can give an approximate value of the damping. But the only way to determine the actual damping is to perform measurements on the operational structure (SIS, 2008). Sétra (2006) urges that it is important not to overestimate the structural damping.

4.1 Damping in design guidelines

Design guidelines often give a damping ratio to be used in the design of bridges. Damping ratios specified for four different codes are presented in Table 4.1 for the service state. Noteworthy is that the damping ratio specified in Eurocode for timber can be found in Eurocode 5 – part 2 and is 1.0% if no mechanical joints are present and 1.5% if mechanical joints are present (SIS, 2004). Damping ratios for the rest of the material can be found in Eurocode 1 – part 2, and if the spans are shorter than 20 m, they may be increased by a factor related to the length of the span (SIS, 2003).

For large amplitude vibrations, which may occur during earthquakes or intentional loads the damping ratio increases significantly. For large amplitude vibrations, only Eurocode has any values given, which can be found in Eurocode 8 – Part 2 (CEN, 2005) and are originally intended for earthquake design. However, both JRC and Sétra refer to this part of Eurocode regarding design for large amplitude vibrations. The damping ratio for large amplitude vibrations according to Eurocode is given in Table 4.2.

Table 4.1 Damping ratios for different materials for serviceability conditions from European Commission, Joint Research Centre (Heinemeyer et al., 2009), the International Federation for Structural Concrete (as cited in Sétra, 2006),Eurocode(SIS, , 2003),(SIS, 2004) and ISO 10137 (SIS, 2008), Sétra (2006)

	JRC		CEB/fib		EC	ISO	Setra
Material	Min. ζ	Ave. ζ	Min. ζ	Ave. ζ	ζ	ζ	ζ
Reinforced concrete	0.8%	1.3%	0.8%	1.3%	1.5%	0.8%	1.3%
Prestressed concrete	0.5%	1.0%	0.5%	1.0%	1.0%	0.8%	1%
Composite steel-concrete	0.3%	0.6%	0.3%	0.6%	0.5%	0.6%	0.6%
Steel	0.2%	0.4%	0.2%	0.4%	0.5%	0.5%	0.4%
Timber	1.0%	1.5%	1.5%	3.0%	1.0% / 1.5% [a]	-	1%
Stress-ribbon	0.7%	1.0%	-	-	-	-	

[a] 1.0% if no mechanical joints are present, 1.5% otherwise

Table 4.2 Damping ratio according to construction material for large amplitude vibrations according to European Commission, Joint Research Centre (JRC) (Heinemeyer et al., 2009), Sétra, (2006) and Eurocode 8 – Part 2 (CEN, 2005).

Material	Damping ratios according to Eurocode
Reinforced concrete	5%
Prestressed concrete	2%
Steel, welded joints	2%
Steel, bolted joints	4%

4.2 Influence of asphalt pavement

Several papers have shown that timber bridges with asphalt pavement have a higher damping ratio than bridges without. For example, out of 19 timber bridges, the bridges without asphalt pavement had a damping ratio varying between 0.23% and 1.35%. Bridges with asphalt pavement on the other hand had a damping ratio from 1.13% to 3.37%. And when adding asphalt on a 20 m timber bridge in the laboratory, the damping ratio increased significantly (Schubert et al., 2010).

Schubert et. al. (2010) studied the influence of asphalt pavement on two timber bridges; a cable-stayed bridge and a shorter simply-supported bridge. In addition decks made from both cross-laminated timber and a stress-laminated plate were tested. On the simply-supported bridge the damping ratio increased as much as 10 times, while at the cable-stayed bridge it increased with 4-5 times when asphalt pavement was added. The tests were performed at room temperature, but FE simulations indicate that the damping will change at extreme temperatures. Low temperatures give a significantly lower damping ratio, while high temperatures only give a small increase of the damping. This however, the study says, has to be verified by measurements at different temperatures.

4.3 Influence of humans

The human body is very sensitive to vibrations due to its biological structure and biodynamic actions. This leads to large interactions with a vibrating structure. How people influence the damping behaviour of a structure cannot be predicted before construction. Tests and studies on the topic have recently been made (Shahabpoor & Pavic, 2012).

Three different research groups, presented in this section, have independent from each other conducted several tests to study how the damping varies in a structure exposed to different loading situation. This makes it possible to see how the difference in damping varies between an empty structure, a structure with passive people and a structure with active people.

Shahabpoor and Pavic (2012), studied a simply-supported, in-situ cast and post-tensioned concrete slab in the laboratory at the University of Sheffield. Measurements of the damping of the slab were made for the first two vertical modes. The result showed that if the slab was occupied with people the damping ratio was almost twice as big for the two first modes. In Table 4.3 all values of the damping ratio is presented for the first two vertical modes.

Table 4.3 Experimental results of the damping ratio, ζ, for the empty slab and for the occupied slab, after Shahabpoor and Pavic (2012).

Mode	Empty Slab ζ	Occupied Slab ζ	Increase ratio
1	0.98%	1.71%	1.74
2	0.61%	1.17%	1.92

Similar experiences were made by Pedersen (2012), when accelerometers were attached and moved around on a sport hall floor to determine the natrual freqeuncy and the corresponding damping ratio of the empty floor. To aqcuire experience on how the damping ratio changes due to the number of passive people, five tests were carried out with different number of people standing on the floor. The results from the tests is shown in Table 4.4.

Table 4.4 Values of the damping ratio for a sport hall floor with different number of passive people,afterPedersen (2012).

People	0	2	4	5	10	15
Damping ratio ζ	1.24%	1.33%	1.36%	1.40%	1.56%	1.71%
Increase ratio	1.0	1.07	1.10	1.13	1.26	1.38

Another labratory test was performed by Wang et al. (2011). A small, light timber beam, supported by steel shutter at the ends, was exposed vibrations by an electric shaker placed in the middle of the beam. The natural frequency and corresponding damping ratio was measured for an empty beam, a beam with a passive pedestrian and finally a beam with a slight more active pedestrain. The observations from the test are presented in Table 4.5.

Table 4.5 Damping ratio for a light timber beam, after Wang et. al. (2011).

	Damping ratio	Increase ratio
Empty beam	0.6%	1.0
Passive pedestrian	11.4%	19
Slightly active pedestrian	8%	13.3

4.4 Analysis of damping

Design guidelines give damping ratios to be used in design of around 1% for the most common materials. These ratios are usually given for pure materials and when they are used in a bridge, non-structural elements tend to influence and in general increase the damping ratio. Asphalt paving for instance, has been shown to sometimes give a significant increase in the damping, however this influence have been shown to be temperature dependent and are not yet ready to be applied in design. The interaction between the structure and humans is an area where some research have been performed, and it is apparent that when people are standing still on the structure an increase in the damping may be expected. However, moving pedestrians does not contribute as much to the damping.

5 Case studies and modelling

This chapter describes the structural system of the studied bridges and how they have been modelled in BRIGADE/Plus to describe the reality as good as possible. The chapter ends by describing how the force models in the design guidelines have been interpreted and modelled.

5.1 Modelling procedure

The modelling procedure followed these five steps:

1. FE modelling to determine mode shapes and natural frequencies
2. Field measurements
3. Refining of original FE models to reflect reality
4. Model according to design guidelines
5. Application of loading according to design guidelines

The models constructed in Step 1, before the field measurements, were necessary to understand the behaviour of bridgesin the form of natural frequencies and corresponding mode shapes. The mode shapes were necessary to know for two main reasons. First, the measuring equipment was only able to collect data from four channels, which means only four points could be measured simultaneously. Hence, the points needed to be selected carefully to be able to capture a good response. The second reason was to know where to apply the external force on the bridge to induce the maximum response of the structure. The models in this phase were basedon the drawings of the bridges.

Description of the field measurements can be found in Chapter 6, while the results can be found in Chapter7. In Step 3, the models were refined by adjusting mass, stiffness and boundary conditions to reflect the measured properties of the bridges. Section 5.5 describes how the relevant force models used in Step 5 are interpreted and applied to the bridges.

5.2 The steel truss bridge in Anneberg

The steel truss bridge in Anneberg with a span of 27 m, see Figure 5.1, is located 20 minutes south of Gothenburg and passes over the highly traffic railway between Gothenburg and Copenhagen. A road is located on the west side of the bridge and on the east side a big stable and a couple houses.

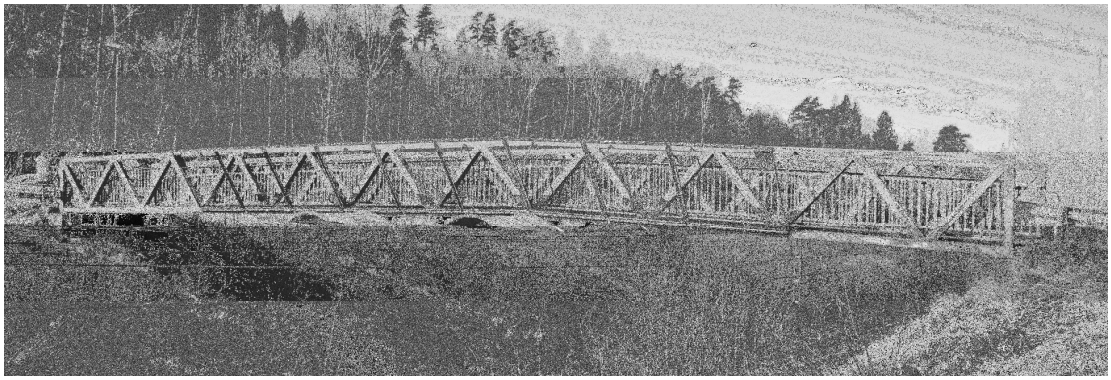

Figure 5.1 Perspective view of the steel truss bridge.

5.2.1 Structural system

The bridge is a truss bridge made of steel. The main frame structural elements are hollow rectangular steel profiles with dimensions of 150x150 mm with a thickness varying between 5 and 10 mm. The bridge deck is a 10 mm thick steel plate attached to the transversal end beams with two bolts to each beam, as seen in Figure 5.2 and Figure 5.3. Railings are fixed along the trusses on each side of the deck. Outside the trusses, a safety fence is fastened to the trusses to protect the overhead line. On all four supports, the bearings are the same and consist of two bolts connected to the concrete foundation, as seen in in Figure 5.3. The truss framework is fixed into the concrete foundation on each side.

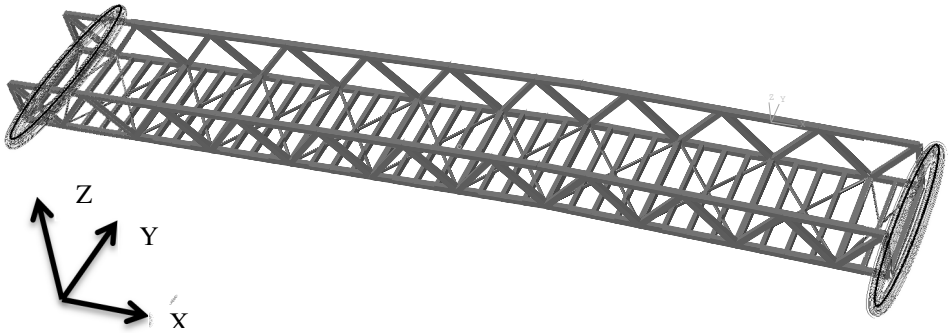

Figure 5.2 *FE model of the steel truss bridge. The end beams where the steel deck is attached are highlighted.*

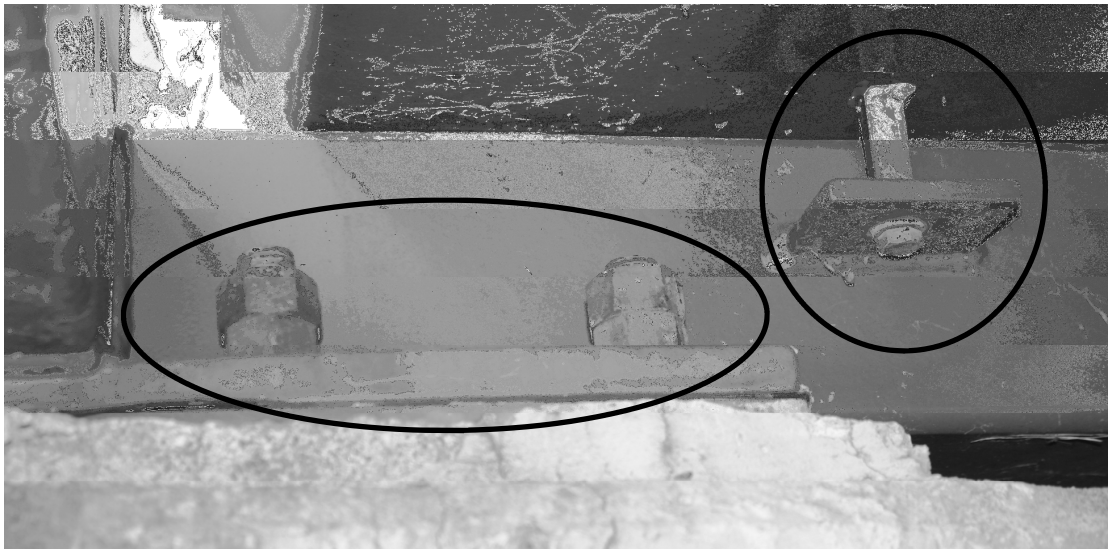

Figure 5.3 *The transversal end beam (highlighted in Figure 5.2), with the bolted connection to the steel deck highlighted to the right, and the bridge's bearing highlighted to the right.*

5.2.2 Structural model

The trusses are modelled as beam elements and are connected together in centre-to-centre points, see Figure 5.2. The assumption was made that the steel deck did not influence the vertical stiffness. The deck was modelled as a horizontal cross bracing with the same stiffness and Poisson's ratio as the steel beams but with a negligible weight to increase the lateral stiffness.The mass of the deck and the epoxy layer on top was modelled as a non-structural mass added to the transversal beams. The material properties used in the FE model are presented in Table 5.1.

The boundary condition of the left end (according to Figure 5.2) of the bridge was locked in xyz-direction in one corner and in xz-direction in the other corner. On the right side the first corner was locked in z-direction and the second corner was locked in yz-direction.

Table 5.1 Material properties of the steel truss bridge usedbefore field measurements.

Material	Steel	Epoxy
FE elements	Beam	-
Approximate mesh size [m]	0.33	-
Density	7850 kg/m^3	10 kg/m^2
Young's modulus [GPa]	210	-
Poisson's ratio	0.3	-

The field measurements did not match the calculated natural frequency. The FE model was calibrated and reconstructed to reflect the real behaviour of the bridge. The assumption that the steel deck did not contribute to the stiffness was proven wrong.Hence, the steel deck was attached to the transversal beams of the bridge with full interaction between the deck and the beams. The deck was modelled with shell elements with a thickness of 10 mm andthe material properties of the deck were the same as for the beams, see Table 5.1. The weight from the outside safety fence was excluded at first but calibrated as a mass of 55 kg/m acting along the bottom. The epoxy layer was neglecteddue to its limited thickness. .

To test the bridge according to the different force models in Section 5.5a third model was created. This time, the material parameters were taken from Eurocode. This model was almost the same as the model used before the field measurements. The changes were the safety fence and change in the material parameters, according toTable 5.2.The same boundary conditions, geometry and elements as in the previous model were used.

Table 5.2 Material parameters of the steel bridge according to force models the material parameters are according to Eurocode. The damping ratio is according to Eurocode, Setra and ISO.

The steel bridge	Eurocode / Setra / ISO
FE elements trusses	Beam
Approximate mesh size truss [m]	0.33
Youngs modulus steel [GPa]	210
Density steel [kg/m^3]	7850
Density safety fence [kg/m^2]	100
Damping ratio steel	0.5% / 0.4% / 0.5%

5.3 The box-beam bridge in Kristinehamn

The box-beam bridge in Kristinehamn, called Stolpen, can be seen in Figure 5.4 and spans 33 m over the highway E18, which goes from Oslo to Stockholm. A bus stop is located on the north side of the bridge and an elementary school 500 m from the south end of the bridge.

Figure 5.4 Stolpen bridge, spanning over the motorway E18, between Oslo and Stockholm. Photo: Carl Westerlund

5.3.1 Structural system

The bridge is simply-supported with a vertical radius of 250 m and has a span of 33 m. The bridge has an arched shape and is constructed with glulam of quality L40c.

Dimensions of the cross section can be seen in Figure 5.5. The bridge has railings on both sides and they are bolted into the box with two bolts. On top of the walkway isan 80 mm layer of asphalt.The end supports are resting on a large concrete foundation.

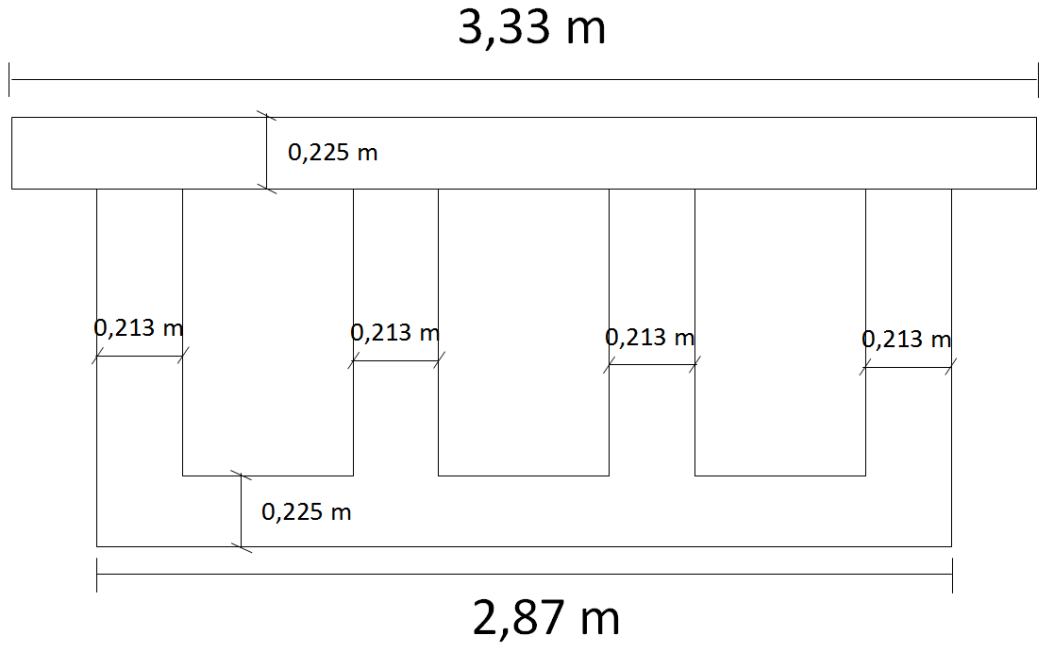

Figure 5.5 Cross sectionand dimensions of the box-beam made of glulam.

5.3.2 Structural model

The bridge is modelled seen inFigure 5.6 with shell elements. The railings and the asphalt on the bridge are assumed not to influence the stiffness of the bridge. The 80 mm thick asphalt layer is modelled as a non-structural mass with of 195 kg/m^2 added to the top flange. The railings are modelled as a non-structural mass applied on the top flange on the area outside of web.

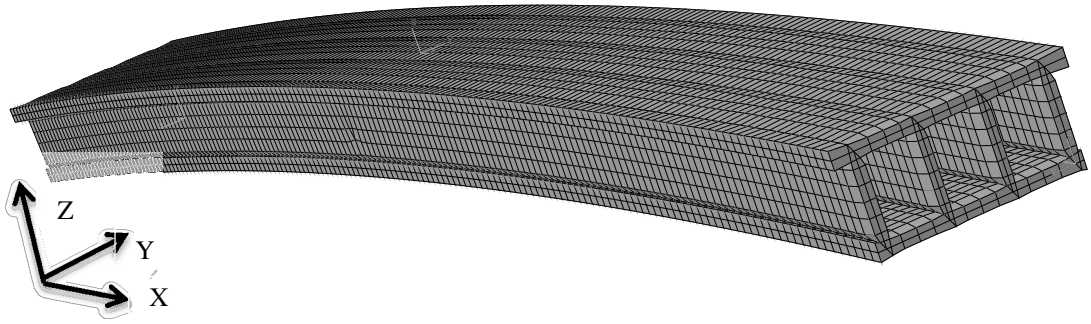

Figure 5.6 FE model of the box-beam bridge.

The bridge was locked in xyz-direction along the end of the bottom flange at the left side (according to Figure 5.6) and yz-direction at the right side. The material properties used in the model are presented in Table 5.3.

On this bridge, even the static response was tested, by measuring the vertical displacement caused by a heavy vehicle. To calibrate the model the following

changes were made. First of all the model was divided in two different models, onestatic and one dynamic. The boundary conditions were also changed, in reality the bridge was simply-supported on rubber bearings in both ends. With the new boundary conditions, the bridge was locked in yz-direction at both ends. The x-direction at both ends was modelled as "Spring-to-ground" with a stiffness of 77 MN/m. The new boundary conditions are shown in Figure 5.7. The material properties were changed in the two different models according to Table 5.4.

Table 5.3 Material properties for the box-beam before field measurements, (Johansson, 2011)

Material	Glulam
FE elements	Shell
Approximate mesh size [m^2]	0.2x0.2
Density [kg/m^3]	500[2]
Young's modulus $E_{0,mean}$[GPa]	13
Young's modulus $E_{90,mean}$ [GPa]	0.41
Shear modulus $G_{90,mean}$ [GPa]	7.6
Shear modulus $G_{0,mean}$ [GPa]	12.75
Poisson's ratio	0
Spring-to-ground stiffeners [MN/m]	-
Damping ratio	-

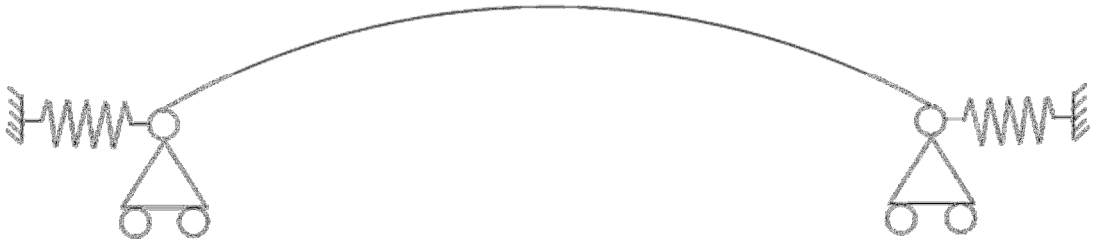

Figure 5.7 Refined boundary conditions of the box-beam.

[2]Peter Jacobsson, Martinssons Trä AB, [Personal Communication], 12.03.2013

Table 5.4 Material parameters in refined model of the box-beam.

Design model	After	
Type of model	Dynamic	Static
Material	Glulam	Glulam
FE elements	Shell	Shell
Approximate mesh size [m^2]	0.2x0.2	0.2x0.2
Density [kg/m³]	500[3]	500[4]
Young's modulus $E_{0,mean}$[GPa]	13	10.8
Young's modulus $E_{90,mean}$ [GPa]	0.41	0.41
Shear modulus $G_{90,mean}$ [GPa]	7.6	6.33
Shear modulus $G_{0,mean}$ [GPa]	12.75	6.33
Poisson's ratio	0	0
Spring-to-ground stiffeners [MN/m]	77	77
Damping ratio	-	-

The third model was used to model the design guidelines, and modelled with material properties according to Table 5.5, and had the boundary conditions of the refined model.

[3]Peter Jacobsson, Martinssons Trä AB, [Personal Communication], 12.03.2013
[4]Peter Jacobsson, Martinssons Trä AB, [Personal Communication], 12.03.2013

Table 5.5 Material properties for the box-beam bridge according to the different force models (Johansson, 2011)

	Eurocode / Sétra / ISO
FE elements	Shell
Approximate mesh size [m^2]	0.2x0.2
Young's modulus Glulam, L40c [GPa]	13
Shear modulus L40c [GPa]	7.6
Density Glulam L40c [kg/m^3]	400
Poisson's ratio	0
Spring-to-ground stiffeners [MN/m]	77
Damping ratio	1.0%

5.4 The multi-span bridge in Mariestad

The multi-span bridge in Mariestad is called Ekudden and is a five span bridge crossing the river Tidan, and can be seen in Figure 5.8. The bridge connects two residential areas with the main city.

Figure 5.8 Ekudden Bridge in Mariestad, crossing the river Tidan.

5.4.1 Structural system

The bridge has a continuous stress laminated glulam deck of quality L40h on six concrete supports. The length of the bridge is 103.4 m. The timber deck has a size of 4.06x0.495 m. It is symmetric and has two balconies, see Figure 5.9, on the two supports closes to the river banks. On top of the glulam deck is a thin insulation mat and an 80 mm layer of asphalt. Along the bridge, the railings are mounted into the side of the deck.

Figure 5.9 One of the balconies on the multi-span bridge.

5.4.2 Structural model

The bridge is modeled with shell elements. It is symmetric, with six supports and two balconies, see Figure 5.10. The balconies are modeled with beam elements and are tied to each other with the TIE command in BRIGADE/Plus. The base beams of the balconies are then tied to the main deck to achieve full interaction with the timber shell elements.

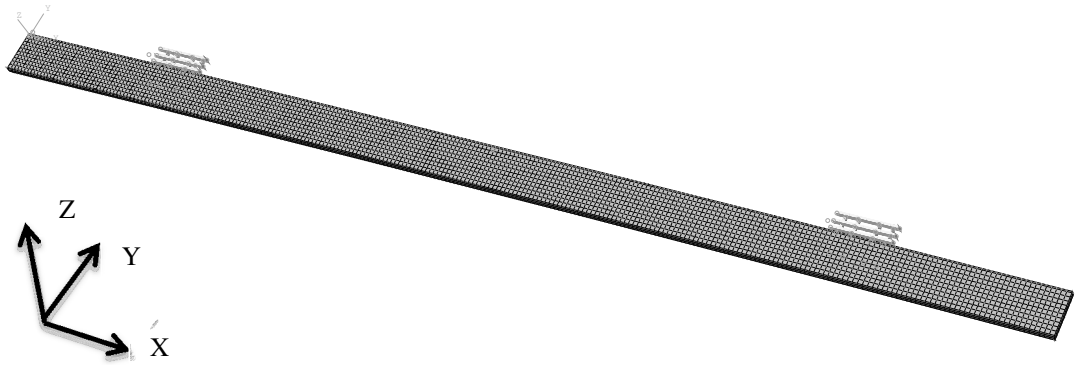

Figure 5.10 FE model of the multi-span bridge in Mariestad

The bridge has five span and six supports. The middle support is locked in xyz-direction and the five remaining supports are locked in yz-direction. The material properties are presented in Table 5.6.

Table 5.6 Material properties for the multi-span bridge before field measurements (Johansson, 2011)

Material	Glulam
FE elements	Shell
Approximate mesh size [m^2]	0.4x0.4
Density [kg/m³]	500
Young's modulus $E_{0,mean}$[GPa]	13.7
Young's modulus $E_{90,mean}$ [GPa]	0.46
Shear modulus $G_{90,mean}$ [GPa]	8.5
Shear modulus $G_{0,mean}$ [GPa]	12.75
Poisson's ratio	0
Damping ratio	-

The railings along both sides were modelled as a non-structural mass of 367.4 kg/m^2 added to the outer 120 mm of the bridge deck. The asphalt was modelled on the rest of the bridge deck with a weight of 195 kg/m^2. The balconies were only model as beams but all the material above the beams are modelled as non-structural masses on top of the three balcony beams.

For the calibration of the FE model, the following changes were made. The weight of the timber was changed to 470 kg/m^3 and the rest of the material properties were left unchanged[5]. The railing on both long side of the bridge was only modelled as masses but when the refinement was made. The top part of the railing was modelled as solid beam elements at a constant vertical distance from the deck and was attached to the deck using the TIE command. The command gives 100% interaction with the deck. Therefore, the young modulus of the timber in the railing was determined to be 1.7 GPa to match the measured natural frequencies.

The last FE model was the one to be used for the calculations of the dynamic design. All geometry and element types were the same as in the pre-measurements model. The material properties were changed according to Table 5.7.

[5]Erik Johansson, Moelven Töreboda AB, [Personal Communication], 12.03.2013

Table 5.7 Material properties of the multi-spanbridge according to different force models (Johansson, 2011)

	Eurocode / Sétra / ISO
Young's modulus Glulam, L40h [GPa]	13.7
Shear modulus L40h [GPa]	0.85
Density Glulam L40h [kg/m^3]	430
Damping ratio timber	1.0%

5.5 Force models

This section describes how the force models from UK NA, Sétra and ISO 10137 are interpreted and applied in the FE software BRIGADE/Plus

5.5.1 Eurocode 5-2

Hand calculations according to EC 5-2 were performed with equation (3.1) and (3.2). The mass and natural frequencies and damping ratios used were taken from the FE models according to Eurocode for each bridge. The calculations can be found in Appendix D. Eurocode 5-2 is only valid for simply-supported bridges, hence only the longest span on the multi-span bridge was calculated while being assumed to be simply-supported.

5.5.2 UK National Annex

All three bridges are assumed to be in bridge class B, which means they are situated in a "*suburban location likely to experience slight variations in pedestrian loading intensity on an occasional basis"*(BSI, 2008, pp. 25). UK NA givesforce models for both group crossings and under crowded conditions where a continuous stream of pedestrians is crossing the bridge. Only the crowded conditions were modelled in this thesis with a crowd density, ρ, of 0.4 pedestrians/m², as given for bridge class B. The crowded conditions were modelled with Equation (3.8) as uniformly-distributed load with directions according to Figure 5.11.

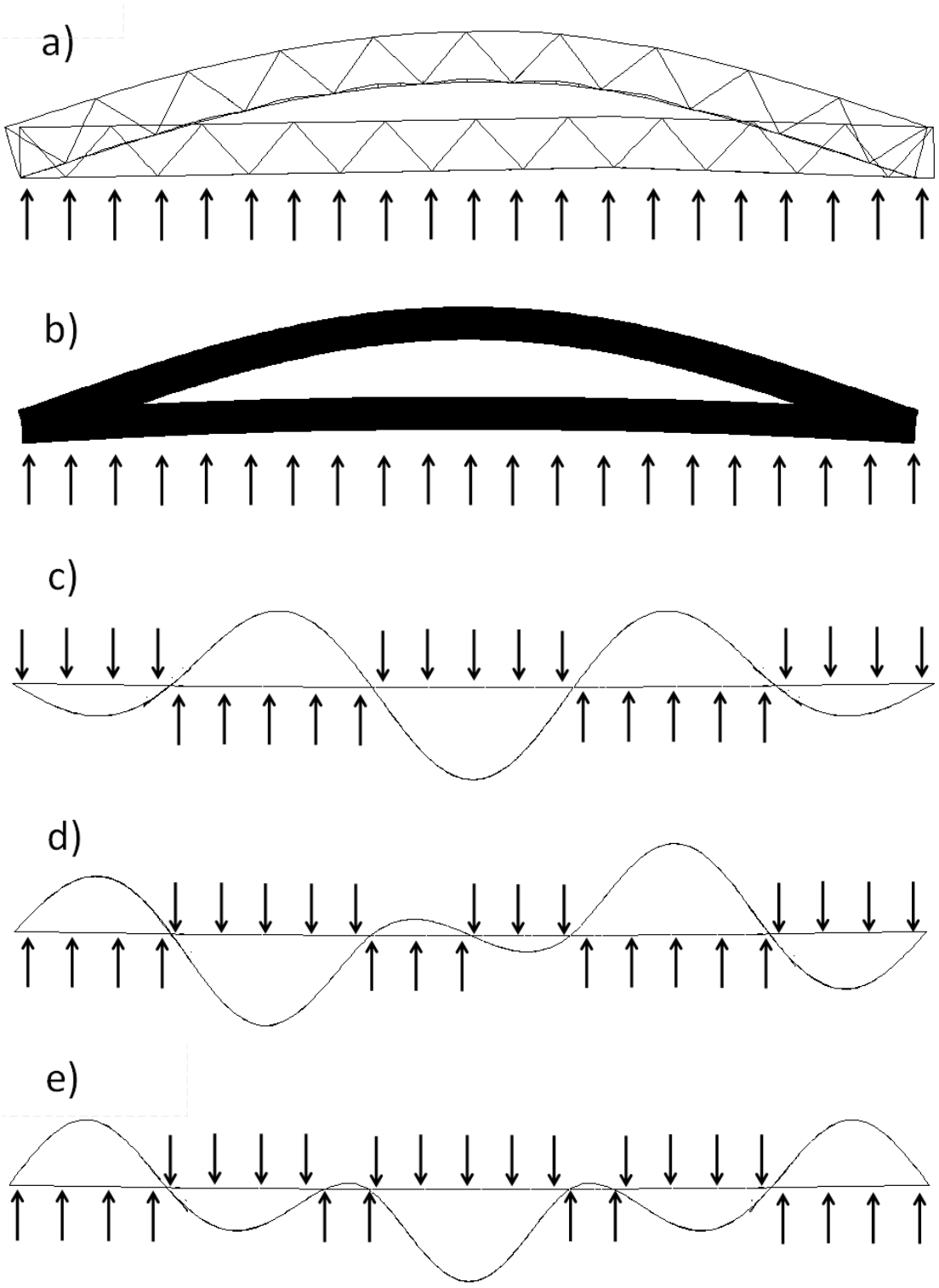

Figure 5.11 Direction of the applied loads for the three bridges and their relevant mode shapes. a) Steel truss bridge, b) Box-beam bridge, c) Multi-span bridge first mode, d) Multi-span bridge second mode and e) Multi-span bridge third mode.

The mode shape also influences the applied load for each span based on the effective span length, S_{eff}, which was approximated according to Figure 5.12. For the multi-span bridge, which have different span lengths and where the influence of mode shapes differ each span have a different load applied to it.

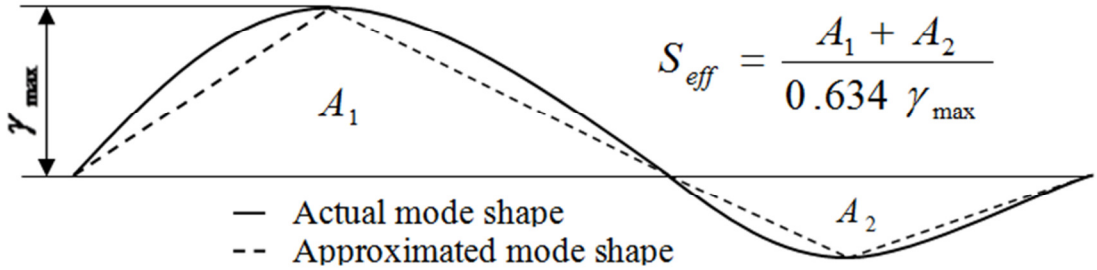

Figure 5.12 Approximation of mode shapes used to calculate S_{eff}.

The applied load for all bridges can be seen in Table 5.9. On the box-beam- and the multi-span bridge, the area load could be applied directly to the shell elements, while at the steel bridge the load were applied as line loads on the transversal beams. The load was applied in time domain as a harmonic load with the natural frequency of the investigated mode as forcing frequency until steady state response was reached.

The comfort criteria according to UK NA were calculated from response modifiers related to location, usage and height of the structures. All bridges were, as earlier stated, assumed to be in a suburban location and all are the primary route, but have different routes available. The multi-span bridge is lower than 4 m, while the other two are between 4 and 8 m gives only one different response modifier. The allowable peak acceleration and the response modifiers use to calculate it is shown in Table 5.8.

Table 5.8 Values for the response modifiers, k_i, and the limiting accelerations according to UK NA.

	k_1	k_2	k_3	k_4	a_{lim} [m/s^2]
Steel	1.3	1.0	1.0	1.0	1.3
Box-beam	1.3	1.0	1.0	1.0	1.3
Multi-span	1.3	1.0	1.1	1.0	1.43

Table 5.9 The amplitude of the applied load for UK NA.

Bridge, mode and span	Applied Load
Steel truss bridge	2.98 N/m [a]
Box-beam	7.01 N/m^2
Multi-span	
Mode 1	
Span 1 and 5	14.54 N/m^2
Span 2, 3 and 4	12.90 N/m²
Mode 2	
Span 1 and 5	12.21 N/m²
Span 2, 3 and 4	10.84 N/m²
Mode 3	
Span 1 and 5	4.07 N/m²
Span 2 and 4	4.00 N/m^2
Span 3	3.61 N/m^2

[a] Applied load per meter on the transversal beams

5.5.3 Sétra

All three bridges are assumed to be in Class III, which means a "*footbridge for standard use, that may occasionally be crossed by large groups of people but that will never be loaded throughout its bearing area"*(Sétra, 2006, pp. 31). According to Figure 3.11 for frequency range 1 (1.7 Hz < f_v < 2.1 Hz) load case 1 (Equation (3.10)) was used and for frequency range 2 and 3 (1.0 Hz < f_v < 1.7 Hz and 2.1 Hz < f_v < 5 Hz) load case 3 were used, both with a crowd density, d, of 0.5 pedestrians/m². Calculations are performed on an empty bridge and on a bridge occupied by d =0.5 pedestrians/m², the difference being the forcing frequency and the minus factor affecting the applied load. Calculations are performed in range 2 and 3 for comparison even though it is not necessary for Class III bridges. The applied load for all bridges can be seen in Table 5.10.

As for UK NA, the load was modelled as uniformly distributed load with directions according to the direction of the relevant mode shapes in Figure 5.11. The box-beam bridge and the multi-span bridge and line loads at the steel truss bridge. Even here the

load was applied in time domain as a harmonic load with the natural frequency of the investigated mode as forcing frequency until steady state response was reached.

The comfort criteria were selected according to Table 5.11 to reflect the location and usage of the bridges. The steel truss bridge was located in a remote location and was hence given the minimum comfort requirement. The box-beam- and the multi-span bridge were deemed to have denser traffic and sensitive pedestrians and were hence given the medium comfort requirement.

Table 5.10 The amplitude of the applied load for the Sétra load model.

Bridge, mode and span	Load case	Applied load
Steel truss (empty)	3	2.43 N/m [a]
Steel truss (occupied)	3	1.51 N/m [a]
Box-beam (empty)	3	5.49 N/m^2
Box-beam (occupied)	3	5.49 N/m²
Multi-span		
Mode 1 (empty)	1 (Sparse crowd)	10.76 N/m²
Mode 1 (occupied)	1 (Sparse crowd)	10.76 N/m^2
Mode 2 (empty)	1 (Sparse crowd)	3.51 N/m²
Mode 2 (occupied)	1 (Sparse crowd)	3.51 N/m^2
Mode 3 (empty)	3	1.74 N/m²
Mode 3 (occupied)	3	1.74 N/m^2

[a] Applied load per meter on transversal beams

Table 5.11 Comfort criteria for the three studied bridges according to Sétra.

	Comfort range	Maximum accelerations [m/s^2]
Steel truss	Minimum	2.5
Box-beam	Medium	1.0
Multi-span	Medium	1.0

5.5.4 ISO 10137

ISO 10137 was modelled as the concentrated force in Equation (5.1) applied at the centreline of the walkway, according to Figure 5.13 for the three bridges.

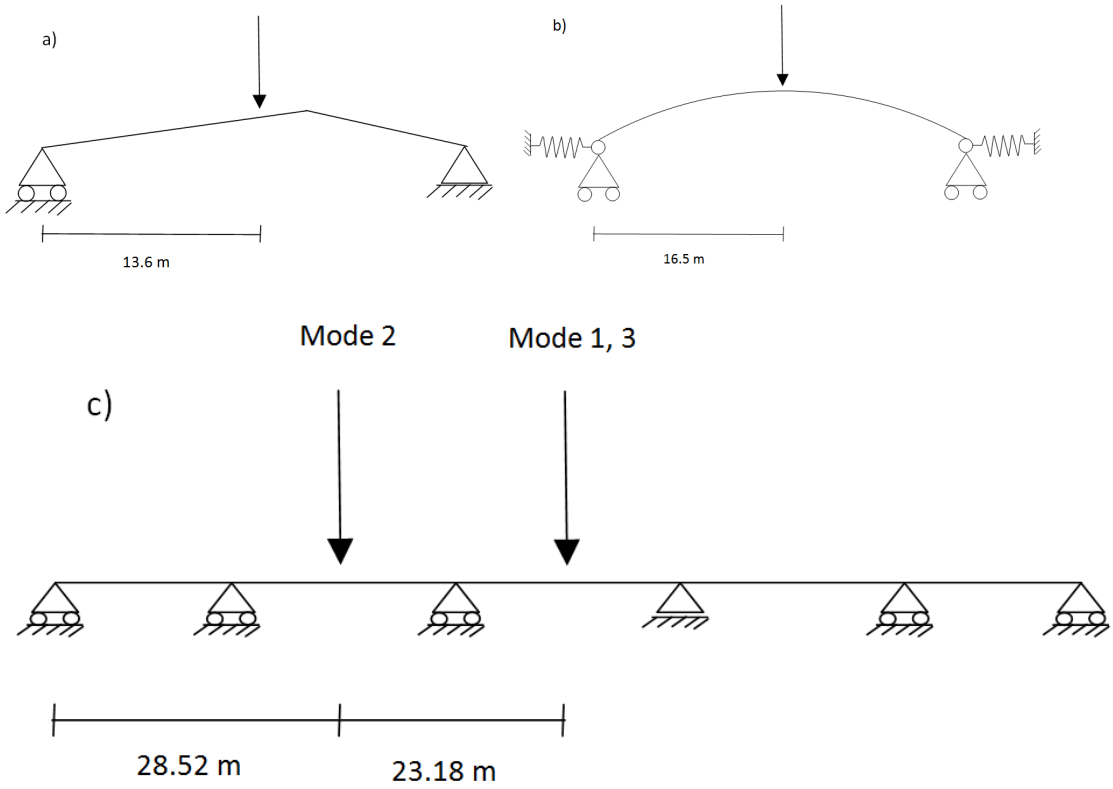

Figure 5.13 Modeling of the ISO 10137 force model. a) The steel truss bridge, b) The box-beam bridge and c) The multi-span bridge.

Calculations were performed for one walking and 2 running pedestrians and in addition for groups of pedestrians corresponding to a loading of 0.4 pedestrians/m² and 0.6 pedestrians/m². The force was applied in the time domain as a tabulated force calculated in Microsoft Excel with a forcing frequency equal to the natural frequencies of the bridge. For the cases when the natural frequency was larger than 2.4 Hz, the α_1-factor was calculated with half the natural frequency to achieve a more realistic force. The comfort criterion is dependent on natural frequency and whether pedestrians are standing or walking on the bridge. For more information about ISO 10137, see Jansson and Svensson (2012).

$$F(t)_N = C(N) \cdot Q \cdot (1 + \sum_{n=1}^{3} \alpha_n \sin(2\pi nft + \varphi_n)) \quad (5.1)$$

Where

$F(t)$	Pedestrian force from N participating pedestrians
$C(N)$	Coordination factor, to account for randomness in walking frequencies, calculated as $C(N) = \sqrt{N}/N$
N	Number of pedestrians
Q	Static load from one pedestrian
α_n	Numerical coefficient corresponding to the n -th harmonic, and is given in Table 5.12
n	Number of the harmonic
f	Frequency of the loading
t	Time
φ_n	Phase angle for the n -th harmonic set to 0 for the 1st harmonic and 90 degrees for the 2nd and 3rd

Table 5.12 The vertical numerical coefficient, α_n, for one person.

	Harmonic number, n	Common range of forcing frequency, $n \cdot f$	Numerical coefficient, α_n
Walking	1	1.2 – 2.4	0.37(f -1.0)
	2	2.4 – 4.8	0.1
	3	3.6 – 7.2	0.06
Running	1	2 – 4	1.4
	2	4 – 8	0.4
	3	6 – 12	0.1

6 Field measurements

The field measurements were performed on three different occasions during the spring of 2013. The measurements of the box-beam- and multi-span bridge were both executed on April 12 while the measurements on the steel bridge were performed on April 5 and April 18. The steel truss bridge needed two test dates because the post processing of the results clearly showed error in the assumptions used when calculating the natural frequency of the bridge. Due to this error the natural frequency were evaluated through Fast Fourier Transform (FFT) in the field at the box-beam- and the multi-span bridge, so the jumping tests could be performed in the right frequency. This chapter will first describe the equipment used and the tests procedures similar for all bridges, and will finish with specific details for each bridge.

6.1 Measuring equipment

The equipment used to measure the response during the tests consisted of piezoelectric accelerometers connected to a data acquisition module, in turn connected to a computer. The computer software VIBpoint Framework was used to collect the data and turn export it to.csv-files for processing. The data acquisition module used was of model DT9837A and were automatically configured in the used software. This module had the possibility to gather data from four accelerometers at the same time, which was used in all tests. The ICP accelerometers used were of model number 393B12. Calibration certificates for the accelerometers can be found in Appendix A. The accelerometers are calibrated and recommended for frequencies between 5 and 1000 Hz.They work well for frequencies below 5 Hz if the data are passed through a low pass frequency filter.

6.1.1 Test setup

Equipment setup for the field measurement was the same on the box-beam- and the multi-span bridge. The accelerometers were screwed to a piece of wood to achieve a stiff connection. The piece of wood was then glued to the asphalt paving with a chemical metal called "Plastic Padding", which can be seen in Figure 6.1.

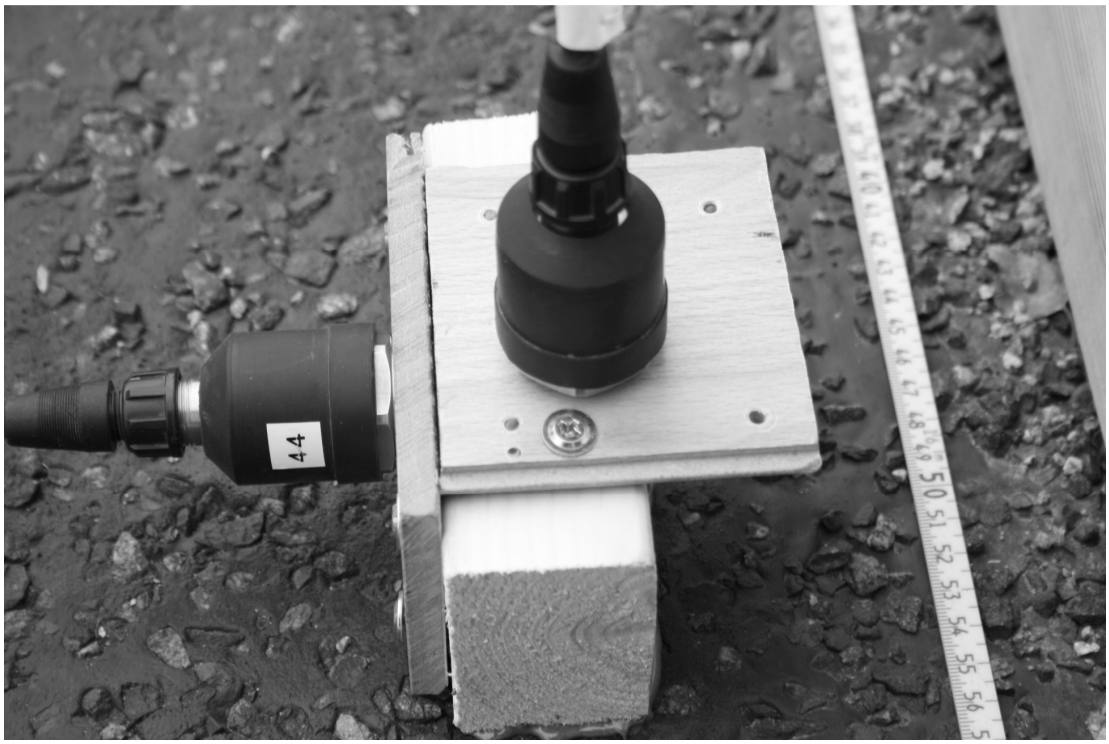

Figure 6.1 *Connection between the accelerometers and the box-beam bridge. The bottom of the piece of wood is glued to the asphalt with "Plastic Padding". Photo: Carl Westerlund*

On the steel truss bridge a different method to connect the accelerometers were used. The accelerometers were fastened to a strong magnet. Two magnets were attached to the bottom chord to measure the vertical vibrations, and two were attached to the truss to measure lateral vibrations, which can be seen in Figure 6.2.

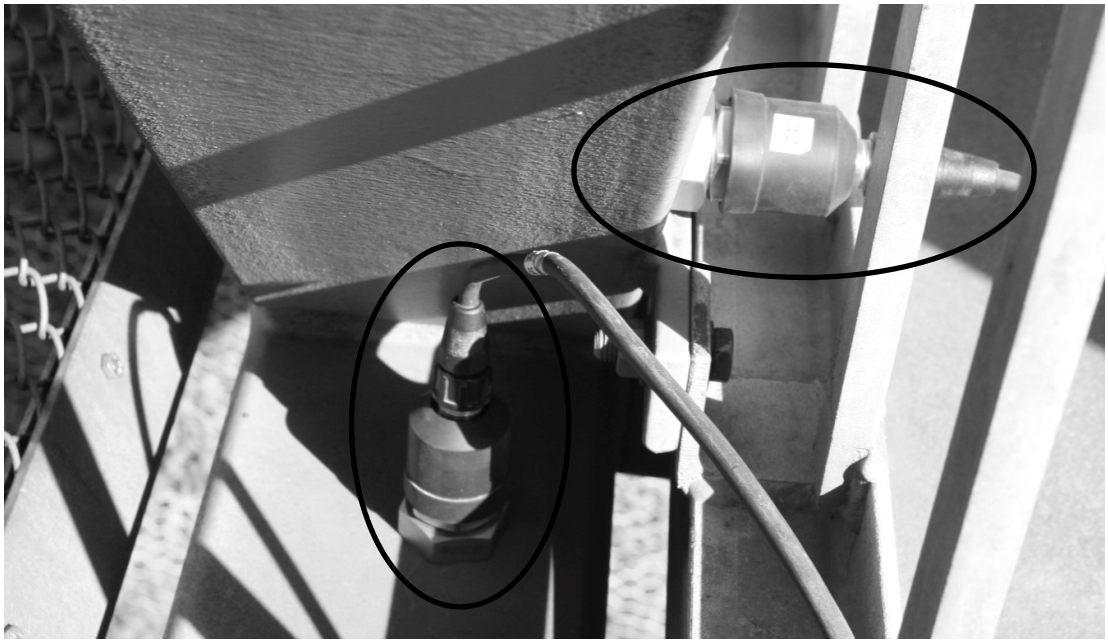

Figure 6.2 *Connection between the accelerometers and the steel bridge, vertical accelerometer to the left and horizontal to the right.*

6.2 Performed tests

Previous authors, among others Jansson and Svensson (2012), have thoroughly described the theory behind the performed tests. Hence this chapter only intends to describe how the tests were performed.

6.2.1 Heel-impact test

The idea was to do an impact test to estimate the damping of the structure. Other ways to perform this test would be with a hammer- or snap-back test. But out of simplicity and lack of equipment the heel-impact test was performed.

All participants were standing on their heels and on a given signal everyone dropped down on their heels. The test was then repeated after 30 seconds.

6.2.2 Jumping test

The jumping test intended to simulate an electrodynamic shaker, by having a group of people jumping at a given frequency at a given location, and then measure the response. The group induced a periodic load, which also would be possible to model in FE software. For all jumping tests the group jumped for 30 seconds and then stood still for the next 30 seconds before another 30 seconds of jumping was performed. The jumping was executed close to the expected natural frequencies. The jumping tests aimed to excite the natural frequency both as part of determining it, and to measured maximum accelerations.

6.2.3 Controlled walking/running

The controlled walking tests aimed to simulate a normal loading situation. In the test a group of eight people were crossing the bridge in 1.7 Hz, 2.0 Hz and with random walking frequencies. At the box-beam bridge, this last test was replaced by a test simulating a more extreme case and is explained in detail in Chapter 6.3.2. In addition two runners crossed the bridge with a running frequency of 3 Hz and a last test of one person sprinting as fast as possible across the bridge.

6.3 Site specific

This section describes tests specific for each location, for instance, specific jumping frequency.

6.3.1 The steel truss bridge

At the steel bridge the accelerometers were placed at mid span and quarter span, as shown in Figure 6.3. At both of these locations accelerometers were placed to register vibrations in both vertical and lateral direction. The points coincided with the maximum of the first vertical and first and second lateral vibration modes calculated before the field measurements. All tests at the steel bridge were executed at mid span due to the lack of a second vertical mode with a low frequency.

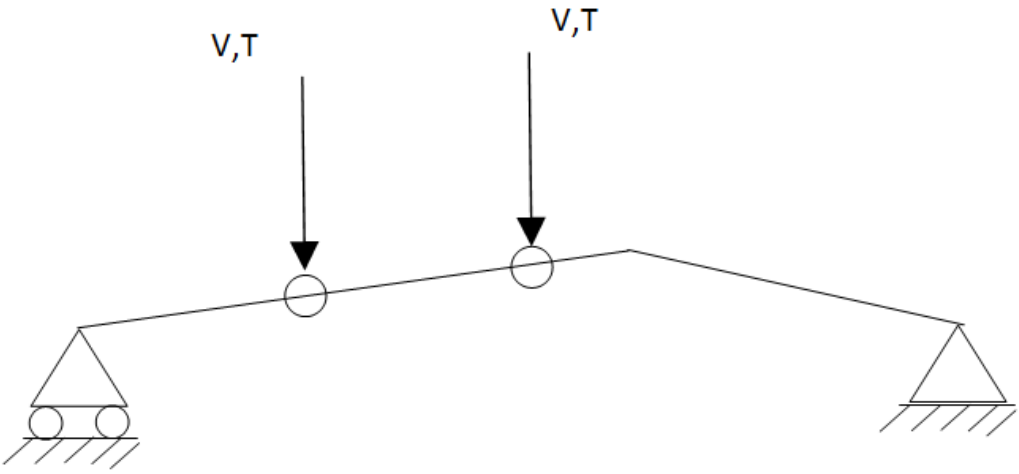

Figure 6.3 *The accelerometers placed in vertical (V) direction and in transversal (T) direction on the middle of the span and in one quarter of the span on the steel bridge.*

Controlled walking tests were performed for 2, 4 and 8 persons both in 1.7 Hz and 2.0 Hz and the running test in 3.0 Hz with 2 persons. At the first occasion, April 5, jumping tests were performed for the frequencies in Table 6.1 and on the second occasion, April 18, the frequencies as shown in Table 6.2. All umping frequencies used on the first occasion are based on the pre-calculated natural frequency of 3.95 Hz. The jumping frequencies used on the second occasion were based on the measured natural frequency of 5.1 Hz from the first occasion. Due to this high natural frequency, which was difficult to performed, the jumping on the second occasions was performed in half of the expected natural frequency.

Table 6.1 *Jumping tests performed on the first measuring occasion.*

Jumping frequency [Hz]
1.9
2.0
3.9
4.0

Table 6.2 Jumping tests performed on the second measuring occasion.

Jumping frequency [Hz]
2.35
2.4
2.45
2.5
2.55

6.3.2 The box-beam bridge

At the box-beam bridge the accelerometers were, as at the steel bridge, placed at mid span and quarter span, as shown in Figure 6.4, and set up to register accelerations in both vertical and lateral direction. The points coincided with the maximum of the first and second vertical calculated before measurements. All jumping- and heel impact tests were performed at mid span. Even a static load case was performed at the box-beam bridge. To apply the static load a vehicle weighing 11.43 metric tons was used. The exact placement and weight of the axles are shown in Figure 6.5.

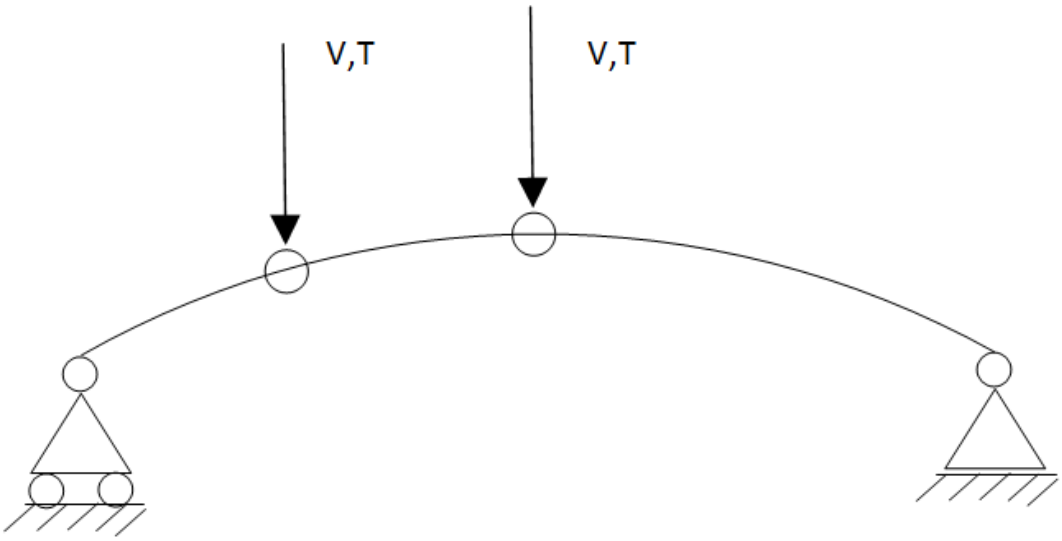

Figure 6.4 The accelerometers placed in vertical (V) direction and in transversal (T) direction on the middle of the span and in one quarter of the span on the steel bridge.

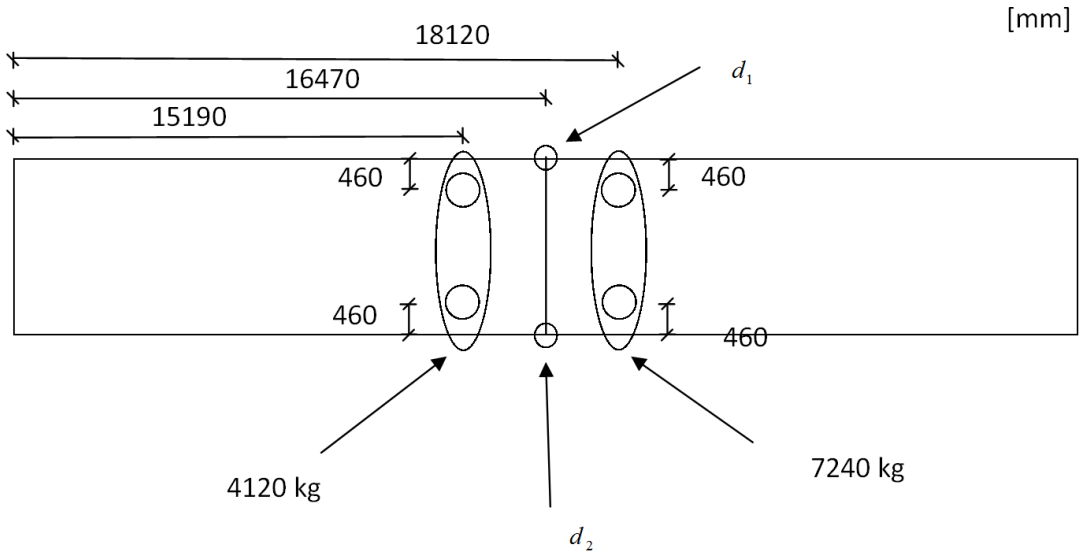

Figure 6.5 *Position of the working vehicle. d_1 and d_2 are the measuring points for the displacement.*

As explained earlier, two simulations of an extreme loading case were tested. In both tests a group of 38 children between 4 and 12 years of age and 4 adults were on the bridge for a total of 5 minutes. In the first test, the group were running, jumping and playing while tracing back and forth following the path in Figure 6.6. In the second test, the group were walking with approximately 1.5 m distance between each other in an orderly fashion, still following the route in Figure 6.6.

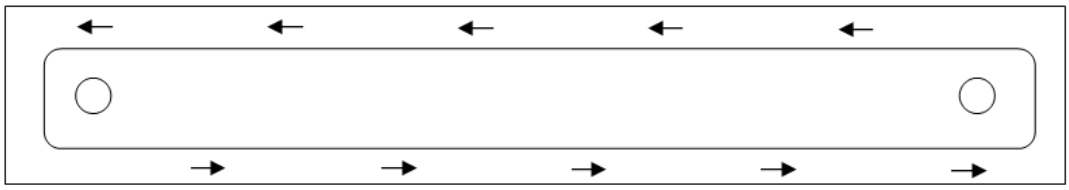

Figure 6.6: *Walking path for the group of children and adults when testing of the box-beam bridge.*

The jumping tests were performed in the pre calculated and measured natural frequency for the first vertical mode. The actual jumping frequencies are shown in Table 6.3. The calculated natural frequencies for the second vertical and first lateral mode were so high (9.13 Hz and 4.62 Hz) they were considered out of range for human induced vibrations.

Table 6.3 Jumping tests performed at the box-beam bridge.

Jumping frequency [Hz]	Comment
2.6	Pre calculated
1.7	Measured, jumping in half the frequency
1.75	Measured, jumping in half the frequency
1.8	Measured, jumping in half the frequency
1.85	Measured, jumping in half the frequency
1.9	Measured, jumping in half the frequency

6.3.3 The multi-span bridge

At the multi-span bridge, no lateral modes with natural frequencies below 5 Hz was found. Hence, the accelerometers were place according to Figure 6.7 at mode maximums. The jumping frequencies at this bridge are shown in Table 6.4.

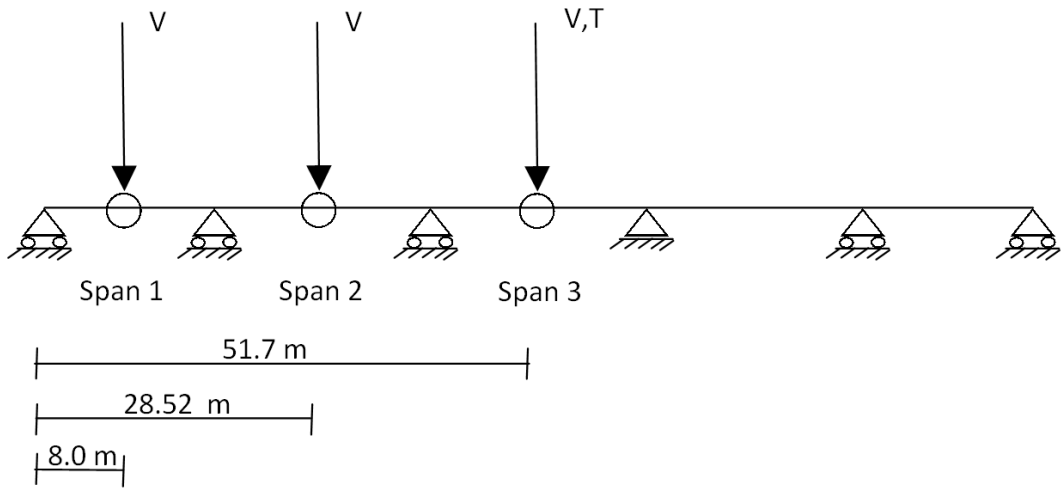

Figure 6.7 The accelerometers placed in vertical (V) direction and in transversal (T) direction at the bridge. They were placed at 8 m, 28.5 m and 51.7 m from the end of the bridge (as seen in the figure).

Table 6.4 Jumping tests performed at the multi-span bridge.

Jumping frequency [Hz]	Load placement	Comment
1.867	Span 1	Pre calculated
2.0	Span 1	Measured
1.9	Span 2	Measured
2.0	Span 2	Measured
1.7	Span 3	Measured
1.8	Span 3	Measured
1.9	Span 3	Measured
2.0	Span 3	Measured
2.1	Span 3	Measured

7 Results

This chapter presents the results acquired from the three studied bridges. For each bridge, the results of the field measurements are presented before the modelling of the design guidelines.

7.1 The steel truss bridge

The following sections are presenting the results of the field measurements and the dynamic design performed at the steel truss bridge.

7.1.1 Field measurements

The measurements at the steel bridge were conducted at two occasions, April 5 and April 18, 2013. On the first occasion it was sunny and around +13ºC and 5 m/s wind speed. On the second occasion it had just stopped raining, the temperature was around +5ºC and the wind speed was a little lower. Trains passed underneath the bridge during a few of the tests, but most of the passages happened between actual tests and did not affect the general result.

The data were processed through a MATLAB built in lowpass-filter so that frequencies between 0.3 Hz and 6 Hz remain. A upper limit of 6 Hz are used due to the fact that the natural frequency is just under 5 Hz, and hence using 5 Hz as a limit would be a little too close to determine the natural frequency.

7.1.1.1 Controlled walking

A total of 13 different controlled walking tests were performed at the steel bridge. The tests with 8 persons walking in random frequencies, two persons jogging in 3 Hz and one person sprinting were performed on all bridges and are the ones presented in this section. From the test with eight persons walking in random frequencies, plots showing the time history and the corresponding frequency spectrum are shown in Figure 7.1 and Figure 7.2. The maximum accelerations from the performed tests are presented in Table 7.1and the natural frequencies calculated form the FFT analyses are shown in Table 7.2.

Table 7.1 Controlled walking tests on the steel bridge. Maximum measured accelerations and test occasion presented.

Test occasion	Test type	Maximum acceleration [m/s^2]
First	8 persons walking in 1.7 Hz	0.45
First	8 persons walking in 2.0 Hz	0.20
Second	8 persons walking with random frequencies	0.15
First	2 persons jogging in 3.0 Hz	0.46
First	1 person sprinting	1.0

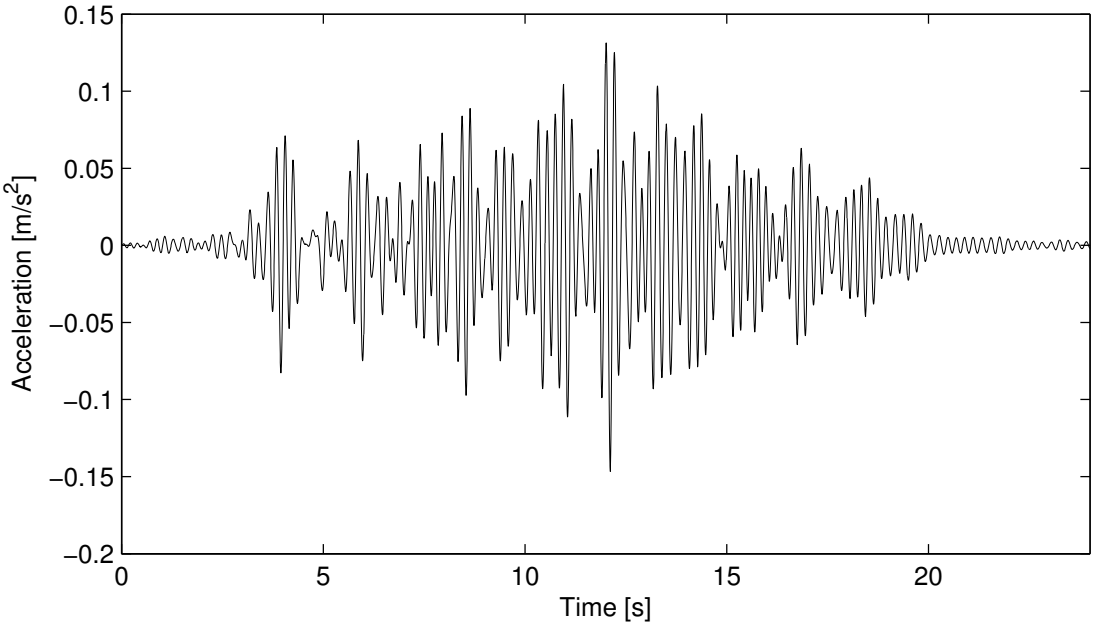

Figure 7.1 Vertical accelerations, measured at midspan from the controlled walking test with eight persons walking in a group with random frequencies. The test was performed on the second occasion.

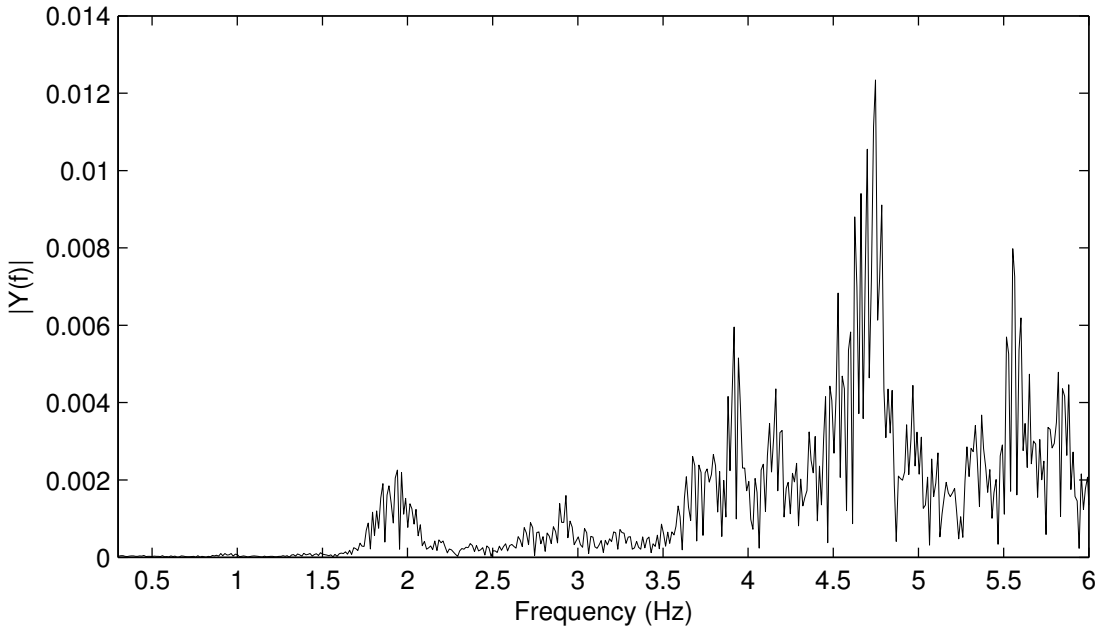

Figure 7.2 Frequency analysis of the vertical accelerations measured at midspanfrom eight persons crossing the bridge with random walking frequencies (the time history showed in Figure 7.1. The test wasperformed on the second occasion.

Table 7.2 Result from the FFT analyses from the two field measure occasions.

Test occasion	Natural frequency [Hz]
First	5.05
Second	4.75

7.1.1.2 Heel impact

Measurements of the heel impact tests performed on the first occasion were used as basis for the results in this section. The main aim of the heel impact tests was to extract the total damping ratio for the bridge. In addition the natural frequency was calculated through FFT analyses. The damping ratio was calculated through logarithmic decrement (Equation (7.1)) on a curve fitted to the peaks of the decreasing acceleration. The curve is fitted by the use of built-in MATLAB exponential curve fitting. The MATLAB program for the curve fitting can be found in Appendix C.

$$\zeta = \frac{1}{2\pi} \ln\left(\frac{a_i}{a_{i+1}}\right) \tag{7.1}$$

Where:

ζ	Structural damping ratio
a_i	Acceleration at the peak in cycle i
a_{i+1}	Acceleration at the peak in cycle i+1

Data from 12 measurements from the heel impact tests were evaluated to calculate the damping ratio of the bridge. A typical fit performed on a heel impact test is shown in Figure 7.3. The calculated damping ratio varied from 2.76% to 5.73%, with a mean value of 3.68% and a standard deviation of 0.92%

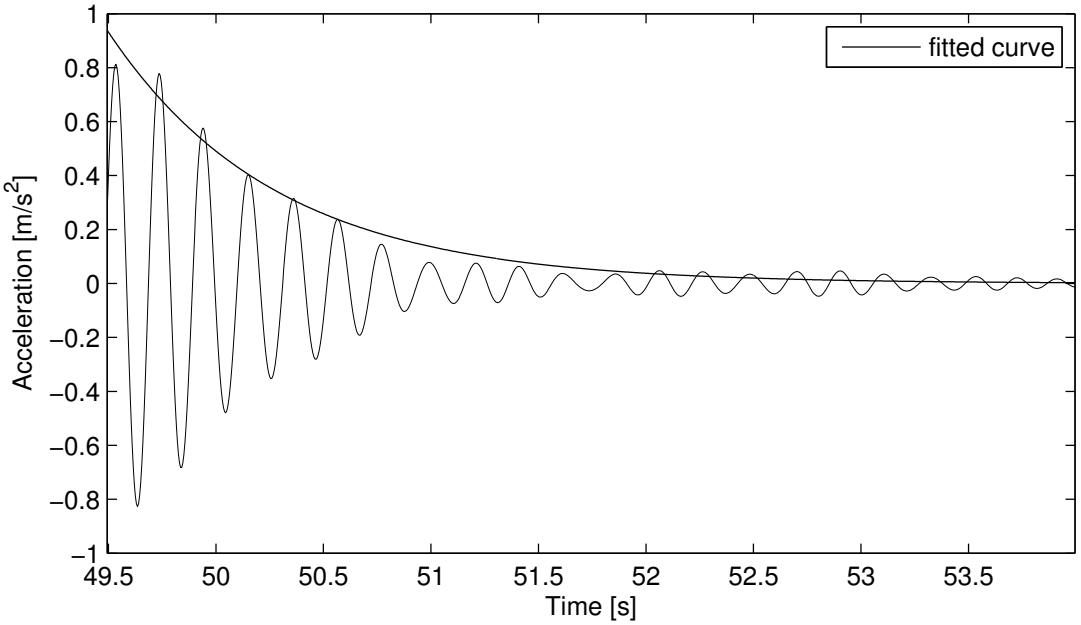

Figure 7.3 Curve fit from a heel impact test with a weight of 632,4 kg. Accelerations measured for the vertical direction at the midspan. This test gives a damping ratio of 4.26%.

7.1.1.3 Jumping tests

The jumping tests were performed with different frequencies. All the jumping tests with corresponding acceleration are shown in Table 7.3. In Figure 7.4 the jumping test with a jumping frequency of 2.4 Hz is shown, which is half the bridge's natural frequency. It provided the largest acceleration with a magnitude of 4.6 m/s^2.

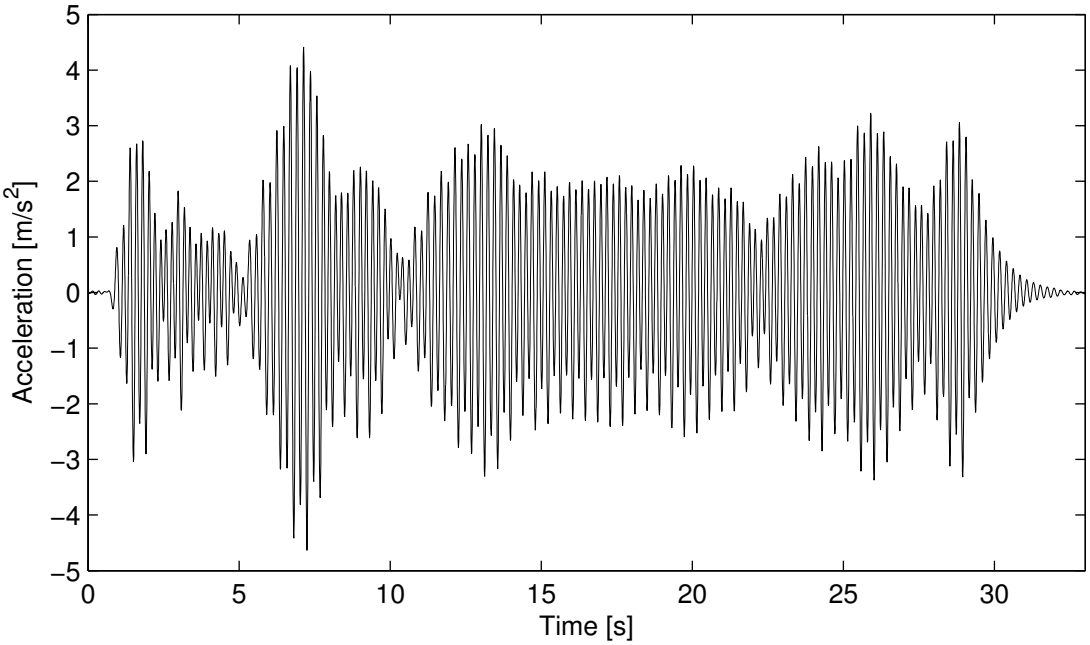

Figure 7.4 Vertical accelerations measured at midspan from a jumping test in 2.4 Hz. Most acceleration peaks are between 2 and 3 m/s^2, but highest peak 4.6 m/s^2.

Table 7.3 Maximum measured acceleration from each jumping tests.

Jumping frequency [Hz]	Maximum acceleration [m/s^2]
1.9	1.65
2.0	2.58
2.35	3.77
2.4	4.6
2.45	3.92
2.55	2.57
3.9	2.42
4.0	2.14

As for the heel impact tests, the damping ratio was calculated by curve fitting and logarithmic decrement (Equation (7.1)). The average damping ratios from the two occasions are listed in Table 7.4.The damping ratio varied between 2.48% and 6.76% on the first and 3.0% and 7.77% on the second occasion. The mean value from both occasions was 4.78%. At the first occasion the jumping was not in very good synchronisation, so someone often had an extra jump after everyone else had stopped, and the free decay had started.

Table 7.4 Calculated damping ratios from jumping tests performed on the steel bridge after how well the calculated curve fit catches the real damping behaviour of the bridge. N is the number of measurements used to calculate the relevant damping ratio.

Occasion	Damping ratio	N	Standard deviation
First	4.99%	16	1.29%
Second	4.59%	17	1.52%
Combined	4.78%	33	1.43%

7.1.1.4 Human perception of the bridge

According to Tomas Svensson, an experienced engineer, who participated in the field measurements, the bridge was fully acceptable with regards to movements, even though it felt like a slim construction. When pedestrians were crossing the bridge, the vibrations were noticeable, especially when one single runner was crossing it[6].

7.1.2 Frequency analyses

Frequency analyses were performed on the four different FE models of the steel truss bridge. The higher natural frequency of the calibrated model is due to the interaction from the steel deck. The lower frequency with Eurocode, however, is due to the added mass of the safety fence. The large difference between an empty and occupied bridge is due to the low weight of the steel truss bridge. Hence the pedestrians will give a large increase in the total weight.

Table 7.5 Natural frequency of the three different FE models of the steel truss bridge.

Model	Natural frequency [Hz]
Before field measurements	4.03
Calibrated model after field measurements	4.76
With material parameters in Eurocode (Empty)	3.57
With material parameters in Eurocode (Occupied)	3.10

[6]Tomas Svensson, COWI AB, [Personal Communication], 13.05.2013

7.1.3 Dynamic design

The resulting peak accelerations from the four force models are presented in Table 7.6. From the table it can be seen that the peak accelerations varies a lot between the different force models, even for the approximately same assumption of pedestrians on the bridge. For instance, for a continuous stream of pedestrians both UK NA and Sétra provided peak accelerations of approximately 2.3 m/s^2, while Eurocode provided 6.6 m/s^2 and ISO 10137 13.3 m/s^2. The difference of 1 $m/s^{2,}$ for empty versus occupied bridge, with Sétra is due to a large increase of the mass of the bridge and hence a changed natural frequency of the bridge. The lower natural frequency for the occupied bridge causes a modified minus factor of half that for the empty bridge.

Table 7.6 Calculated peak accelerations for the four used design models applied at the model for the steel bridge.

Design guideline	Maximum accelerations [m/s^2]
Eurocode simplified approach	
1 pedestrian	1.00
13 pedestrians	1.71
50.4 pedestrian (0.6 m^{-2})	6.62
UK National Annex	
Stream of pedestrians (0.4 m^{-2})	2.27
Sétra	
Empty bridge (0.5 m^{-2})	2.30
Occupied bridge (0.5 m^{-2})	1.07
ISO 10137	
1 walking	2.24
2 running	21.6
35 walking (0.4 m^{-2})	13.3
50 walking (0.6 m^{-2})	15.9

7.2 The box-beam bridge

The next sections are presenting the results of the field measurements and the dynamic design performed at the box-beam bridge.

7.2.1 Field measurements

The measurements at the box-beam bridge were conducted in the morning of April 12 2013. The weather was cloudy and the temperature was a few degrees above zero. During the tests several large trucks and a lot of smaller cars passed underneath the bridge. These may have affected the measurements, but the vibrations were not felt, and were therefore considered negligible. Also the wind speed was very low, probably less than 5 m/s and was also considered negligible for the acceleration measurements.

The data are processed through a MATLAB built in lowpass filter so that frequencies between 0.3 Hz and 5 Hz were left.

7.2.1.1 Static test

The deflections were measured at both edges of the bridge at mid span, as shown in Figure 6.5. The deflections for the applied load were: $d_1 = 12$ mm and $d_2 = 13$ mm.

7.2.1.2 Controlled walking

At the box-beam bridge, six controlled walking tests were performed. Here, instead of having eight persons walking in random frequency, two school classes with a total of 38 children and four adults were used. An acceleration plot and a corresponding frequency spectrum are shown inFigure 7.5 andFigure 7.6. The FFT analyse produced the natural frequency of the bridge is 3.5 Hz. The peak accelerations from the tests are presented in Table 7.7.

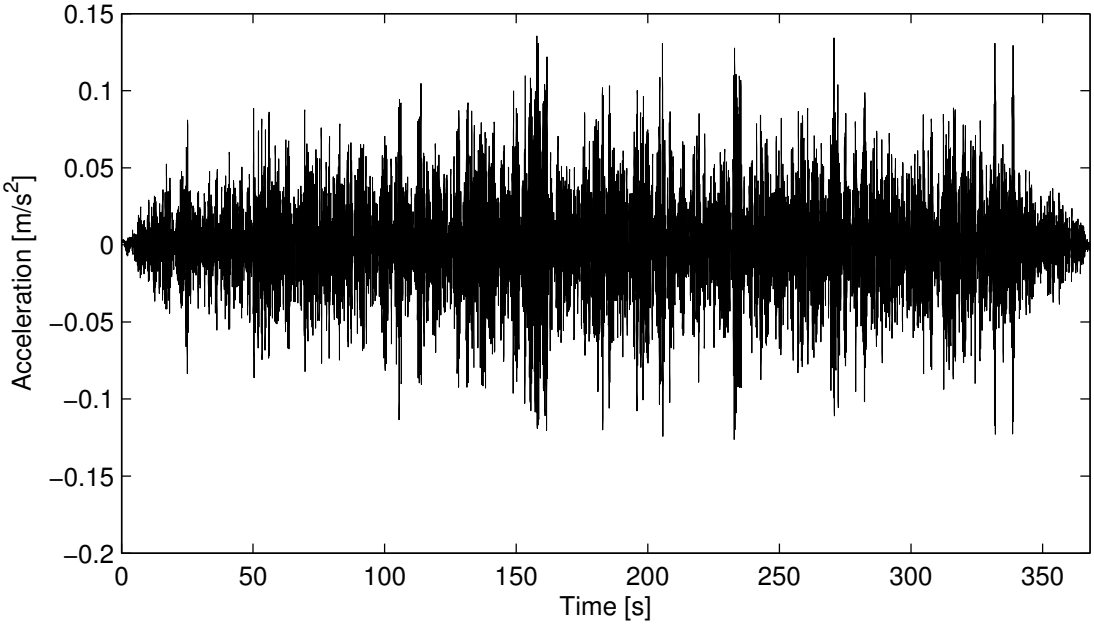

Figure 7.5 Vertical accelerations measured at midspan for 38 children and four adults walking organized on the bridge.

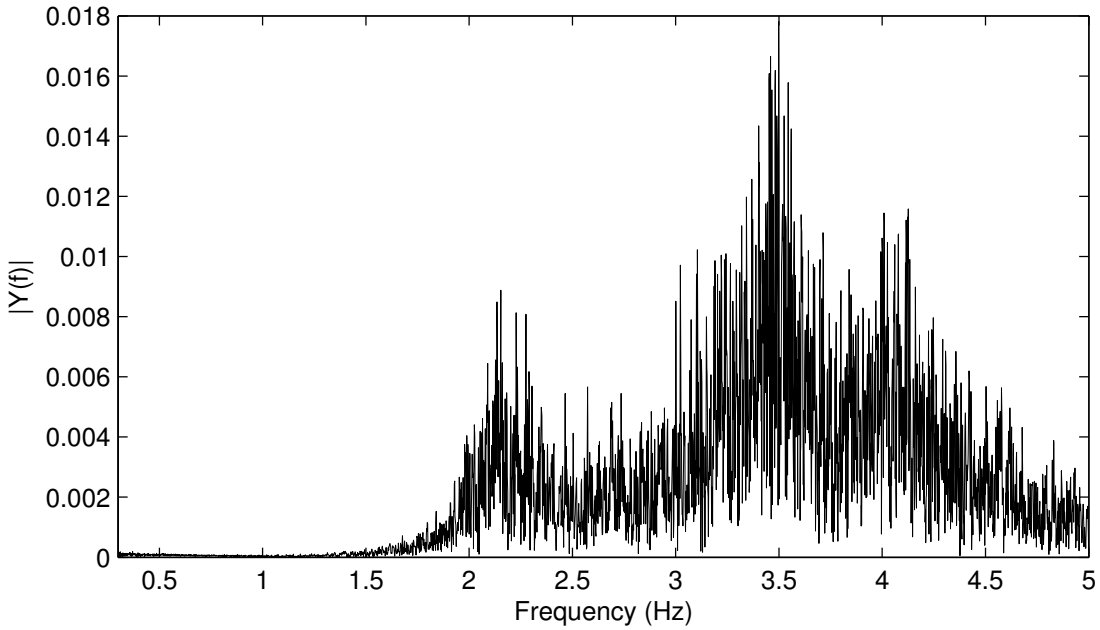

Figure 7.6 *Frequency analysis of the vertical accelerations measured at midspan 38 children and 4 adults playing and having fun on the bridge. The test indicates the natural frequency to be 3.5 Hz.*

Table 7.7 *Controlled walking tests on the box-beam bridge. Test type and vertical peak accelerations are presented.*

Test type	Maximum acceleration [m/s^2]
8 persons walking in 1.7 Hz	0.12
8 persons walking in 2.0 Hz	0.09
2 school classes walking random	0.14
2 persons jogging in 3.0 Hz	0.29
1 person sprinting	0.35

7.2.1.3 Heel Impact test

The damping ratio was calculated from logarithmic decrement with the use of curve fitting from MATLAB and Equation (7.1). Data from 16 measurements from heel impact tests were evaluated to calculate the damping ratio of the bridge. The curve fit produced values for the damping ratio between 4.12% and 5.6%.With a calculated mean value of 4.64% and a standard deviation of 0.47%. A typical heel impact test from the box-beam bridge is shown in Figure 7.7.

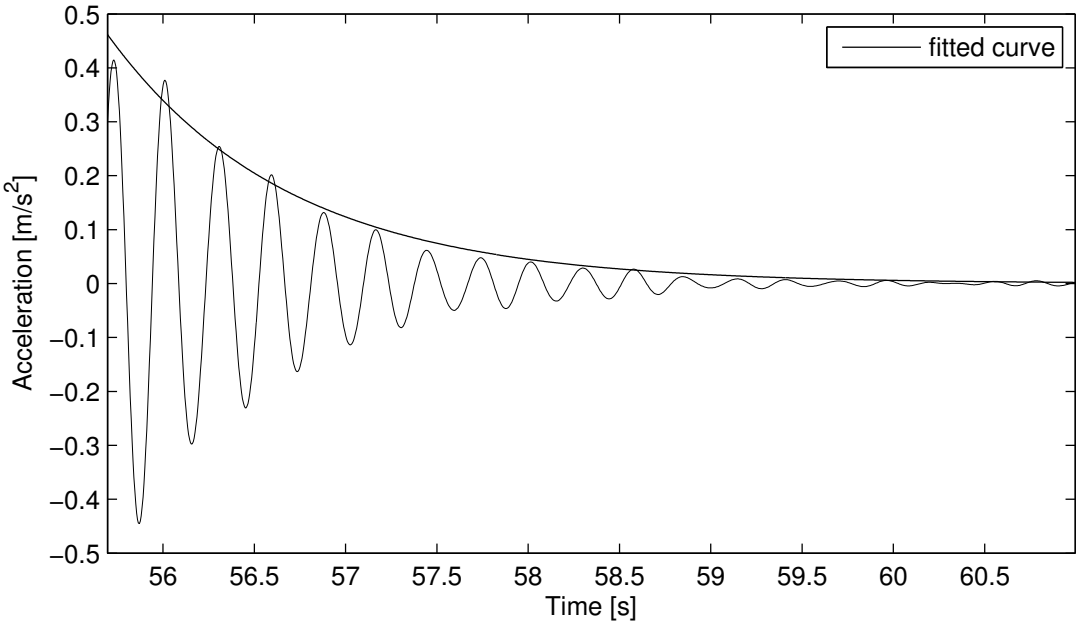

Figure 7.7 Curve fit from a heel impact test with a weight of 676,4 kg. Accelerations measured for the vertical direction at the midspan. This test gives a damping ratio of 4.51%.

7.2.1.4 Jumping test

Jumping tests were performed in steps of 0.05 Hz around half the expected natural frequency. The largest accelerations reached 1.45 m/s^2 and were measured while jumping in 1.75 Hz and are shown in Figure 7.8. However, only slightly smaller accelerations were measured while jumping in 1.80 Hz. This indicates a natural frequency somewhere between 3.5 and 3.6 Hz, but closer to 3.5 Hz than 3.6 Hz. All the jumping frequencies together with corresponding acceleration are shown in Table 7.8. A mean damping ratio of 4.36% with a standard deviation of 0.56% was calculated with curve fit from 24 measurements.

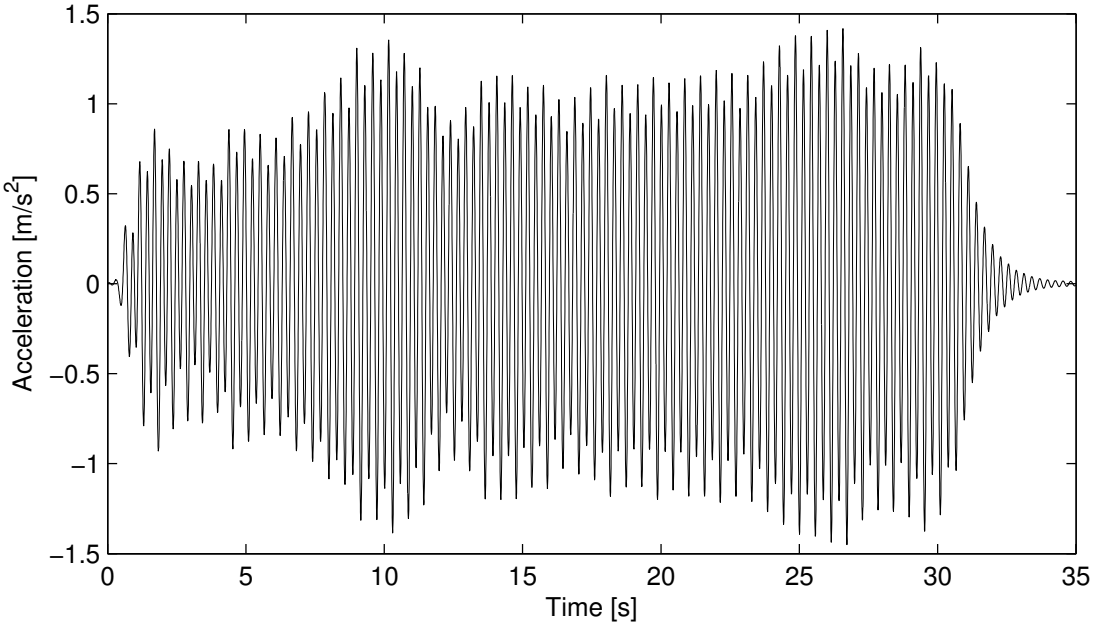

Figure 7.8 Vertical accelerations measured at midspan from the jumping test while jumping in 1.75 Hz. Most peaks between 1 and 1.5 m/s^2, with the highest peak of 1.45 m/s^2.

Table 7.8 Maximum measured acceleration from each jumping frequency.

Jumping frequency [Hz]	Maximum acceleration [m/s^2]
1.7	1.26
1.75	1.45
1.8	1.36
1.85	1.15
1.9	1.00
2.6	0.69

7.2.1.5 Human perception of the bridge

According to Tomas Svensson, only small movements of the bridge deck were noticed during all performed tests, and the bridge's function was good with regards to vibrations[7].

7.2.2 Frequency analyses

Frequency analyses were performed on the four different FE models of the box-beam bridge. The higher natural frequency of the calibrated model is due to the spring

[7]Tomas Svensson, COWI AB, [Personal Communication], 13.05.2013

effect from the rubber bearings. The somewhat higher according to Eurocodeis due the difference in density of glulam as expected by the manufacturer and used in design.

Table 7.9 Natural frequency of the three different FE models of the box-beam bridge.

Model	Natural Frequency [Hz]
Before field measurements	2.61
Calibrated model after field measurements	3.50
With material parameters in Eurocode (Empty)	3.74
With material parameters in Eurocode (Occupied)	3.62

7.2.3 Dynamic design

The resulting peak accelerations from the four force models are presented in Table 7.10. The smallest peak accelerations to be used in design according to each guideline were provided by Sétra with an acceleration of 0.66 m/s^2, and the largest from ISO 10137 with an acceleration of 4.50 m/s^2. UK NA provided accelerations of 0.86 m/s^2 and Eurocode of 1.29 m/s^2.

Table 7.10 Calculated peak accelerations for the four used design models applied at the model for the box-beam bridge.

Design guideline	Maximum accelerations [m/s^2]
Eurocode simplified approach	
1 pedestrian	0.196
13 pedestrians	0.295
56.8 pedestrian (0.6 m^{-2})	1.290
UK National Annex	
Stream of pedestrians (0.4 m^{-2})	0.855
Sétra	
Empty bridge (0.5 m^{-2})	0.664
Occupied bridge (0.5 m^{-2})	0.620
ISO 10137	
1 walking	0.511
2 running	4.498
38 walking (0.4 m^{-2})	3.153
57 walking (0.6 m^{-2})	3.856

7.3 The multi-span bridge

The following sections are presenting the results of the field measurements and the dynamic design performed at the multi-span bridge.

7.3.1 Field measurements

The measurements at the multi-span bridge were conducted in the afternoon of April 12, 2013. During the tests it was a combination of snow and rain with a temperature pending around zero degrees Celsius and the wind speed was very low, probably less than 5 m/s and was considered negligible for the acceleration measurements.

The data were processed through a MATLAB built in lowpass filter so that frequencies between 0.3 Hz and 5 Hz are left.

7.3.1.1 Controlled walking

Five controlled walking tests were performed. The test when eight people walking in random frequency is plotted in Figure 7.9 and the corresponding frequency spectrum is presented in Figure 7.10. The rest of the controlled walking tests are presented in Table 7.11 together with the peak acceleration of each frequency.

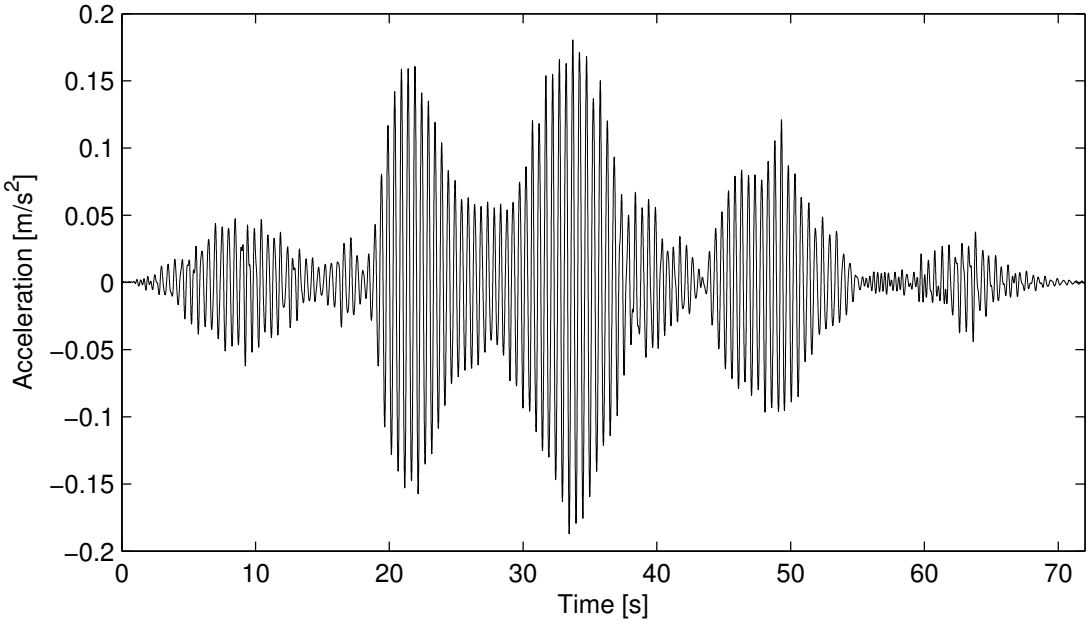

Figure 7.9 Vertical accelerations measured in the middle span (span 3) from the walking test with 8 persons walking in random frequency. The accelerations reach 0.19 m/s^2 when the group passes over the span.

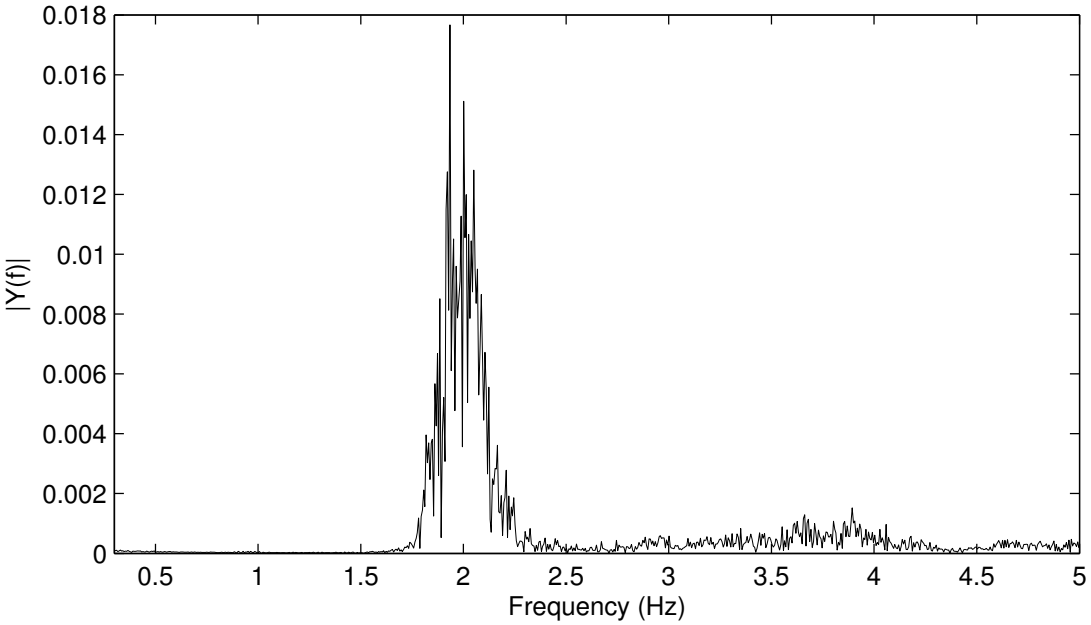

Figure 7.10 Frequency spectrum from span 3 of the walking test performed in random frequency indicating natural frequencies of around 2.0 Hz.

Table 7.11 Controlled walking tests on the multi-span bridge. Test type and maximum measured accelerations are presented.

Test type	Maximum acceleration [m/s^2]
8 persons walking in 1.7 Hz	0.12
8 persons walking in 2.0 Hz	0.49
8 persons walking with random frequencies	0.19
2 persons jogging in 3.0 Hz	0.29
1 person sprinting	0.31

7.3.1.2 Heel impact test

The damping ratio was calculated from logarithmic decrement as described in Section 7.1.1.2. Data from six heel impact tests were evaluated to calculate the damping ratio of the bridge. The calculated damping ratio varies from 2.18% and 7.93% with an average of 4.01% and a standard deviation of 1.11% based on 48 measurements. A typical heel impact test from the multi-span bridge is shown in Figure 7.11. A frequency spectrum from a heel impact test is shown in Figure 7.12, clearly indicating the natural frequencies according to Table 7.12.

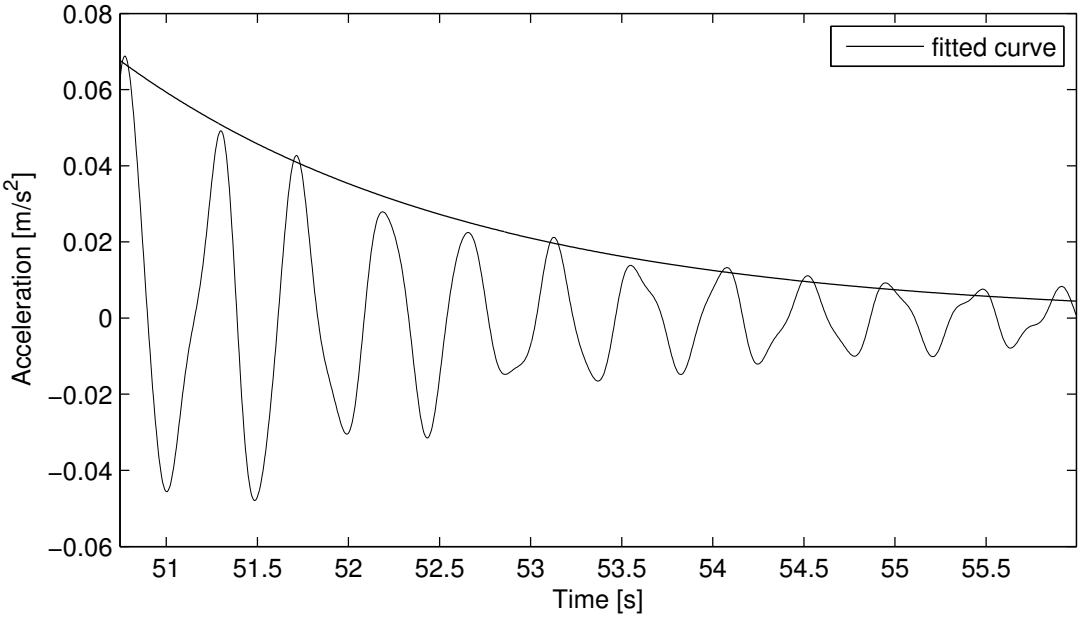

Figure 7.11 Curve fit from a heel impact test in span 3 with a weight of 582.9 kg. Accelerations measured for the vertical direction in span 3. This test gives a damping ratio of 4.38 %.

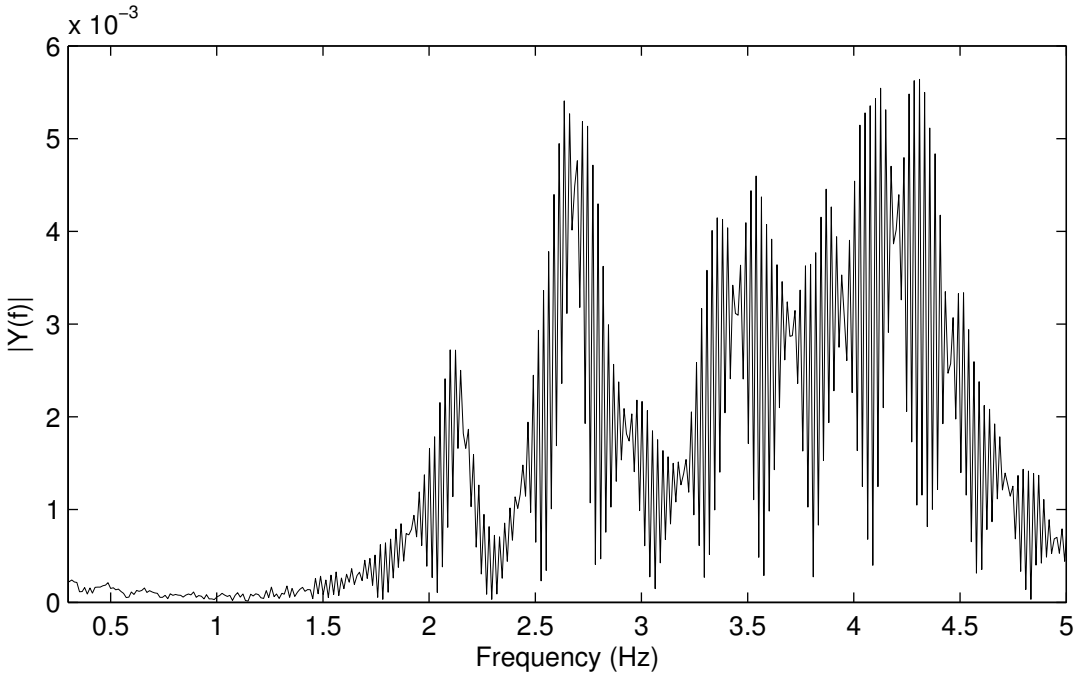

Figure 7.12 Frequency spectrum from one of the heel impact tests performed in span 2, and are based on the accelerations from the accelerometer in span 1.

Table 7.12 Natural frequencies of the first four modes extracted from the frequency spectrum through FFT from the six performed heel impact tests.

Mode	Frequency [Hz]
1	2.15
2	2.7
3	3.35
4	4.25

7.3.1.3 Jumping test

A total of 18 jumping tests in different frequencies and in different spans were performed on the bridge. The test, when jumping in 2.1 Hz in span 3 gave the highest acceleration, with a magnitude of 2.8 m/s^2. The test is plotted in Figure 7.13. The rest of the results from the jumping tests are shown in Table 7.13. Damping ratios were calculated according to Section 7.1.1.2. The damping ratio varied between 1.32% and 6.95% with an average of 3.50% and a standard deviation of 0.87% calculated from 63 measurements.

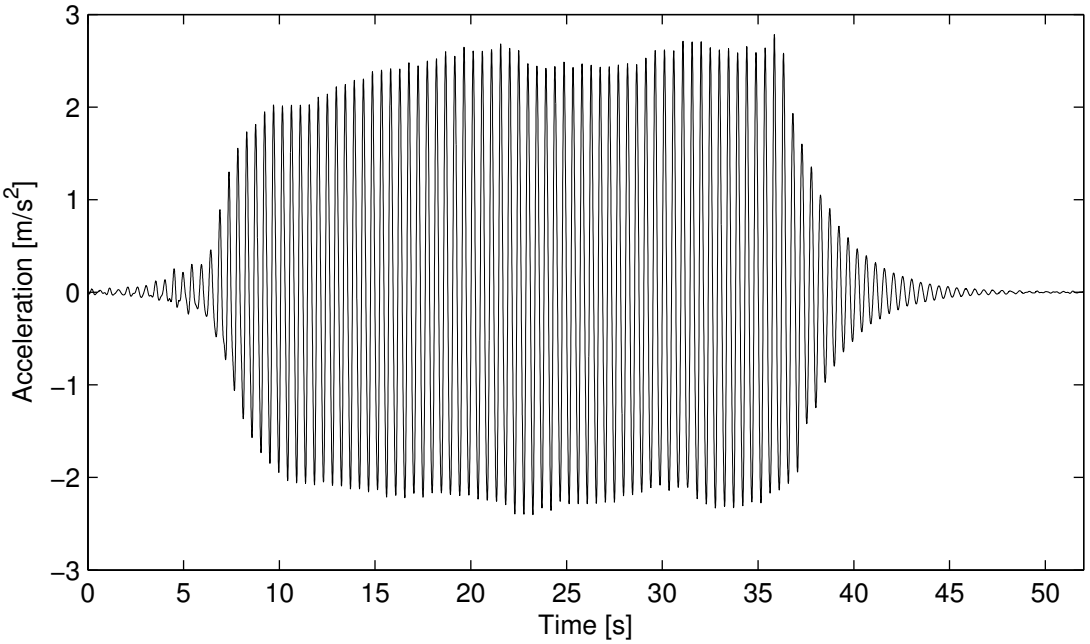

Figure 7.13 Vertical accelerations measured in span 3, from the jump test in 2.1 Hz performed in span 3. Acceleration level reached 2.8 m/s^2.

Table 7.13 Maximum measured acceleration from each jumping test.

Jumping frequency [Hz]	Span	Maximum acceleration [m/s^2]
1.87	1	0.85
2.0	1	1.61
1.9	2	1.49
2.0	2	1.88
1.7	3	1.0
1.8	3	1.19
1.9	3	2.45
2.0	3	2.49
2.1	3	2.78

7.3.1.4 Human perception of the bridge

According to Tomas Svensson the bridge seemed acceptable with regard to vibrations during expected daily use. With denser crowds, however, it was more doubtful if the bridge still would feel comfortable to a person standing on it. During the jumping

tests, where a small group was jumping in the same frequency as resonance, it was easy to excite the bridge so that severe and apparent movements were observed[8].

7.3.2 Frequency analyses

Frequency analyses were performed on the four different FE models of the multi-span bridge. Very small variations can be seen between the different models, which probably were due to the simple structure of the bridge. The higher frequency of the calibrated model was caused by the influence of the railings, which increase the total stiffness of the bridge. The provided natural frequencies from the models with material parameters from Eurocode was higher than the first model due to a lower mass assumption and lower because no railings were included in the model.

Table 7.14 Natural frequency of the three different FE models of the multi-span bridge.

Model	Mode 1 [Hz]	Mode 2 [Hz]	Mode 3 [Hz]	Mode 4 [Hz]
Before field measurements	1.89	2.34	3.00	3.74
Calibrated model after field measurements	2.15	2.69	3.43	4.21
With material parameters in Eurocode (Empty)	1.94	2.43	3.12	3.89
With material parameters in Eurocode (Occupied)	1.94	2.44	3.12	3.89

7.3.3 Dynamic design

The peak accelerations from all design guidelines are shown in Table 7.15.For the Eurocode, UK NA and Sétra guidelines the largest accelerations were provided when the force was applied to the first mode. For ISO 10137 however, almost the same accelerations were provided for both the first and third mode. ISO 10137 was applied at the same place for both modes. Hence it is possible that the modes interacted with each other and caused the large accelerations for the third mode. Sétra provided the smallest peak accelerations of 1.93 m/s^2 and Eurocode the largest of 5.94 m/s^2. Between these two, UK NA provides peak accelerations of 2.31 m/s^2 and ISO 10137 of 4.41 m/s^2.

[8]Tomas Svensson, COWI AB, [Personal Communication], 13.05.2013

Table 7.15 Calculated peak accelerations for the four used design models applied at the model for the multi-span bridge.

Design guideline	Maximum accelerations [m/s^2]		
	Mode 1	Mode 2	Mode 3
Eurocode simplified approach			
1 walking pedestrians	0.499	-	-
13 pedestrians	1.49	-	-
51.8 pedestrian (0.6 m^{-2})	5.94	-	-
1 running person	1.47	-	-
UK National Annex			
Stream of pedestrians (0.4 m^{-2})	2.31	1.93	0.758
Sétra			
Empty bridge (0.5 m^{-2}) – mode 1	1.93	0.605	0.339
Occupied bridge (0.5 m^{-2}) – mode 1	1.89	0.600	0.339
ISO 10137			
1 walking – mode 1	0.289	0.237	0.286
2 running – mode 1	2.39	1.89	2.31
50 walking – mode 1	2.03	1.67	2.03
158 walking (0.4 m^{-2}) – mode 1	3.60	2.98	3.60
237 walking (0.6 m^{-2}) – mode 1	4.41	3.65	4.41

8 Analysis of case studies

The aim of this chapter is to perform some analysis of the case studies. First, a comparison between the performed and simulated tests executed at the bridges and second a comparison between the results of the different force models applied to the bridges. These results are also compared to the measured accelerations from the field experiments.

8.1 Field measurements and simulations

To achieve a good correlation between the field measurements and the FE simulations, some material properties were changed from what is stated in Eurocode to reflect the actual behaviour of the bridges. The material properties used in the calibrated models and the ones stated in Eurocode are listed in Table 8.1. Most properties were the same, notable however isthe Young's modulus of the timber railing at the multi-span bridge, which was reduced to match the measured natural frequencies of the bridge. The mass of the timber used in the calibrated models was higher than the design values, which was in accordance with the view of the manufacturers.

Table 8.1 Material properties used in models developed in BRIGADE/Plus that reproduce reality well, in Eurocode, Sétra and ISO 10137.

	Steel truss	Box-beam	Multi-span	Eurocode / Sétra / ISO
Young's modulus Glulam, L40c [GPa]	-	13	-	13
Young's modulus Glulam, L40h [GPa]	-	-	13.7	13.7
Young's modulus steel [GPa]	210	-	-	210
Young's modulus timber railing [GPa]	-	-	1.8	-
Shear modulus L40c [GPa]	-	0.76	-	0.76
Shear modulus L40h [GPa]	-	-	0.85	0.85
Density Glulam L40c [kg/m^3]	-	500	-	400
Density Glulam L40h [kg/m^3]	-	-	470	430
Density steel [kg/m^3]	7850	-	-	7850
Stiffness rubber bearing [kN/m]	-	77 000	-	77 000

[a] The damping ratio given is the average of the damping ratios from the jump- and heel impact-tests.

[b] No value is given for the damping ratio of timber in ISO 10137, hence the value from Eurocode 5 is used.

In Table 8.2 the measured natural frequencies are displayed together with the calculated natural frequencies from the calibrated and the design models. The calibrated models had good correlation with the measured frequencies, even though it differs slightly at the higher modes at the multi-span bridge. The design models gave a lower natural frequency than the actual for the steel truss bridge and the multi-span bridge, while at the box-beam the measured natural frequency was higher than what was given in the design model.

Table 8.2 Natural frequencies of the three studied bridges according to the field measurements, calibrated models and design models (Properties from Eurocode). Both an occupied and empty bridge are used to calculate natural frequencies with the design models.

	Measured frequencies [Hz]	Calibrated models [Hz]	Design models (Empty / Occupied) [Hz]
Steel truss			
First Vertical	4.75	4.76	3.57 / 3.10
Box-beam			
First Vertical	3.5	3.50	3.74 / 3.62
Multi-span			
First vertical	2.15	2.15	1.94 / 1.94
Second vertical	2.73	2.69	2.43 / 2.44
Third vertical	3.35	3.43	3.12 / 3.12
Fourth vertical	4.25	4.21	3.89 / 3.89
Fifth vertical	-	4.46	4.12 / 4.12

In Table 8.3, the measured damping ratios of the studied bridges, and the cable-stayed bridge Älvsbackabron, studied by Jansson and Svensson (2012) are listed togheter with the given values from Eurocode and Sétra. The measured ratios were significantly higher than the design values for the three bridges studied in this thesis, but have a better correlation at Älvsbackabron.

Table 8.3 Damping ratios for the studied bridges and from relevant design documents.

	Heel impact	Jumping	Sétra	Eurocode
Steel truss	3.68%	4.78%	0.4%	0.5%
Box-beam	4.64%	4.36%	1.0%	1.0%
Multi-span	4.01%	3.50%	1.0%	1.0%
Cable-stayed[a]	1.2%	0.6%	-	1.5%

[a] The values from the cable-stayed bridge is taken from Jansson and Svensson (2012).

8.2 Dynamic design

In this study, the given force models for the dynamic design of pedestrian loading according to EC 5-2, Sétra, UK NA and ISO 10137 were investigated. These force models were described in Chapter 3, except ISO 10137, which were thoroughly described by Jansson and Svensson (2012). The application of the loads on the studied bridges is described in Section 5.5. The group loading in EC 5-2 was a group of 13 people and the stream loading was corresponding to a deck loaded with 0.6 pedestrians/m². Sétra was calculated for a load of 0.5 pedestrians/m² and UK NA for 0.4 pedestrians/m². ISO 10137 were calculated for stream loadings of 0.4 and 0.6 pedestrians/m² for ease of comparison.

In Table 8.4, the measured vertical peak accelerations are displayed. These are in good correlation with the perception of the bridges, which stated that the box-beam bridge had a very good behaviour with regards to vibrations. According to the acceleration measurements the steel truss bridge had the worst behaviour, but the human perception was that the multi-span bridge was worse. However, on both the steel truss bridge and the multi-span bridge the vibrations were deemed acceptable, but with large crowds on the multi-span bridge it may be doubtful if it is acceptable.

Table 8.4 Vertical peak accelerations from field measurements.

	Steel truss	Box-beam	Multi-span	Cable-stayed[a]
Heel Impact [m/s^2]	0.84	0.50	0.50	0.1
Jumping [m/s^2]	4.6	1.45	2.8	1.66
Controlled walking [m/s^2]	0.45	0.14	0.49	0.5
Running [m/s^2]	1.0	0.35	0.31	-

[a] The values from the cable-stayed bridge is taken from Jansson and Svensson (2012).

The vertical peak accelerations from the modelled load configurations of the four design guidelines are shown in Table 8.5. For the three studied bridges, EC 5-2, UK NA and Sétra had good correlation with the controlled walking test with the same level of accelerations at the steel truss bridge and the multi-span bridge, and significantly lower accelerations at the box-beam bridge. However, none of the design guidelines gave accelerations equal to the actual measured from the controlled walking tests. However, the force models did not model the exact group sizes as were used in the field measurements. At the box-beam bridge, the test resembled a continuous stream of pedestrians with a density of approximately 0.4 pedestrians/m². The test group however, consisted of mostly children, and hence the applied load in the force models was too large. In general, the vertical peak accelerations from Sétra were closest to the measured accelerations.

With UK NA and Sétra, the comfort criterion may vary, as described in Section3.5. As seen in Table 8.5, a somewhat higher allowable acceleration for the multi-span bridge than the two other bridges was proposed in guideline UK NA. This is due to

the lower height of the bridge. In Sétra, the choice of comfort level is decided by the client. In this thesis, medium comfort were selected for the box-beam- and the multi-span bridge, and minimum comfort for the steel truss bridge.

Table 8.5 Vertical peak accelerations from the force models from the design guidelines, compared to the maximum allowable acceleration according to the code (in parenthesis)

	Steel truss	Box-beam	Multi-span	Cable stayed[a]
EC 5-2 (1 walking pedestrian) [m/s^2]	0.998 (0.7)	0.196 (0.7)	0.499 (0.7)	-
EC 5-2 (group) [m/s^2]	1.71 (0.7)	0.295 (0.7)	1.49 (0.7)	-
EC 5-2 (stream) [m/s^2]	6.62 (0.7)	1.29 (0.7)	5.94 (0.7)	-
EC 5-2 (1 running pedestrian) [m/s^2]	-	-	1.50 (0.7)	-
UK NA (stream) [m/s^2]	2.27 (1.3)	0.86 (1.3)	2.31 (1.43)	-
Sétra (empty / occupied) [m/s^2]	2.30 / 1.07 (2.5)	0.664 / 0.620 (1.0)	1.93 / 1.89 (1.0)	-
ISO 10137 (1 walking pedestrian) [m/s^2]	2.24 (0.159)	0.511 (0.155)	0.289 (0.215)	0.05 (0.234)
ISO 10137 (2 running pedestrians) [m/s^2]	21.59 (0.159)	4.50 (0.155)	2.39 (0.215)	0.09[b] (0.234)
ISO 10137 (0.4 pedestrians/m²) [m/s^2]	13.27 (0.318)	3.15 (0.310)	3.60 (0.431)	0.99[c] (0.467)
ISO 10137 (0.6 pedestrians/m^2) [m/s^2]	15.86 (0.318)	3.86 (0.310)	4.41 (0.431)	

[a] The values from Älvsbackabron is taken from Jansson andSvensson (2012).

[b] Corresponding to one running pedestrian

[c] The accelerations corresponds to 50 persons on the bridge, which is equal to a density of 0.06 pedestrians/m².

The utilisation ratio between calculated peak acceleration and maximum allowable peak acceleration based on the design guidelines for each bridge can be seen in Table 8.6. Proposed comfort criteria based on guidelines EC 5-2 and ISO 10137 were outside the range for all studied bridges. The box-beam bridge also had allowable peak accelerations for UK NA and Sétra. In addition, the steel truss bridge was inside

the limits according to Sétra, but not UK NA. The multi-span bridge did not satisfy any of the modelled design guidelines.

Table 8.6 Utilisation ratios between calculated peak acceleration and maximum allowable peak acceleration for the design guidelines for each of the bridges.

	Steel truss	Box-beam	Multi-span	Cable stayed[a]
EC 5-2	946%	184%	849%	-
UK NA	175%	66.2%	162%	-
Sétra	92%	66.4%	193%	-
ISO 10137	13 579%	2 903%	1 112%	212%

[a] The values from Älvsbackabron is taken from Jansson and Svensson (2012).

9 Discussion

In this chapter, the results and the comparison are discussed by the authors. The discussion is based on the literature presented in the first chapters and assumptions made by the authors.

9.1 Design guidelines

The least detailed of the design guidelines studied in Chapter 3, EC 5-2, is very straightforward. It only has the three input variables natural frequency, mass of the bridge and damping ratio, where the latter is given in the code. A distinct and no-negotiable peak acceleration limit of 0.7 m/s^2, makes it an easy code to follow. However, the force model is only applicable to simply-supported beam and truss-like bridges in timber and is a crude simplification of the pedestrian load and response. EC 5-2 should also, in theory, be applicable to other construction materials, but this was not allowed by the code when this thesis was written. Considering the mentioned oversimplification the designer should think twice before using this in the design of pedestrian bridges.

The two other treated design guidelines, UK NA and Sétra, are more complicated and needs good communication between the designer and the client, especially in the early stages of the design. In both codes the choice of bridge class is very important. The bridge class gives the loading which are to be expected on the bridge. The smallest crowd loads considered are 0.4 pedestrians/m^2 for UK NA and 0.5 pedestrians/m^2 for Sétra. These limits seem a little high for Swedish conditions, where a lot of bridges never will be subjected to these large crowds and it may be acceptable to exceed these crowds once or twice in the bridge's lifetime. Hence, smaller crowd densities should probably be applied for Swedish conditions. The comfort criteria for the UK NA and Sétra both have a lowest peak acceleration of 0.5 m/s^2, while the highest are 2.0 m/s^2 for UK NA and 2.5 m/s^2 for Sétra. The actual limit between these two extreme values will be decided by the client. For Sétra, the limit is decided by the comfort level desired, from maximum to minimum comfort, while UK NA has modification factors dependent on the availability of alternative routes, usage and height. Both methods seem to have their own advantages, UK NA is methodical and it is just to apply the recommended values. Sétra however, gives the client a choice on how they want the bridge to be perceived, specific limits within a comfort range is probably also possible to decide by the client.

For both UK NA and Sétra, the application of the load are the same, a uniformly-distributed load is applied with a forcing frequency equal to the natural frequency and directions according to the relevant mode shape, as shown in Figure 3.4. This will then give the worst case loading to be expected on the bridge In addition to this distributed load, UK NA gives a point load representing different groups crossing the bridge at a constant velocity, both walking and running. Worth noting is that Sétra does not cover any load cases for runners due to the short crossing time. Even so, a force model for runners exists in the appendix if it is deemed necessary for calculations. This is probably the case for most bridges, but in the authors opinion this should be checked for longer bridges since the crossing time increases and disturbance over a longer period of time may occur.

To model the complete behaviour with UK NA and Sétra it is necessary to perform the calculations in 3D, since even torsional modes have to be included in the design. However, it should be possible to perform preliminary design for the uniformly

distributed load on simple structures in 2D. If the bridge is beamlike, solutions should be readily available and may diminish the need for FE analysis in the early phases.

The magnitude of the load to be applied with UK NA and Sétra is dependent on several factors, where the natural frequency, the density of pedestrians and the damping ratio are the most important. The natural frequency influences the magnitude through Figure 3.5 and Figure 3.16, where peaks are centred round the first and second harmonics. The easiest magnitude of the two to calculate is Sétra, which have factors easily determined and it would be possible to create a standardised spreadsheet incorporating all factors to give the design load for all possible cases. If load case 3 is incorporated in 1 and 2 by the modified minus factor in Figure 3.16, it will be even easier. For UK NA, most of the modification factors are described by non-linear figures and more manual work needs to be done before the magnitude of the load can be determined.

When calculating the natural frequency of the occupied bridge, a density of one pedestrian per square meter should be used according to Sétra. However, in this thesis the occupied bridge was calculated with a density in accordance with the specified pedestrian density. The authors found this to be a better representation of the actual loading to be expected on the bridge.

9.2 Damping

As earlier stated, the damping is influenced by many factors, in particular non-structural elements fastened after construction and not modelled in the design. This makes it difficult to evaluate the damping exact in the design phase, and hence has to be selected in accordance with the design guideline in use. The influence of human-structure interaction and asphalt pavement have been highlighted in is this thesis. From the few studies investigated it seems possible to increase the damping in some cases, however this is not thoroughly investigated and further studies are needed before any conclusions can be made.

In this thesis, the total damping of the bridges were calculated, this includes the effects of all kind of structural and non-structural elements on the bridge and the people participating in the tests. The calculated damping ratios were in the range of 4%, which is 10 times higher than specified in Eurocode for steel, and five times higher than for timber. Eurocode however, gives the structural damping for the pure material, so the actual structural damping may be somewhat smaller. For the steel truss bridge, which was very light, the people on the bridge probably contribute significantly to the damping than for the timber bridges. In the timber bridges, most of the larger damping probably could be explained by the influence of asphalt and non-structural elements. The timber bridges also have a damping ratio close to the average for timber bridges given in Table 4.1 by the CEB/fib.

9.3 Field measurements

During the field measurements, none of the studied bridges behaved as expected by the original FE models, which were based on the drawings. These models were also used, with small modifications, when the design guidelines were applied. The structural changes made were; at the steel bridge the steel deck had to be included, at the box-beam bridge springs had to be added to simulate the rubber bearing and at the

multi-span bridge the railing had to be included with a reduced Young's modulus. With these changes, the calibrated FE models had good correlation with the measured natural frequencies. The most unexpected of these changes were the contribution from the steel plate at the steel truss bridge. The plate is only fastened with two bolts at each end of the bridge and should in theory not contribute to any stiffness, but in reality it did. A possible explanation for this could be that rust has formed between the transversal beams and the plate and hence not allowing movement between the parts. At the box-beam bridge, the springs were even used in the design model, to reflect the actual behaviour and because it could have been approved in a design phase.

At the box-beam bridge, the measured natural frequency was higher than used in the design model, which was due to the lower mass used in design. At the steel- and box-beam bridge however, the natural frequency were lower in the design model. This is due to the extra stiffness from the steel plate and the railings, which for the multi-span bridge gives a larger influence on the natural frequency than the decrease in density of timber. Some uncertainty however, exists about the actual natural frequency at the steel bridge. At the two occasions the field measurements were performed, the natural frequency differed with 0.25 Hz. The highest natural frequency was measured at the warmest day, which raises the question of whether the natural frequency is temperature dependent in this bridge. A reason for this could be that the bearings of the bridge did not allow movement in the longitudinal direction, due to for instance corrosion, and hence introducing a compressive force in the chord.

9.4 Dynamic design

All the force models were applied in the time domain until steady state response wasreached. For Sétra and UK NA guidelines the steady state response describes the continuous stream of pedestrians in a good way. ISO 10137 describes a group of pedestrians crossing the bridge, and for the studied bridges the crossing time would not be sufficiently long to reach steady state. For example for runners, which only uses a few seconds to cross, the calculated peak accelerations were too high.

In general, the internal relation between the studied bridges with regards to peak accelerations from the design guidelines were in correlation with the measured accelerations on and the experience of the bridges. When it comes to the magnitude of the accelerations from the design guidelines however, the correlation was low for ISO 10137 and EC 5-2. The design following these guidelines highly overestimated the accelerations in the bridges. Sétra and UK NA on the other hand gave accelerations more in accordance with the observations from the field experiments. This was not surprising results, considering the two first are simplifications that does not fully explain the pedestrian loading, at least not when a crowd is concerned. The two latter models however, are better prepared and intended to capture the actual pedestrian loading from continuous streams of pedestrians. Hence, the better correlation was expected from the beginning.

According to the peak accelerations obtained in this study, none of the studied bridges should have been built if they had been designed according to EC 5-2 or ISO 10137, and the multi-span bridge not according to any of the codes. The steel truss and the box-beam bridge had lower peak acceleration than the comfort criteria according to Sétra. These two bridges would even have been deemed acceptable with

too high accelerations because they are in Bridge class III, and hence no calculations are needed since the natural frequencies were higher than 2.1 Hz. The multi-span bridge however, would have needed calculations, because it was within the frequency span of 1.7 Hz and 2.1 Hz. Another issue with the multi-span bridge is the possibility of interaction between different modes due to the closeness of the first two modes, and therefore the actual response may be even higher than the one predicted by the Sétra and UK NA.

From the field experiments, it was noted that jumping in half the natural frequency caused large accelerations in the bridge deck. This was most apparent when the bridge had a high natural frequency, which is difficult to maintain while jumping. This should be something to consider in the design phase, if the bridge has a natural frequency of approximately 4 Hz, a forcing frequency of half the natural frequency may give excessive accelerations.

For very light bridges, like the steel bridge, performing calculations on both an unloaded and loaded bridge according to Sétra may give a huge difference in the calculated accelerations. This depends on the lower natural frequency on the loaded bridge, which may give a different minus factor but also on the added mass, which will give the bridge more inertia and make it more difficult to set in motion.

10 Conclusion

Acceleration measurements were performed on three bridges, a steel truss bridge, a timber box-beam bridge and a five span timber bridge with a stress laminated deck. Table 10.1 displays the measured peak accelerations, the first vertical natural frequency and the calculated damping ratios for the three bridges, and in Table 10.2 the peak accelerations and utilisation ratios between calculated peak acceleration and maximum allowable peak acceleration from the modelled design guidelines are shown. None of the studied design guidelines provided peak accelerations corresponding to the field measurements simulating normal usage, but Sétra and UK NA had the best predictions. These two models also provided utilisation ratios, which in general coincided with the measurements and perception of the bridges. EC 5-2 and ISO 10137 provided a lot higher peak accelerations far exceeding both the measurements and comfort criteria. Due to all presented results, in combination with the ease of application for Sétra, the authors recommend Sétra as a design guideline to be used in future design of pedestrian bridges.

Table 10.1 Results of the field measurements.

	Steel	Box-beam	Multi-span
Peak acceleration, jumping [m/s^2]	4.6	1.45	2.8
Peak acceleration, normal usage [m/s^2]	0.45	0.14	0.49
First vertical natural frequency [Hz]	4.75	3.50	2.15
Damping ratio (total damping) [-]	4.14%	4.38%	3.86%

Table 10.2 Vertical peak accelerations and utilisation ratios for the four modelled design guidelines.

	Steel truss		Box-beam		Multi-span	
	Peak acc. [m/s^2]	Utilisation ratio [-]	Peak acc. [m/s^2]	Utilisation ratio [-]	Peak acc. [m/s^2]	Utilisation ratio [-]
EC 5-2	6.62	946%	1.29	184%	5.94	849%
UK NA	2.27	175%	0.86	66.2%	2.31	162%
Sétra	2.30	92%	0.66	66.4%	1.93	193%
ISO 10137	21.6	13 579%	4.50	2 903%	4.41	1 112%

To reflect the measured behaviour of the bridges, the mass of the timber were increased according to specifications from the manufacturers. In addition, these structural changes were made:

- At the steel truss bridge, the bridge deck was modelled to interact with the transversal beams.
- At the box-beam bridge, springs were added in the longitudinal direction to simulate the rubber bearings.
- At the multi-span bridge, the top of the railing were added with a reduced stiffness to account for the partly interaction.

Damping of bridges are a complex phenomenon and are influenced, among others, by non-structural elements like asphalt pavement and railings. In addition, humans influence and generally increase the total damping of a bridge. The total damping may be higher than the structural damping as given by design guidelines. Due to all this uncertainty, the damping should be selected on the conservative side in design.

10.1 Further studies

This thesis highlighted the subject of damping, and it should be even further studied by a more extensive literature review and evaluation of the real damping through several methods. Especially the influence of asphalt, humans and other non-structural elements would be interesting to study in more details.

As described in the previous section, this study has indicated that in some cases even the railing may influence the stiffness of the bridge. This interaction has to be better studied before it can be implemented in design of bridges.

During the performed field experiments, large acceleration amplitudes were reached when jumping in half the natural frequency of the bridge. When the natural frequency of the bridge is approximately 4 Hz, it is possible that a walking frequency of half the frequency may excite the bridge and give unacceptable vibrations. This was not covered in this study, but should be further investigated.

The minimum pedestrian crowd density for a stream of pedestrians are 0.4, 0.5 and 0.6 pedestrians/m^2 according to UK NA, Sétra and EC 5-2, and seems very high for Swedish conditions with a lot of bridges rarely or never reaching these densities. And if a bridge reaches this crowd density once or twice in its lifetime, it may be acceptable with higher accelerations.

11 References

Bachmann, H., & Ammann, W. (1987): *Vibration in structures,* 3rd ed., IABSE-AIPC-IVBH , Zürich.

BSI. (2008):*UK National Annex to Eurocode 1: Actions on structures - Part 2: Traffic loads on bridges,* Corrigendum No. 1, British Standard Institution, London

CEN. (2005):*EN 1998-2 - Eurocode 8: Design of structures for earthquake resistance - Part 2: Bridges,* European comittee for standardization, Brussels.

Chopra, A. K. (2007):*Dynamics of structures,* 3rd ed., Pearson Education, Upper Saddle River.

Craig Jr, R. R., & Kurdila, A. J. (2006):*Fundamentals of structural dynamics*, 2nd ed., John Wiley & Sons, Hoboken.

Dallard, P., Fitzpatrick, A. J., Flint, A., Le Bourva, S., Low, A., Ridsdill Smith, R. M., Willford, M. (2001):The London Millenium Footbridge,*Structural Engineer,* Vol. 79, No. 22, pp. 17-33.

Heinemeyer, C., Butz, C., Keil, A., Mark, S., Goldack, A., Trometer, S., Lukić, M., Chabrolin, B., Lemaire, A., Martin, P., Cunha, Á., Caetano, E., (2009):*Design of lightweight footbridges for human induced vibrations. Background document in support to the implementation, harmonization and furter development of the Eurocdes* JRC European Commission, Luxembourg.

Ingólfsson, E. T., Georgakis, C. T., & Jönsson, J. (2012): Pedestrian-induced lateral vibrations of footbridges: A literature review,*Engineering Structures,* Vol. 45, pp.21-52.

Jansson, H., & Svensson, I. (2012):*Vibrations in timber bridges du to pedestrian induced forces - A case study of Älvsbackabron,* MSc Thesis, Department of Civil and Environmental Engineering, Chalmers University of Technology, Göteborg.

Johansson, C-J, (2011): *CE-märkning av svenskt limträ, limmat konstruktionsvirke och klyvbalkar,* SP report BMt F617031 rev 2011.

Nakamura, S. (2004): Model for Lateral Excitation of Footbridges by Synchronous Walking,*Journal of structural engineering,* Vol. 130, 32-37.

Nakamura, S.-i., & Kawasaki, T. (2006): Lateral vibration of fottbridges by synchronous walking,*Journal of Constructional Steel Research,* Vol. 62, pp. 1148-1160.

Pedersen, L. (2012): *Damin effect of humans*, In Topics on the Dynamics of Civil Structures, Volume 1: *Conference proceedings of the Society for Experimental Mechanics, Series 26*, eds. Caicedo et al., pp. 1-6.

Schubert, S., Gsell, D., Stieger, R., & Feltrin, G. (2010): Influence of asphalt pavement on damping ratio and resonance frequencies of timber bridges,*Engineering Structures,*Vol. 32, pp. 3122-3129.

Sétra. (2006):*Footbridges. Assessment of vibrational behaviour of footbridges under pedestrian loading.* The Technical Department for Transport, Roads and Bridges Engineering and Road Safety, Paris

Shahabpoor, E., & Pavic, A. (2012):*Comparative Evaluation of Current Pedestrian Traffic Models on Structures*, In Topics on the Dynamics of Civil Structures,

Volume 1: *Conference proceedings of the Society for Experimental Mechanics, Series 26*, eds. Caicedo et al., pp. 41-52.

SIS. (2003):SS-EN 1991-2 *Eurocode 1 – Actions on structures - Part 2: Traffic loads on bridges,* Stockholm: 1st Ed., Swedish Standard Institute.

SIS. (2004): *SS-EN 1995-2:2004* Eurocode 5:*Design of timber structures - Part 2: Bridges,* Stockholm: 1st Ed., Swedish Standard Institute tute.

SIS. (2005):*SS-EN 1990/A1:2005 Eurocode – Basis of structural design,* Stockholm: 1st Ed., Swedish Standard Institute

SIS. (2006):*SS-EN 1993-2:2006: Eurocode 3: Design of steel structures - Part 2: Steel bridges,* Stockholm: 1st Ed., Swedish Standard Institute

SIS. (2008). *SS-ISO 10137:2008 Bases for design of structures - Serviceability of buildings and walkways against vibratiosn (ISO 10137:2007, IDT),* Stockholm: 1st Ed., Swedish Standard Institute

Wang, D., Shiqiao, G., Kasperski, M., Liu, H., Jin, L. (2011): The dynamic characteristics of a couple system by pedestrian bridge and walking persons, *Applied Mechanics and Materials,* Vol 71-78, pp 1499-1506.

Zivanovic, S., Pavic, A., & Ingólfsson, E. T. (2010): Modeling spatially unrestricted pedestrian traffic on footbridges. *Journal of structural engineering,*Vol. 136, No. 10, pp. 1296-1308.

Živanović, S., Pavić, A., & Reynolds, P. (2005). Vibration serviceability of footbridges under human-induced excitation: a literature review. *Journal of Sound and Vibration,* Vol. 279, No. 1-2, 1-74.

Appendix A – Calibration Certificates

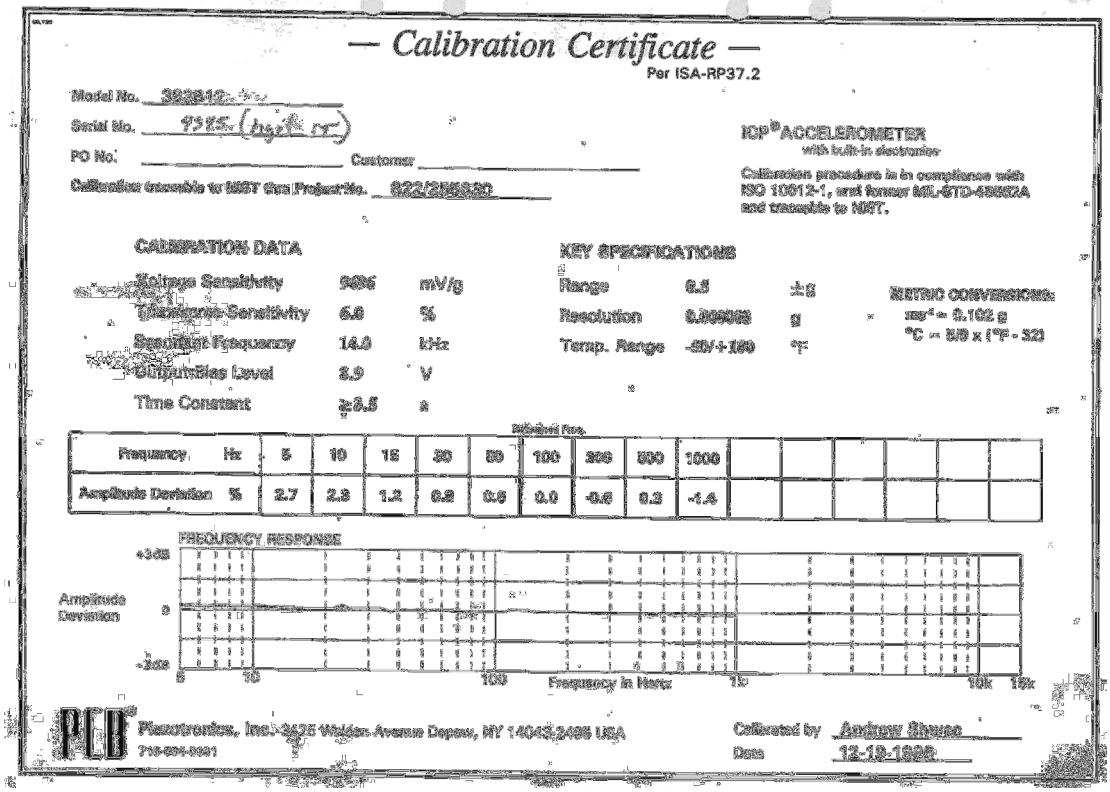

— Calibration Certificate —

Per ISA-RP37.2

Model No. 352B10

Serial No. 9915 (high range)

PO No. _____ Customer _____

Calibration traceable to NIST thru Project No. 822/255930

ICP® ACCELEROMETER
with built-in electronics

Calibration procedure is in compliance with ISO 10012-1, and former MIL-STD-45662A and traceable to NIST.

CALIBRATION DATA

Voltage Sensitivity	9896	mV/g
Transverse Sensitivity	6.8	%
Resonant Frequency	14.0	kHz
Output Bias Level	8.9	V
Time Constant	≥8.5	s

KEY SPECIFICATIONS

Range	0.5	±g
Resolution	0.000098	g
Temp. Range	-59/+120	°F

METRIC CONVERSIONS:
m/s² = 0.102 g
°C = 5/9 x (°F - 32)

Reference Freq.

Frequency Hz	5	10	15	30	50	100	300	500	1000						
Amplitude Deviation %	2.7	2.3	1.2	0.2	0.0	0.0	-0.6	0.3	-1.4						

FREQUENCY RESPONSE

PCB® Piezotronics, Inc. 3425 Walden Avenue Depew, NY 14043-2495 USA
716-684-0001

Calibrated by Andrew Shreve
Date 12-19-1996

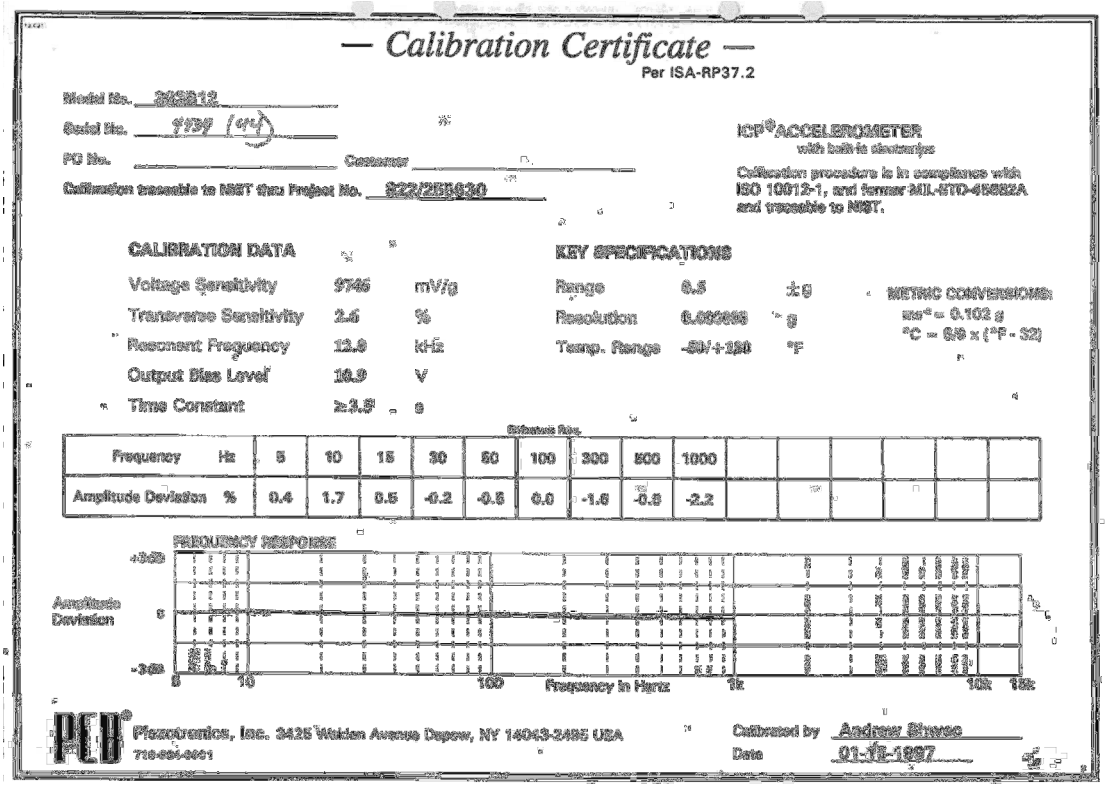

— Calibration Certificate —

Per ISA-RP37.2

Model No. 352B10

Serial No. 9739 (low)

PO No. _____ Customer _____

Calibration traceable to NIST thru Project No. 822/255930

ICP® ACCELEROMETER
with built-in electronics

Calibration procedure is in compliance with ISO 10012-1, and former MIL-STD-45662A and traceable to NIST.

CALIBRATION DATA

Voltage Sensitivity	9746	mV/g
Transverse Sensitivity	2.6	%
Resonant Frequency	12.9	kHz
Output Bias Level	10.9	V
Time Constant	≥3.5	s

KEY SPECIFICATIONS

Range	0.5	±g
Resolution	0.000098	g
Temp. Range	-59/+120	°F

METRIC CONVERSIONS:
m/s² = 0.102 g
°C = 5/9 x (°F - 32)

Reference Freq.

Frequency Hz	5	10	15	30	50	100	300	500	1000						
Amplitude Deviation %	0.4	1.7	0.5	-0.2	-0.5	0.0	-1.6	-0.8	-2.2						

FREQUENCY RESPONSE

PCB® Piezotronics, Inc. 3425 Walden Avenue Depew, NY 14043-2495 USA
716-684-0001

Calibrated by Andrew Shreve
Date 01-15-1997

— Calibration Certificate —

Per ISA-RP37.2

Model No. 393B12

Serial No. 4396 (32)

PO No. _____ Customer _____

Calibration traceable to NIST thru Project No. 822/265430

ICP® ACCELEROMETER
with built-in electronics

Calibration procedure is in compliance with ISO 10012-1, and former MIL-STD-45662A and traceable to NIST.

CALIBRATION DATA			KEY SPECIFICATIONS		
Voltage Sensitivity	10095	mV/g	Range	0.5	±g
Transverse Sensitivity	2.4	%	Resolution	0.000095	g
Resonant Frequency	13.5	kHz	Temp. Range	-58/+150	°F
Output Bias Level	10.3	V			
Time Constant	≥3.5	s			

METRIC CONVERSIONS:
m/s² = 0.102 g
°C = 5/9 x (°F - 32)

Reference Freq.

Frequency Hz	5	10	15	30	50	100	300	500	1000						
Amplitude Deviation %	2.5	1.5	0.2	-0.2	-0.4	0.0	-1.7	-0.5	-2.4						

FREQUENCY RESPONSE

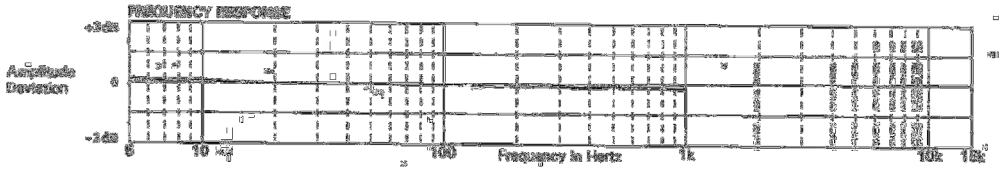

PCB® Piezotronics, Inc. 3425 Walden Avenue Depew, NY 14043-2495 USA
716-684-0001

Calibrated by Andrew Sinnes
Date 12-12-1996

— Calibration Certificate —

Per ISA-RP37.2

Model No. 393B12

Serial No. 4366 (3)

PO No. _____ Customer _____

Calibration traceable to NIST thru Project No. 822/265430

ICP® ACCELEROMETER
with built-in electronics

Calibration procedure is in compliance with ISO 10012-1, and former MIL-STD-45662A and traceable to NIST.

CALIBRATION DATA			KEY SPECIFICATIONS		
Voltage Sensitivity	10175	mV/g	Range	0.5	±g
Transverse Sensitivity	2.4	%	Resolution	0.000095	g
Resonant Frequency	14.0	kHz	Temp. Range	-58/+150	°F
Output Bias Level	9.9	V			
Time Constant	≥3.5	s			

METRIC CONVERSIONS:
m/s² = 0.102 g
°C = 5/9 x (°F - 32)

Reference Freq.

Frequency Hz	5	10	15	30	50	100	300	500	1000						
Amplitude Deviation %	2.8	1.8	0.7	0.4	0.1	0.0	-1.0	-0.0	-1.8						

FREQUENCY RESPONSE

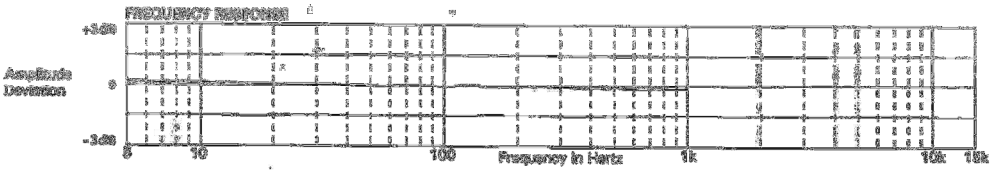

PCB® Piezotronics, Inc. 3425 Walden Avenue Depew, NY 14043-2495 USA
716-684-0001

Calibrated by Andrew Sinnes
Date 12-23-1996

Appendix B – FE modelling of the bridges

Steel truss bridge

The FE models in BRIGADE/Plus of the steel bridge were built from a perception of the drawings of the bridge. By using the following figures and tables, it is possible to model the steel truss bridge in an arbitrary FE software.

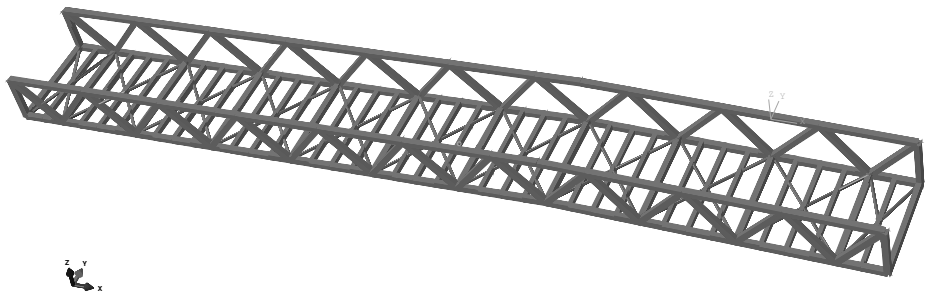

Figure B.1 3D view of the FE model in BRIGADE/Plus.

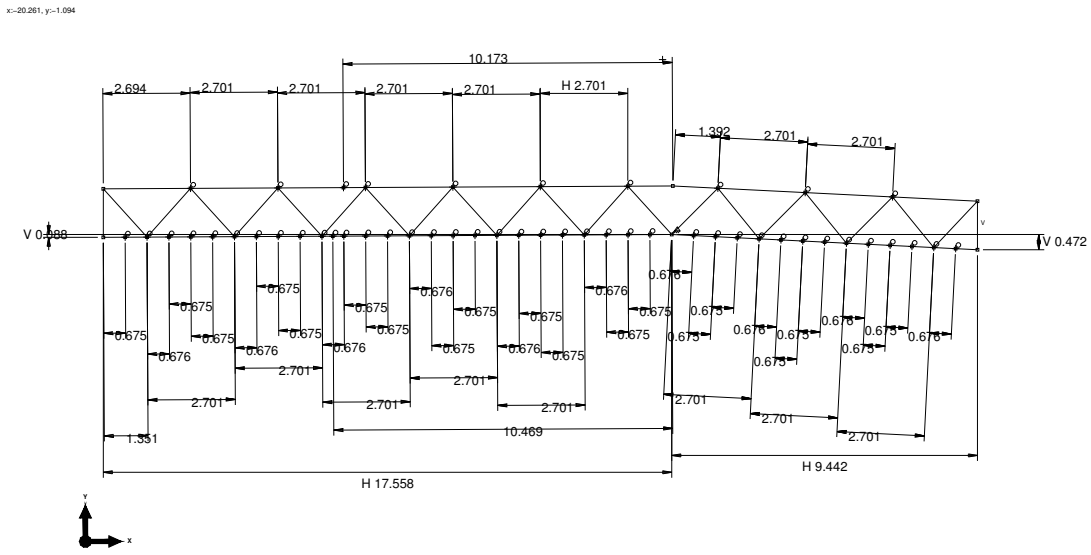

Figure B.2 A sketch from the side of the steel bridge. These dimensions were used for the FE model in BRIGADE/Plus.

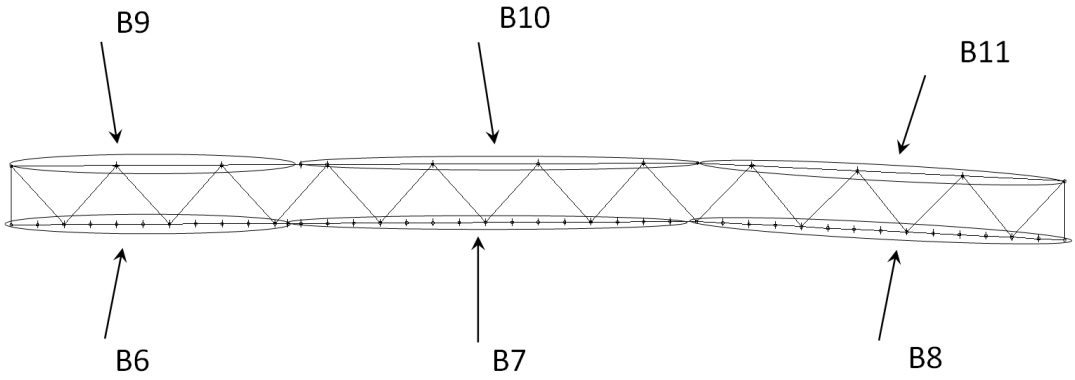

Figure B.3 *Sketch from the side of the steel bridge how the different beam types are place in the FE model. Both side of the bridge have the same. See Table B.2 for dimensions.*

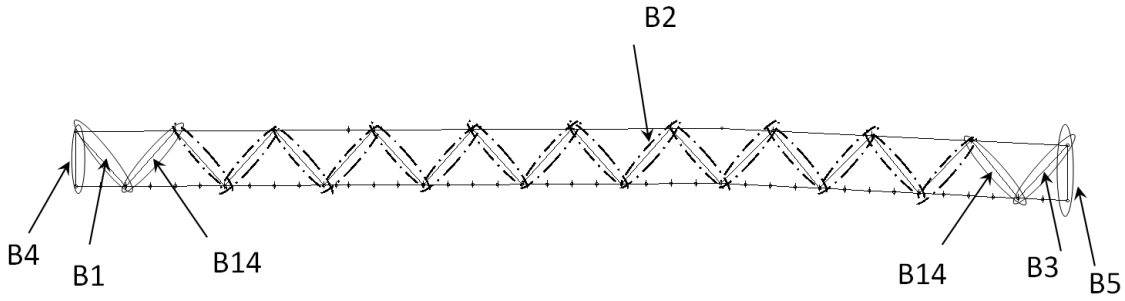

Figure B.4 *Placement of the beams in the truss. Both sides of the bridge are the same. See Table B.2 for dimensions.*

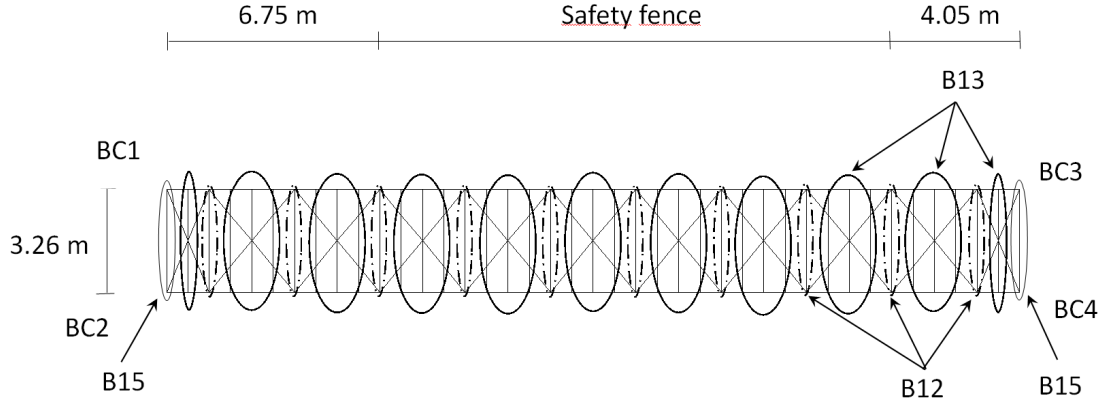

Figure B.5 *Placement of horizontal beams when looking from above the bridge. The boundary conditions of the corners are marked with BC and description of how they are lock can be found in Table B.1.*

Table B.1 Boundary conditions of each corner of the bridge. The positions of the corners are shown in Figure B.5

Position	Locked directions
BC1	x y z
BC2	x z
BC3	y z
BC4	z

Table B.2 Dimension of the beams in the steel bridge according to Figure B.6

Name	Dimensions [mm] b x h x t
B1	150x150x6.3
B2	150x150x5
B3	150x150x6.3
B4	150x150x10
B5	150x150x10
B6	150x150x6.3
B7	150x150x8
B8	150x150x8

Name	Dimensions [mm] b x h x t
B9	150x150x8
B10	150x150x10
B11	150x150x10
B12	150x150x5
B13	100x150x5
B14	150x150x6.3
B15	150x150x10

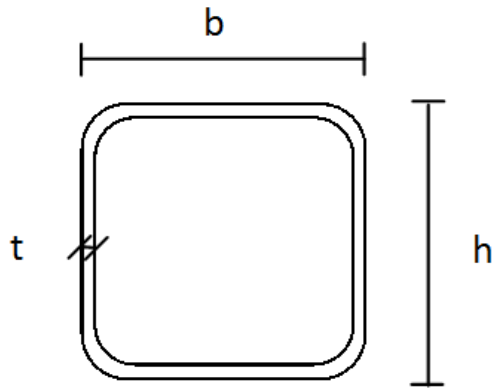

Figure B.6 Cross section of the hollow rectangular beams in Table B.2

Table B.3 Material properties used in the FE models in BRIGADE/Plus.

Design model	Before	After	Setra	UK NA	ISO
Element type	Beam	Beam	Beam	Beam	Beam
Approximate mesh size [m^2]	0.33	0.33	0.33	0.33	0.33
Young's modulus steel [GPa]	210	210	210	210	210
Density steel [kg/m^3]	7850	7850	7850	7850	7850
Density epoxy [kg/m^3]	10	0	0	0	0
Poisson's ratio	0.3	0.3	0.3	0.3	0.3
Density safety fence [kg/m^2]	0	55	100	100	100
Damping ratio steel	-	-	0.4%	0.5%	0.5%
Density diagonal steel stiffeners [kg/m^3]	1e-5	-	1e-5	1e-5	1e-5
Young's modulus diagonal steel stiffeners [GPa]	210	210	210	210	210

Box-beam bridge

The FE models in BRIGADE/Plus of the box-beam bridge were built from a perception of the drawings of the bridge. By using the following figures and tables, it is possible to model the steel truss bridge in an arbitrary FE software. The analysis line is in the middle of all shell elements.

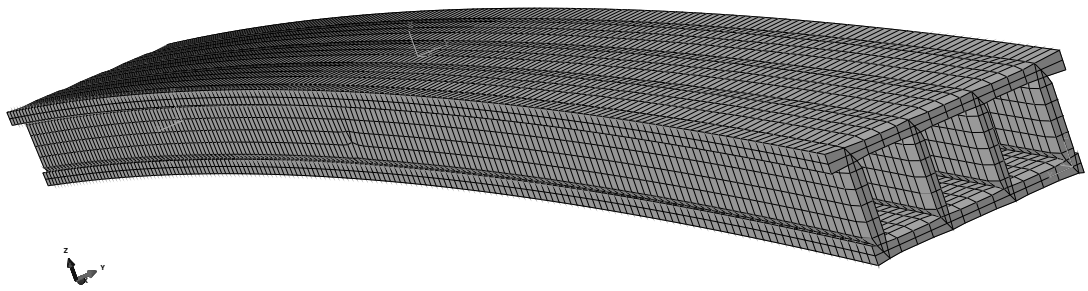

Figure B.0.7 3D FE model of the box-beam bridge.

The box-beam bridge is modelled with a curvature radius of 250 m from the bottom flange. The distance in x direction from the bottom short end side corners are 33 m.

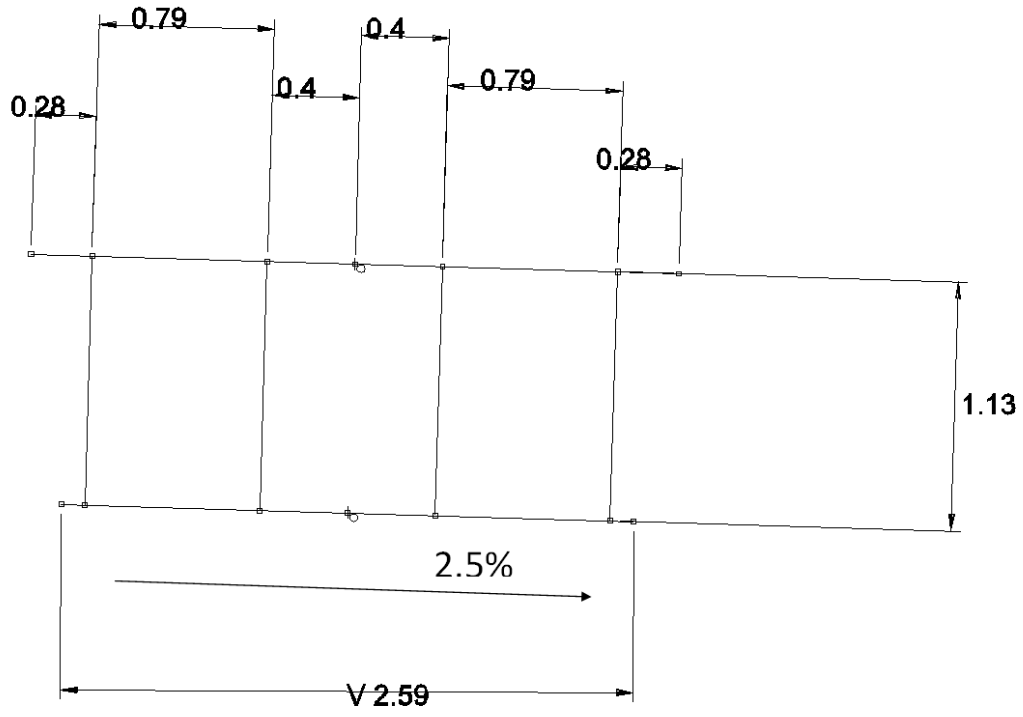

Figure B.8 Cross-section of the box-beam bridge.

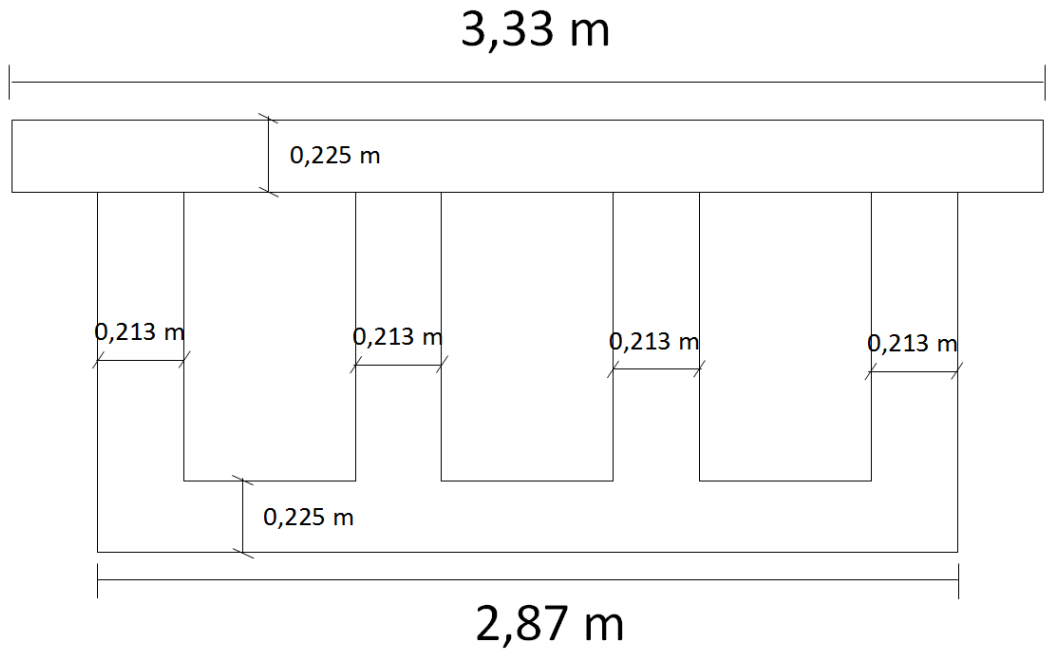

Figure B.9 Dimensions of the cross section

Table B.4 Material parameters in the FE models for the box-beam bridge.

Design model	Before	After		Setra	UK NA	ISO
Type of model	Static	Dynamic	Static	Dynamic	Dynamic	Dynamic
Material	Timber	Timber	Timber	Timber	Timber	Timber
FE element type	Shell	Shell	Shell	Shell	Shell	Shell
Approximate mesh size [m]	0.2x0.2	0.2x0.2	0.2x0.2	0.2x0.2	0.2x0.2	0.2x0.2
Density [kg/m³]	500	500	500	400	400	400
Young's modulus $E_{0,mean}$[GPa]	13	13	10.8	13	13	13
Young's modulus $E_{90,mean}$ [GPa]	0.41	0.41	0.41	0.41	0.41	0.41
Shear modulus $G_{90,mean}$ [GPa]	7.6	7.6	6.33	7.6	7.6	7.6
Shear modulus $G_{0,mean}$ [GPa]	12.75	12.75	6.33	12.75	12.75	12.75
Poisson's ratio	0	0	0	0	0	0
Spring-to-ground stiffeners [MN/m]	-	77	77	77	77	77
Damping ratio timber	-	-	-	1.0%	1.0%	1.0%

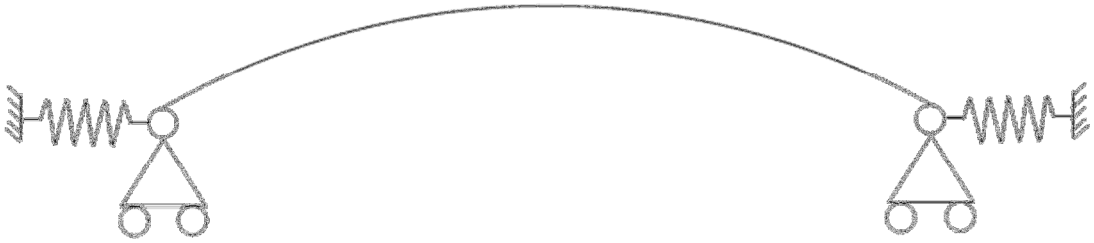

Figure B.10 "Spring-to-ground" stiffeners on the box-beam bridge.

Table B.5 Boundary conditions for the box-beam bridge. the Stiffness is place along both lower short end sides.

Directions	Stiffness
x	77 000 000 N/m
y	Locked along entire short end
Z	Locked along entire short end

The multi-span bridge with stress laminated deck

The FE models of the multi-span bridge are built in BRIGADE/Plus. By using the following figures and tables, it is possible to model the steel truss bridge in an arbitrary FE software. The analysis line is in the middle of all shell elements of the deck.

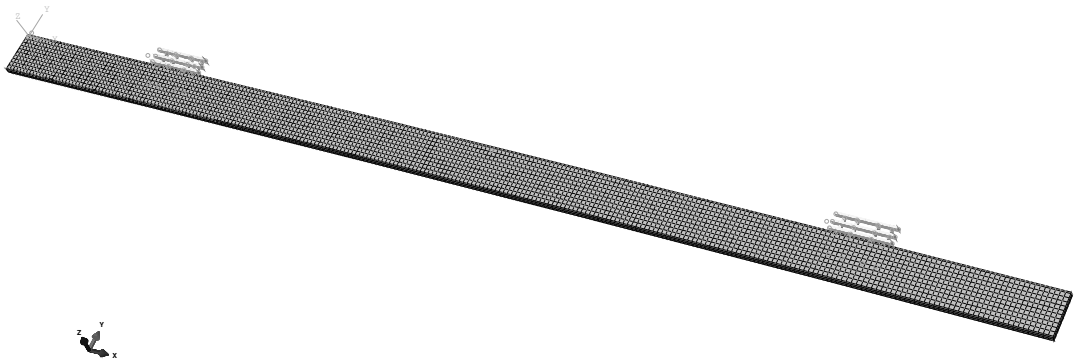

Figure B.11 3D FE model of the muli span bridge.

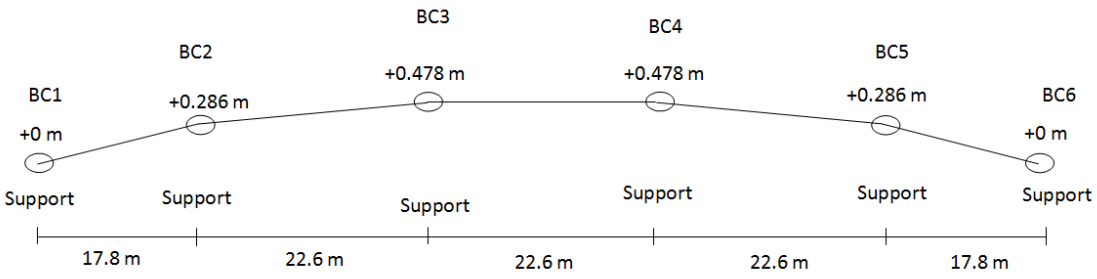

Figure B.12 View from the side of the FE model.

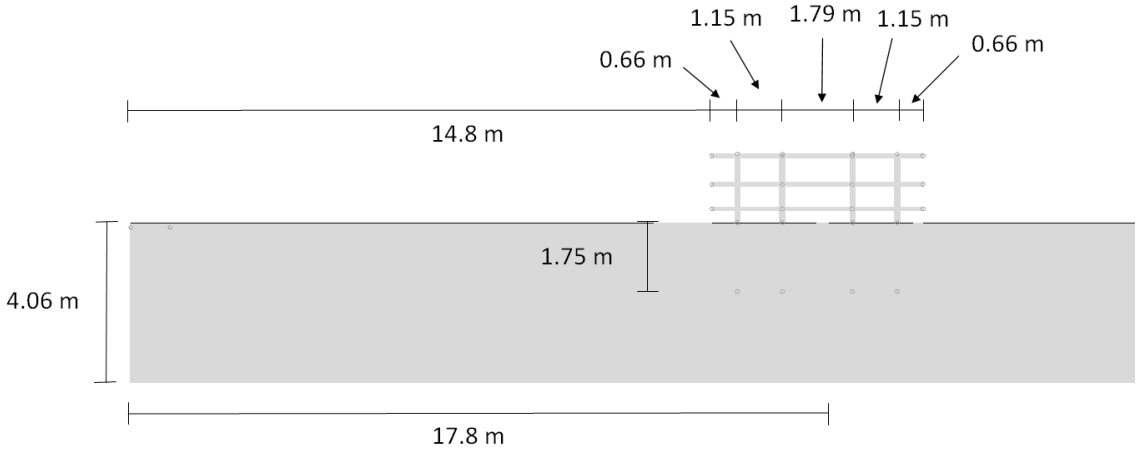

Figure B.13 Placement of the balcony beams. Hence, the bridge is symetric the beams were placed with the same distance from each other on the right side.

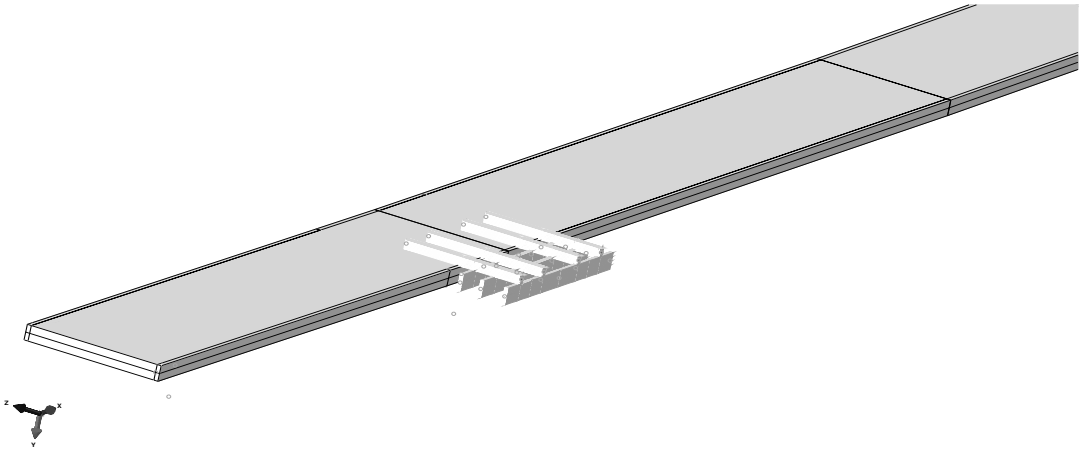

Figure B.14 View of how the balconies are model from beneath the bridge.

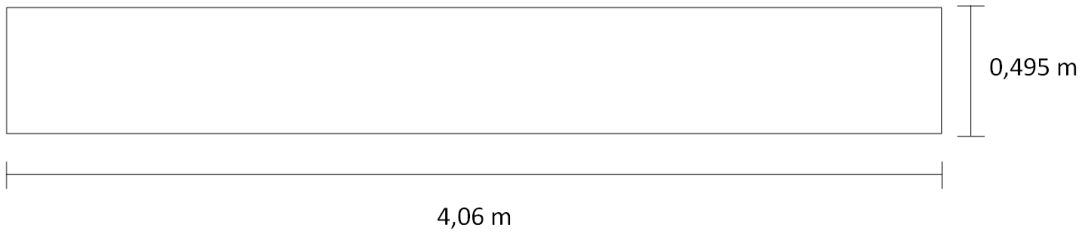

Figure B.15 Dimensions of the cross section

Table B.6 Material parameters in the FE models for the box-beam bridge.

Design model	Before	After	Setra	UK NA	ISO
Material	Timber	Timber	Timber	Timber	Timber
FE element type	Shell	Shell	Shell	Shell	Shell
Approximate mesh size [m^2]	0.4x0.4	0.4x0.4	0.4x0.4	0.4x0.4	0.4x0.4
Density [kg/m³]	500	470	430	430	430
Young's modulus $E_{0,mean}$[GPa]	13.7	13.7	13	13	13
Young's modulus $E_{90,mean}$ [GPa]	0.46	0.46	0.41	0.41	0.41
Shear modulus $G_{90,mean}$ [GPa]	8,5	8.5	7.6	7.6	7.6
Shear modulus $G_{0,mean}$ [GPa]	12.75	12.75	12.75	12.75	12.75
Poisson's ratio	0	0	0	0	0
Damping ratio timber	-	-	1.0%	1.0%	1.0%
Railing	NO	YES	NO	NO	NO
Material		Timber			
FE element type		Beam			
Density [kg/m³]		430			
Young's modulus $E_{0,mean}$[GPa]		1.7			

Table B.7 Dimension of the beams in the balconies and the railing beam according to Figure B.16

Name	Dimensions [mm]
Beam-To-Deck	140x300
Beam-To-Beam	90x530
Railing	190x122

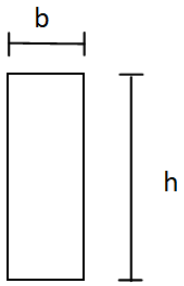

Figure B.16 Cross section of the beams in Table B.7

Table B.8 Boundary conditions of the multi-span bridge

Position	Direction (Locked along whole support)
BC1	y z
BC2	y z
BC3	x y z
BC4	y z
BC5	y z
BC6	y z

Appendix C – MATLAB scripts

The scripts are based on the MATLAB scripts used by Jansson and Svensson (2012)

```
%% Calculation of damping ratio
t = filtery.time ; % Time from filtered measurements
y = filtery.data ; % Accelerations from filtered measurements
t_start=50 ; % Test dependent variable, unique for each test
t_stop=60 ; % Test dependent variable
sampleRate = 1/(t(2)-t(1)) ;
startTime = t_start * sampleRate ; % Test dependent variable
endTime = t_stop * sampleRate ; % Test dependent variable
upOrDown = sign(diff(y)) ;
maxPos = [upOrDown(1)<0 ; diff(upOrDown)<0 ; upOrDown(end)>0] ;
tops = find(maxPos) ;
t_coord = [] ; % Coordinates in "time-direction"
a_coord = [] ; % Coordinates in "acceleration-direction"
fori = 1:length(tops)
if (tops(i) >startTime) && (tops(i) <endTime)
t_coord = [t_coord t(tops(i))] ;
a_coord = [a_coord y(tops(i))] ;
end
end
fit_damp = fit(t_coord',a_coord','exp1') ;
plot(t,y,'-r',t_coord,a_coord,'ok')
hold on
plot(fit_damp,'b')
damp_factor = 1/(2*pi) * log(fit_damp(t_coord(1)) / fit_damp(t_coord(2)))
```

```
%% Function to calculate Fast Fourier Transformation
function [] = FFTtransformation(y,t)
L = length(y);
Fs = L / t(end);
NFFT = 2^nextpow2(L);
Y = fft(y,NFFT)/L;
f = Fs/2*linspace(0,1,NFFT/2+1);
plot(f,2*abs(Y(1:NFFT/2+1)))
freq_int=5 ; % Bridge depended frequency interval
xlim([0  freq_int])
xlabel('Frequency (Hz)')
ylabel('|Y(f)|')
```

Appendix D – Peak accelerations according to EC 5-2

Calculation of peak accelerations according to Annex B of Eurocode 5, part 2, for the steel truss bridge

Indata

The indata are taken from the models in BRIGADE/Plus

$L_{span} := 27m$

$b_{plate} := 3.112m$

$M := 20045.02kg$

$\zeta := 0.5\%$

$f_{1V} := 3.57Hz$

Vertical accelerations for one person crossing

$$a_{vert1} := \frac{100N}{M \cdot \zeta} = 0.998 \frac{m}{s^2}$$

For group of pedestrians, with n=13 and a stream of pedestrians with n=0.6*A

$$k_{vert} := 1 - \frac{(f_{1V} - 2.5Hz)}{2.5Hz} = 0.572$$

$n_1 := 13$

$$a_{vert.13} := 0.23 \cdot a_{vert1} \cdot n_1 \cdot k_{vert} = 1.706 \frac{m}{s^2}$$

$$n_2 := 0.6 \cdot b_{plate} \cdot L_{span} \cdot \frac{1}{m^2} = 50.414$$

$$a_{vert0.6A} := 0.23 \cdot a_{vert1} \cdot n_2 \cdot k_{vert} = 6.618 \frac{m}{s^2}$$

Calculation of peak accelerations according to Annex B of Eurocode 5, part 2, for the box beam bridge

Indata

The indata are taken from the models in BRIGADE/Plus

$L_{span} := 33m$

$b_{walk} := 2.87m$

$M := 51070.34kg$

$\zeta := 1.0\%$

$f_{1V} := 3.74Hz$

Vertical accelerations for one person crossing

$$a_{vert1} := \frac{100}{M \cdot \zeta} \cdot (N) = 0.196 \frac{m}{s^2}$$

For group of pedestrians, with n=13 and n=0.6*A

$$k_{vert} := 1 - \frac{(f_{1V} - 2.5Hz)}{2.5Hz} = 0.504$$

$n_1 := 13$

$$a_{vert.13} := 0.23 \cdot a_{vert1} \cdot n_1 \cdot k_{vert} = 0.295 \frac{m}{s^2}$$

$$n_2 := 0.6 \cdot b_{walk} \cdot L_{span} \cdot \frac{1}{m^2} = 56.826$$

$$a_{vert0.6A} := 0.23 \cdot a_{vert1} \cdot n_2 \cdot k_{vert} = 1.29 \frac{m}{s^2}$$

Calculation of peak accelerations according to Annex B of Eurocode 5, part 2, for the multi span bridge

The design method is only valid for simply supported bridges, hence only the largest span is considered in the model, and assumed to be simply supported.

Indata

The indata are taken from the models in BRIGADE/Plus

$L_{span} := 22.6m$

$b_{walk} := 3.819m$

$M := 40096.67kg$

$\zeta := 1.0\%$

$f_{1v} := 1.90Hz$

$f_{2v} := 2.38Hz$

$f_{3v} := 3.05Hz$

Vertical accelerations for one person crossing

$$a_{vert1} := \frac{200N}{M \cdot \zeta} = 0.499 \frac{m}{s^2}$$

For group of pedestrians, with n=13 and n=0.6*A

$n_1 := 13$

$k_{vert1} := 1.0$

$$a_{vert.13} := 0.23 \cdot a_{vert1} \cdot n_1 \cdot k_{vert1} = 1.491 \frac{m}{s^2}$$

$$n_2 := 0.6 \cdot b_{walk} \cdot L_{span} \cdot \frac{1}{m^2} = 51.786$$

$$a_{vert0.6A} := 0.23 \cdot a_{vert1} \cdot n_2 \cdot k_{vert1} = 5.941 \frac{m}{s^2}$$

For one person running across the span

$$a_{vert.run} := \frac{600N}{M \cdot \zeta} = 1.496 \frac{m}{s^2}$$